Diese Arbeit haben begutachtet

....
Ansgar Jüngel

TECHNISCHE UNIVERSITÄT WIEN

DISSERTATION

Kinetic and diffusion equations for socio-economic scenarios

Ausgeführt zum Zwecke der Erlangung des akademischen Grades einer
Doktorin der technischen Wissenschaften
unter der Leitung von

Univ.-Prof. Dr. Ansgar Jüngel

E101
Institut für Analysis und Scientific Computing

eingereicht an der Technischen Universität Wien Fakultät für Mathematik
und Geoinformatic
von

Lara Trussardi
Matrikelnummer: 1328689

Wien, am 12. Mai 2016

CONTENTS

...

Men nearly always follow the tracks
made by others and proceed in their
affairs by imitation.

N. Macchiavelli

ABSTRACT

In this work three different models for describing some socio-economic scenarios are presented. First, a cross-diffusion system modelling the information herding of individuals has been studied; the second model describes the dynamics of agents in a large market depending on the estimated asset value of a product and the rationality of the agents using a kinetic inhomogeneous Boltzmann-type equation. The third model describes the influence of knowledge and wealth in a society where the agents interact with the others through binary interactions via a Boltzmann equation.

The entropy structure of the cross-diffusion system gives us the global-in-time existence of weak solutions and the exponential decay to the constant steady state. Moreover, we investigate local bifurcations from homogeneous steady states analytically and this analysis shows that generically there is a gap in the parameter regime between the entropy approach validity and the first local bifurcation.

In the second model, a nonlinear nonlocal Fokker-Planck equation with anisotropic diffusion is derived. The existence of global-in-time weak solutions to the Fokker-Planck initial-boundary-value problem is proved using the entropy approach.

For the third model we prove the existence of weak solutions for the Boltzmann equation.

For each model studied several numerical simulations has been implemented: for the cross-diffusion system we used numerical continuation methods to track the bifurcating non-homogeneous steady states globally and to determine non-trivial herding solutions. We find that the main boundaries in the parameter regime are given by the first local bifurcation point, the degeneracy of the diffusion matrix and a certain entropy decay validity condition.

In the second model, numerical simulations for the Boltzmann equation highlight the importance of the reliability of public information in the formation of bubbles and crashes. The use of Bollinger bands in the simulations shows how herding may lead to strong trends with low volatility of the asset prices, but eventually also to abrupt corrections.

In the last model we implement the Boltzmann equation. The kinetic code shows the possibility of cluster formation, using certain specific threshold.

ZUSAMMENFASSUNG

In dieser Arbeit werden drei verschiedene Modelle zur Beschreibung einiger sozioökonomischer Szenarien vorgestellt. Zunächst wird ein Kreuzdiffusionssystem untersucht, welches das Herdenverhalten von Individuen modelliert. Das zweite Modell beschreibt die Dynamik von Agenten in einem großen Markt in Abhängigkeit von dem geschätzten Vermögenswert eines Produkts und der Rationalität der Agenten. Dies wird mit einer kinetischen inhomogenen Boltzmann-Gleichung modelliert. Das dritte Modell beschreibt den Einfluss von Wissen und Wohlstand in einer Gesellschaft, in der die Agenten miteinander durch binäre Wechselwirkungen gemäß einer Boltzmann-Gleichung interagieren.

Die Entropiestruktur des Kreuzdiffusionssystems liefert die Existenz von zeitlich globalen schwachen Lösungen und den exponentiellen Abfall zu einem konstanten stationären Zustand. Darüber hinaus untersuchen wir analytisch lokale Abzweigungen von homogenen stationären Zuständen. Diese Analyse zeigt, dass im Allgemeinen eine Lücke existiert zwischen jenem Parameterbereich, in dem der Entropieansatz gültig ist, und jenem, in dem die erste lokale Bifurkation liegt.

Im zweiten Modell wird eine nicht lineare nicht lokale Fokker-Planck-Gleichung mit anisotroper Diffusion hergeleitet. Die Existenz von zeitlich globalen schwachen Lösungen für das Fokker-Planck-Anfangs-Randwertproblem wird mit Hilfe eines Entropieansatzes bewiesen.

Für das dritte Modell beweisen wir die Existenz von Lösungen für die Boltzmann-Gleichung.

Für alle Modelle wurden verschiedene numerische Verfahren implementiert: für das Kreuzdiffusionssystem verwenden wir numerische Fortsetzungsmethoden, um bifurkierende inhomogene stationäre Zustände global zu verfolgen, und um nicht triviale Herdenlösungen zu bestimmen. Wir haben festgestellt, dass die Hauptgrenzen im Parameterbereich durch den ersten lokalen Bifurkationspunkt, die Entartung der Diffusionsmatrix und eine gewisse Gültigkeitsbedingung für den Abfall der Entropie gegeben sind.

Im zweiten Modell stellen numerische Simulationen für die Boltzmann-Gleichung die Bedeutung der Zuverlässigkeit der öffentlichen Information bei der Bildung von Spekulationsblasen und Crashs heraus. Die Verwendung von Bollinger-Bändern in den Simulationen zeigt, wie Herdenverhalten zu starken Preistrends führen kann, aber letztendlich auch zu abrupten Korrekturen.

Im letzten Modell implementieren wir die Boltzmann-Gleichung. Der kinetische Code zeigt die Möglichkeit der Clusterbildung unter Verwendung von bestimmten Schwellenwerten für Wissen und Wohlstand.

INTRODUCTION

Socio-economics is a relatively new science which studies the relationship between the social processes and the economy [BM00, DY00, MS00, Lux98]. It analyses in particular the influence of specific social relationship on the formation of groups, economic systems and institutions [Gra85]. It involves different fields such as sociology, economics, psychology which cooperate in order to understand better, describe and explain the social, economic and political reality.

Due to this wide range of concepts and methods, there is no unique approach to this science and there are several options to investigate the interactions between the processes involved.

Together with the socio-economics, another field of science inspired this work. In the early eighties Galam, Gefen and Shapir introduced the term socio-physics for describing the idea of using the tools of statistical mechanics to model the social behaviour [GGS82, Wei71]. Socio-physics attempts to address a wide range of problems such as social networks, population dynamics, voting, formation of coalitions, opinion dynamics.

This work attempts to merge socio-economics and socio-physics with a model of several socio-economical scenarios. It consists in describing and modelling from a mathematical point of view some socio-economical scenarios using kinetic and diffusion equations.

Since the social behaviour of a community shows a very high degree of complexity and does not represent a physical system, any mathematical model would introduce some limitations and would not be an exact reproduction of the reality.

Nevertheless, a mathematical model also allows studying subjects apparently away from mathematics such as the sociological dynamics.

This work consists of three mathematical models, describing the interactions between individuals in a market and addresses two different scenarios: the herding in financial market and the wealth distribution in a closed society.

1.1 THE TWO SCENARIOS: HERDING AND WEALTH DISTRIBUTION

The first scenario described in this work is the herding in financial markets.

Herding in economic markets is characterized by a homogenization of the actions of the market participants, which behave at a certain time in the same way. Herding may lead to strong trends with low volatility of asset prices, but eventually also to abrupt corrections, so it promotes the occurrence of bubbles and crashes. Numerous socio-economic papers [Ban92, Bru01, DJH$^+$09, RRF09, Roo06] and research in biological sciences [ARNn$^+$05, Ham71] show that herding interactions play a crucial role in social scenarios. Herding behaviour is often irrational because people are not basing their decision on objective criteria. It is driven by emotions and usually occurs because of the social pressure of conformity and the belief that it is unlikely that a large number of people

could be wrong. A market participant might follow the herd in spite of another opinion.

We can observe herding not only in the financial market but also in every day life situations and in panic situations.

One problem in describing herding (or other human behaviour) arises from the fact that the behaviour of every individual in a group has local interactions without centralized coordination, but the global effect can be observed on a macro scale, when we observe all the population. A full understanding of herding behaviour would need the ability to understand both levels: the microscopical one which considers each individual of the crowd separately; and the macroscopic level which deals with all the group of individual, i.e. the herd. The first case usually represents the individual as a particle; the latter one is often represented with a density function depending (continuously) on space and time [BMP11b].

There are many historical examples of herding behaviour in financial and commodity markets, from the so-called Dutch tulip bulb mania in 1637 to the recent credit crunch in the US housing market in 2007. In the last two decades, herding behaviour started to play an increasing role in scientific research although this phenomenon has been studied from a variety of perspectives and at distinct levels of analysis since the XVIII century. Indeed, herding can be seen from a psychological and sociological point of view, but it has also application in medicine and political science.

In 1759 Adam Smith in "The Theory of Moral sentiments" [Smi59] described herding as motor mimicry. More than 100 years later, in 1895, Gustave Le Bon introduced the idea of herding as a form of irrational and unconscious social contagion [LB95]. Veblen, American economist and sociologist, studied sudden shifts in consumers behaviour and in his book "The Theory of the Leisure Class" (1899) he introduced the idea of "conspicuous consumption" in which people engage in actions by making comparison with people who are similar but also slightly better with the goal to express their strength better. But it was only in 1908 that the doctor Wilfred Trotter introduced the phrase "herd behaviour" [Tro06] as an explanatory principle of crowd psychology starting from the work of Le Bon. In 1935 John Maynard Keynes, an English economist, described herding as a contagious "animal spirit" which moves the market [Key36]. For decades the study of this behaviour in social psychology and sociology had a broad description and analysis, but it is in the analysis of the stock market that herding has received most of the recent attention in the social sciences. Everett Roger introduced two research directions [Rog03]: one related to diffusion of innovations and one related to social network analysis. He defined diffusion as "the process by which an innovation is communicated through certain channels over time among the members of a social system". His work found application not only in economics but also in psychology and sociology.

In 1992, two papers have been published which showed that people could follow others even if private information and motivations suggested doing otherwise. The first work by Banerjee [Ban92] describes a situation where the individuals focus more on the behaviour of the others than on their own information, and another work by Bikhchandani,

Hirshleifer and Welch [BHW92], which used the concept of "information cascades". Abrahamson and Rosenkopf also took into account the fact that usually the individuals don't have equal access to the same information [AR97], which implies that the position of the individuals in a social network influences the strength of pressure on others to follow. All these models were based on rational actors. This is what Veblen called a „hedonistic-associational psychology" and a „hedonistic calculus" in which „human conduct is conceived of and interpreted as a rational response to the exigencies of the situation in which mankind is placed" [Veb09].

Psychologists and economists agree on the definition of herding but there are theoretical and methodological differences. From the theoretical point of view there are two main issues [Bad10]: economists' approach focuses on the existence of rational actors while psychologists consider a bounded rationality [Sim55]. Psychologists assume that human limitations lead people to satisfying solutions instead to optimal solution and the simpler solution relies on phrases like "the majority is always right". A second point is the existence of complete information which would always allow individuals to make rational and optimal decisions. But, as Abrahamson and Rosenkopf showed, herding is caused by incomplete and ambiguous information [AR93, AR97]. Also at the methodology level there are different approaches: economics usually focuses on questions like „how much" (how to deal with herd behaviour, how much to benefit from it), while psychology is more interested in questions like „why" and „when" (why and when herding occurs).

The second scenario addressed in this work is the wealth distribution. As for the herding description, there is the microscopic level and the macroscopic one: each individual owns a certain wealth but it is more interesting to focus on the distribution of the money in the whole society.

The so-called socio-physics has been used for analysing this phenomenon.

The term "Social physics" was introduced by Quetelet in 1835 in his book "Sur l'homme et le développement de ses facultés, ou Essai de physique sociale" (in English "Treatise on Man") where he described the social physics concept of the "average man" who is characterized by the mean values of measured variables that follow a normal distribution. His goal was to understand the statistical laws behind the phenomena such as crime rates, marriage rates or suicide rates. The term "social physics" was also used from Comte, a French political philosopher, who, in 1842, defined it as the study of the laws of society. Only afterwards this term became sociology due to his disagreement with Quetelet's collection of statistics.

Later on, Maxwell developed the kinetic theory of gases and in 1876 he claimed that the experiences of "social physicists" gave him confidence that the statistical approach could extract order from the microscopic chaos. So physics became statistical and as Boltzmann said "Molecules are like many individuals, having the most various states of motion, and the properties of gases only remain unaltered because the number of these molecules which on average have a given state of motion is constant" [Bol09].

But the step from microscopic to macroscopic level has been done by two physicists W. Lenz and E. Ising and an economist, T. Schelling. The two physicists simulated different phenomena with the Ising model which had in common the presence of individual components which were interacting in pairs producing collective effects, while Schelling showed that simple agent rules can create complex global patterns or emergent behaviour [Sch71].

As already pointed out the access to the information plays a fundamental role and it should be taken into account. It is complicated to model the way in which individuals learn, however various aspects of learning has been studied in these last years [BdO04, dFC06, GAEM⁺11, LMM13].

This micro-macro approach has been employed both in Chapter 3 and Chapter 4 where we respectively studied the herding behaviour and the wealth distribution starting from binary collision between individuals. In particular, in Chapter 3 a variable which represents the rationality of the individuals has been taken into account, while in Chapter 4 we have considered a knowledge variable.

1.2 MODELS FOR HERDING AND WEALTH DISTRIBUTION

The first question is "how could we model herding?". We consider two different herding models: a cross-diffusion system (Chapter 2) and a kinetic model (Chapter 3). In Chapter 2 we tried to obtain herding non-constant solutions; in Chapter 3 we tried to address and answer to the question "is it possible to obtain a model that would allow us to prevent herding?". In Chapter 4 we tried to reproduce mathematically and simulate the reciprocal influence between knowledge and wealth.

In Chapter 2 we study the following cross-diffusion system:

$$\partial_t u_1 = \text{div}(\nabla u_1 - g(u_1)\nabla u_2), \tag{1.1}$$

$$\partial_t u_2 = \text{div}(\delta \nabla u_1 + \kappa \nabla u_2) + f(u_1) - \alpha u_2, \tag{1.2}$$

where $u_1 = u_1(t, x), u_2 = u_2(t, x)$ for $(t, x) \in [0, T) \times \Omega, T > 0$ is the final time, $\Omega \subset \mathbb{R}^d$ $(d \geq 1)$ is a bounded domain with sufficiently smooth boundary, ∇ denotes the gradient, div $= \nabla\cdot$ is the divergence and $\partial_t = \frac{\partial}{\partial t}$ denotes the partial derivative with respect to time. The equations are supplemented by no-flux boundary conditions and suitable initial conditions

$$
\begin{aligned}
(\nabla u_1 - g(u_1)\nabla u_2) \cdot v &= 0 \quad \text{on } \partial\Omega, \ t > 0, \\
(\delta \nabla u_1 + \kappa \nabla u_2) \cdot v &= 0 \quad \text{on } \partial\Omega, \ t > 0, \\
u_1(0, x) &= u_1^0, \quad \text{in } \Omega, \\
u_2(0, x) &= u_2^0 \quad \text{in } \Omega
\end{aligned}
\tag{1.3}
$$

where v denotes the outer unit normal vector to $\partial\Omega$. The function $u_1(x, t) \in [0, 1]$ represents the density of individuals with information variable $x \in \Omega$ at time $t \geq 0$, and $u_2(x, t)$ is an influence function which modifies the information state of the individuals and possibly may lead to a herding (or aggregation) behaviour of individuals. The influence function acts through the term $g(u_1)\nabla u_2$ in (1.1). The non-negative bounded function $g(u_1)$ is assumed to vanish only at $u_1 = 0$ and $u_1 = 1$,

which provides the bound $0 \leq u_1 \leq 1$ if $0 \leq u_1(0, x) \leq 1$. In particular, we assume that the influence becomes weak if the number of individuals at fixed $x \in \Omega$ is very low or close to the maximal value $u_1 = 1$, i.e. $g(0) = 0$ and $g(1) = 0$, which may enhance herding behaviour. The influence function is assumed to be modified by diffusive effects also due to the random behaviour of the density of the individuals with parameter $\delta > 0$, by the non-negative source term $f(u_1)$, relaxation with time with rate $\alpha > 0$, and diffusion with coefficient $\kappa > 0$.

If $\delta = 0$, equations (1.1)-(1.2) can be interpreted as a nonlinear variant of the chemotaxis Patlak-Keller-Segel model [KS70], where the function u_2 corresponds to the concentration of the chemoattractant. The model with nonlinear mobility $g(u_1)$ was first analysed by Hillan and Painter [HP02], even for more general mobilities of the type $u_1\beta(u_1)\chi(u_2)$. Generally, the mobility $g(u_1) = u_1(1 - u_1)$ models finite-size exclusion and prevents blow-up phenomena [Wrz04], which are known in the original Keller-Segel model. The convergence to equilibrium was shown in [JZ09]. Such models were also employed to describe evolution of large human crowds driven by the dynamic field u_2 [BMP11a]. Although of high interest in the mathematical community, we will not analyse this case but assume that $\delta \neq 0$.

System (1.1)-(1.2) represents one possible model to describe the dynamics of information herding in a macroscopic setting. There exist other approaches to model herding behaviour, for instance using kinetic equations (as in [DL14] and in Chapter 3) or agent-based models [LS08]. The focus in this model is to understand the influence of the parameters δ and α on the solution behaviour from a mathematical viewpoint, i.e., to investigate the interplay between cross-diffusion and damping.

Equations (1.1)-(1.2) with $\delta > 0$ can be derived from an interacting "particle" system modelled by stochastic differential equations, at least in the case $g(u_1) = $ const. (see [GS14]). One expects that this derivation can be extended to the case of nonconstant $g(u_1)$ but we do not discuss this derivation here. The above system with $g(u_1) = u_1$ was analysed in [HJ11] in the Keller-Segel context. The additional cross diffusion with $\delta > 0$ in (1.2) was motivated by the fact that it prevents the blow up of the solutions in two space dimensions, even for large initial densities and for arbitrarily small values of $\delta > 0$. The motivation to introduce this term in our model is different since the nonlinear mobility $g(u_1)$ allows us to conclude that $u_1 \in [0, 1]$, thus preventing blow up without taking into account the cross-diffusion term $\delta\Delta u_1$. Our aim is to investigate the behaviour of the solutions to (1.1)-(1.2) for *all* values for δ, thus allowing for *destabilizing* cross-diffusion parameters $\delta < 0$.

One starting point to investigate the dynamics is to consider the functional structure of the equation. In this context entropy methods are a possible tool [Jün15]. The entropy structure can frequently be used to establish the existence of (weak) solutions. Furthermore, it is helpful for a quantitative analysis of the large-time behaviour of solutions for certain reaction-diffusion systems; see, e.g., [DF07]. The method quantifies the decay of a certain functional with respect to a steady state. An advantage is that the entropy approach can work globally, even for initial conditions far away from steady states. Moreover, the entropy structure may be formulated in the variational framework of gradient flows which allows one to analyse the geodesic convexity of their

solutions [LM13, ZM15]. However, this global view indicates already that we may not expect that the approach is valid for all parameters in general nonlinear systems. Indeed, in many situations, global methods only work for a certain range of parameters occurring in the system. The question is what happens for parameter values outside the admissible parameter range and near the validity boundary.

One natural conjecture is that upon variation of a single parameter, there exists a *single* critical parameter value associated to a first local bifurcation point δ_b beyond which a global functional approach does not extend. In particular, the homogeneous steady state upon which the entropy is built, could lose stability and new solution branches may appear in parameter space. Another possibility is that global bifurcation branches in parameter space are an obstruction. In our context, the generic situation is different from the two natural conjectures.

In the context of (1.1)-(1.2), the *main distinguished parameter* we are interested in is δ. Here we shall state our results on an informal level. Carrying out the existence of weak solutions and the global decay to homogeneous steady states $u^* = (u_1^*, u_2^*)$ via an entropy approach, we find the following results:

(M1) Using the entropy approach, one may prove the existence of weak solutions to (1.1)-(1.2) in certain parameter regimes.

(M2) The global entropy decay to equilibrium does not extend to arbitrary negative δ. Suppose we fix all other parameters, then there exists a critical δ_e (to be defined later) such that global decay occurs only for $\delta > \delta_e$ ($\delta \neq 0$).

(M3) If we consider the limit $\alpha \to +\infty$ then we can extend the global decay up to

$$\delta^* := -\kappa/\gamma < 0, \qquad \text{where } \gamma := \max_{v \in [0,1]} g(v),$$

i.e., global exponential decay to a steady state occurs for all $\delta > \delta^*(\delta \neq 0)$ if α is large enough.

(M4) In the limit $\alpha \to 0$, we find that $\delta_e \to +\infty$. In particular, the entropy method breaks down in this limiting regime.

We stress that the results for the global decay (M2)-(M4) may not be sharp, in the sense that one could potentially improve the validity boundary δ_e. Interestingly, we shall prove that (M3) is indeed sharp for certain steady states, i.e., no improvement is possible in this limit. The proofs of (M1)-(M4) provide a number of technical challenges, which are discussed in more detail in Section 2.1.1 and Section 2.2. We also note that the entropy method definitely does not extend to any negative δ. It is clear that a global decay to steady state is impossible if bifurcating non-homogeneous steady state solutions exist in addition to homogeneous steady states. We use analytical local bifurcation theory for the stationary problem, based upon a modification of Crandall-Rabinowitz theory [Kie04], to prove the following:

(M5) The bifurcation approach for homogeneous steady states can be carried out as long as

$$\delta \neq \delta_d := -\kappa/g(u_1^*).$$

On a generic open and connected domain, local bifurcations of simple eigenvalues occur for

$$\delta_{\mathrm{b}}^{n} = \delta_{\mathrm{d}} + \frac{1}{\mu_{n}}\left[f'(u_{1}^{*}) - \frac{\alpha}{g(u_{1}^{*})}\right],$$

where μ_{n} are the eigenvalues of the negative Neumann Laplacian.

(M6) If $\alpha > 0$ is sufficiently *large* and fixed, $\delta^{*} > \delta_{\mathrm{d}} > \delta_{\mathrm{b}}^{n}$ and the bifurcation points accumulate at δ_{d}.

(M7) If $\alpha > 0$ is sufficiently *small* and fixed, $\delta_{\mathrm{d}} < \delta_{\mathrm{b}}^{n}$ and the bifurcation points again accumulate at δ_{d} as long as $\delta^{*} \neq \delta_{\mathrm{d}}$.

Although these results are completely consistent with the global decay of the entropy functional, they do not yield global information about the bifurcation curves. In general, this is not possible analytically for arbitrary nonlinear systems. Therefore, we consider numerical continuation of the non-homogeneous steady-state solution branches (for spatial dimension $d = 1$). The continuation is carried out using AUTO [DCD^{+}07]. Our numerical results show the following:

(M8) We regularize the numerical problem using a small parameter ρ to avoid higher-dimensional bifurcation surfaces due to mass conservation.

(M9) The non-homogeneous steady-state bifurcation branches starting at the local bifurcation points extend in parameter space and contain multi-bump solutions, which deform into more localized herding states upon changing parameters.

(M10) A second continuation run considering $\rho \to 0$ yields non-trivial herding solutions for the original problem. In particular, solutions may have multiple transition layers (respectively concentration regions) and the ones with very few layers occupy the largest ranges in δ-parameter space.

Combining all the results we conclude that we have the situations in Figure 1(a)-(b) for generic fixed parameter values and a generic fixed domain. These two main cases of interest are:

(C1) $\alpha > 0$ *sufficiently large*: in this limit, the entropy validity boundary, the analytical bifurcation approach, and the numerical methods are organized around the singular limit at $\delta = \delta^{*}$. Indeed, note that

$$\delta^{*} = \delta_{\mathrm{d}}, \quad \text{if } u = u_{1}^{*} \text{ maximizes } g(u) \text{ on } [0, 1],$$

and we show in Section 2.1.1 that $\delta_{\mathrm{e}} \to \delta^{*}$ as $\alpha \to +\infty$. The generic picture for a homogeneous steady state so that u_{1}^{*} does not maximize g and α is moderate and fixed is given in Figure 1(a).

(C2) $\alpha > 0$ *sufficiently small*: in this case, the generic picture is shown in Figure 1(b). The entropy decay only occurs for very large values δ_{e}. Interestingly, the approaches do not seem to collapse onto one singular limit in this case.

We remark that the condition $\kappa \neq -\delta g(u_1)$ does not only occur in the numerical continuation analysis but also in the context of the entropy method as well as the analytical bifurcation calculation. It is precisely the condition for the vanishing of the determinant of the diffusion matrix that prevents pushing existence and decay techniques based upon global functionals further and it is also a condition where the analytical bifurcation theory does not work because the linearised problem does not yield a Fredholm operator. In some sense, this explain the singular limit as $\alpha \to +\infty$ from (C1). Although (C1) is quite satisfactory from a mathematical perspective, one drawback is that the forward problem may not be well-posed in a classical sense if $\delta < \delta_d$; of course, the stationary problem is still well-defined.
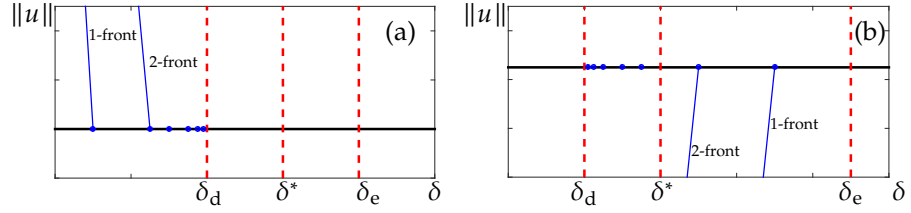
Figure 1: Sketch of the different bifurcation scenarios; for more detailed numerical calculations see Section 2.4. Only the main parameter δ is varied, a homogeneous branch is shown in black and bifurcation points and branches in blue (dots and curves). Only the first two nontrivial branches are sketched which contain solutions with one transition layer. (a) Case (C1) with $\alpha > 0$ sufficiently large; for a suitable choice of u^* and $\alpha \to +\infty$ all three vertical dashed red lines collapse onto one line. (b) Case (C2) with $\alpha > 0$ sufficiently small.

For (C2), we cannot prove sharp global decay via an entropy functional. However, the first nontrivial branch of locally stable stationary herding solutions can be reached in forward time, and not just by adiabatic parameter variation as in (C1). Although we postpone the detailed mathematical study of the the limit $\alpha \to 0$ to future work, the observations raise several interesting problems, which we discuss in the outlook in Chapter 5.

In summary, we study the interplay between three different techniques available for reaction-diffusion systems with cross-diffusion: entropy methods, analytical local bifurcation and numerical global bifurcation theory. Furthermore, for each technique, we have to use, improve, and apply the previously available methods to the herding model problem (1.1)-(1.3). Our results lead to clear insight on the subdivision of parameter space into regimes, where each method is particularly well-suited to describe the system dynamics. We identify two interesting singular limits and provide a detailed analysis for the limit of large damping. Furthermore, we compute via numerical continuation several solutions that are of interest for applications to herding behaviour using a two-parameter homotopy approach to desingularize the mass conservation. From an application perspective, we identify herding states with clustering of individuals in one, or just a few, distinct regions, as the ones occupying the largest parameter ranges. Hence, we expect applications to be governed by homogeneous stationary and relatively simple heterogeneous herding states.

There seem to be very few works [Gab12, AAN96] studying the parameter space interplay between global entropy-structure methods in

comparison to local analytical and global numerical bifurcation approaches. This work seems to be, to the best of our knowledge, the first analysis combining and comparing all three methods, and also the first to consider the global-functional and bifurcations interaction problem for cross-diffusion systems. In fact, our analysis suggests a general paradigm to improve our understanding of global methods for nonlinear spatio-temporal systems, i.e., one major goal is to determine the parameter space *validity boundaries* between *different methods*.

While most approaches to herding in the literature are based on agent models [LM99], in Chapter 3 we use techniques from kinetic theory, similar to opinion-formation models [BS09, DMPW09, Tos06]. Up to our knowledge, the first kinetic models in social sciences were developed by Helbing [Hel93b, Hel93a] to study the social behaviour dynamics of a population, and by Cordier, Pareschi and Toscani [CPT05] to describe a simple market economy. For more details, the reader can refer to [NPT10], in particular [CMPP10, BS10], and the very complete book by Pareschi and Toscani [PT13]. Binary collisions between gas molecules are replaced by interactions of market individuals, and the phase-space variables are interpreted as socio-economic variables in our case: the rationality $x \in \mathbb{R}$ and the estimated asset value $w \in \mathbb{R}^+ := [0, \infty)$, assigned to the asset by an individual. When $x > 0$, we say that the agent behaves rational, otherwise irrational. We refer to the review [DW96] for a discussion of rational herding models.

Denoting by $f(x, w, t)$ the distribution of the agents at time $t \geq 0$, its time evolution is given by the inhomogenous Boltzmann-type equation

$$\partial_t f + [\Phi(x, w)f]_x = \widetilde{Q}_I(f) + \widetilde{Q}_H(f, f), \quad (x, w) \in \mathbb{R} \times \mathbb{R}^+, \, t > 0, \, (1.4)$$

with the boundary condition $f = 0$ at $w = 0$ and initial condition $f = f_0$ at $t = 0$. The first term on the right-hand side describes an interaction that is soley based on economic fundamentals. After the interaction, the individuals change their estimated asset value influenced by sources of public information such as financial reports, balance sheet numbers, etc. The second term describes binary interactions of the agents modelling the exchange of information and possibly leading to herding and imitation phenomena.

When the asset value lies within a certain range around the "fair" prize, determined by fundamentals, the agents may suffer from psychological biases like overconfidence and limited attention [Hir01], and we assume that they behave more irrational. This means that the drift field $\Phi(x, w)$ is negative in that range. When the asset value becomes too low or too large compared to the "fair" prize the asset values are believed to be driven by speculation. We assume that the market agents recognize this fact at a certain point and are becoming more rational. In this case, the drift field $\Phi(x, w)$ is positive. We expect that the estimated asset value will in average be not too far from the "fair" price, and we confirm this expectation by computing the moment of $f(x, w, t)$ with respect to w in Section 3.1.2. For details on the modelling, we refer to Section 3.1.

Let us discuss how our study relates to previous works in the literature. The first paper on kinetic models including herding in markets

seems to be [MP12], while earlier articles are concerned with opinion-formation modelling; see, e.g., [Tos06]. Our setting is strongly influenced by the models investigated by Toscani [Tos06] and Delitala and Lorenzi [DL14]. Toscani [Tos06] described the interaction of individuals in the context of opinion formation, and we employ ideas from [Tos06] to model public information and herding. The idea to include public information and herding is due to [DL14]. In contrast to [DL14], we allow for the drift field $\Phi(x, w)$, leading to the inhomogeneous Boltzmann-type equation (1.4). Such equations were also studied in [DW15] but using a different drift field. The relationship of rational herd behaviour and asset values was investigated in [AZ98] but no dynamics were analysed. The novelty of the present work is the combination of dynamics, transport, public information, and herding.

Our main results are as follows. We derive formally in the grazing collision limit (as in [Tos06]) the nonlinear Fokker-Planck equation

$$\partial_t g + [\Phi(x, w)g]_x = (K[g]g)_w + (H(w)g)_w + (D(w)g)_{ww}, \quad (1.5)$$

$$g(x, 0, t) = 0, \quad g(x, w, 0) = g_0(x, w), \quad (x, w) \in \mathbb{R} \times \mathbb{R}^+, \ t > 0. \quad (1.6)$$

Here, $K[g]$ is a nonlocal operator related to the attitude of the agents to change their mind because of herding mechanisms, $H(w)$ is an average of the compromise propensity, and $D(w)$ models diffusion, which can be interpreted as a self-thinking process, and satisfies $D(0) = 0$. Again, we refer to Section 3.1 for details. A different herding diffusion model in the context of crowd motion was derived and analysed in [BMP11b]. Other kinetic and macroscopic crowd models were considered in [DARM+13].

Equation (1.5) is nonlinear, nonlocal, degenerate in w, and anisotropic in x (incomplete diffusion). It is well known that partial diffusion may lead to singularity formation [HPW13], and often the existence of solutions can be shown only in the class of very weak or entropy solutions [AN03, EVZ94]. Our situation is better than in [AN03, EVZ94], since the transport in x is linear. Exploiting the linear structure, we prove the existence of global *weak* solutions to (1.5)-(1.6). However, we need the assumption that $D(w)$ is strictly positive to get rid of the degeneracy in w. Unfortunately, our estimates depend on $\inf D(w)$ and become useless when $D(0) = 0$.

Moreover, we present some numerical experiments for the inhomogeneous Boltzmann-type equation (1.4) using a splitting scheme. The collisional part (i.e. (1.4) with $\Phi = 0$) is approximated using the interaction rules and a modified Bird scheme. The transport part (i.e. (1.4) with $\widetilde{Q}_I = \widetilde{Q}_H = 0$) is discretized using a combination of an upwind and Lax-Wendroff scheme. The numerical experiments highlight the importance of the reliability of public information in the formation of bubbles and crashes. The use of Bollinger bands in the simulations shows how herding may lead to strong trends with low volatility of the asset prices, but eventually also to abrupt corrections.

Also in Chapter 4 we used the tools of statistical mechanics for the study of the collective behaviour of the wealth distribution.

The advantage of the kinetic formulation is that it allows to study the dynamic effects for a sufficiently large number of people where no one has a dominant role compared to the others [BS09, Tos06].

The model we mathematically and numerically investigate here is quite simple. It may lack some realism, because it involves simplified models with respect to [Tos06, BS09, PT14], to provide a neat mathematical framework. It also allows to recover clustering effects highlighted in [DNAW00, HK02], for example. The main idea relies on the same kind of assessment as [MP12, DL14, PT14, BT15]: the wealth exchanges are also driven by the knowledge/beliefs of each agent in the population. For instance, in [PT14], the population interacts with a fixed, time-dependent background of common knowledge, which behaves like an information mean field which does not depend on the population itself. This background can then be understood as the media. In [MP12], the population is divided into two groups, the chartists and the fundamentalists, whose interactions allow to steer the price formation of a specific good.

The point of view we here choose is different. We assume that all the exchanges, knowledge or wealth, are of binary kind, inside a homogeneous closed community. The wealth is described with a one-dimensional positive real variable v and we suppose that the trading mechanisms leave the total mean wealth unchanged. The knowledge variable x is also positive and real and it does not have an upper bound since the agents can always learn more and more. The microscopic wealth exchange mechanism between two agents is very similar to the one from [PT14]: it depends on the knowledge of each agent. In the same way, the microscopic knowledge exchange takes into account the dependence with respect to the agents' wealth, with the quite natural idea that an agent may consider as more trustworthy another agent who owns more than himself. In other words, knowledge plays a fundamental role to improve the social condition, so that we can safely suppose that the more we know, the more we can earn and, at the same time we can imagine that who owns more is because he/she has a higher knowledge.

For the wealthy exchanges, we only take into account the personal saving propensity, and forget, for the time being, the risk perception of the individuals as described in [PT14]. We consider that each agent can use his own personal knowledge to reduce the risk in a trade.

Denoting by $f(x, v, t)$ the distribution of the individuals at time $t \geq 0$, its time evolution is given by the Boltzmann-type equation

$$\partial_t f = Q_K(f, f) + Q_W(f, f), \quad (x, v) \in \mathbb{R}^+ \times \mathbb{R}^+, \ t > 0, \tag{1.7}$$

with initial condition $f = f_0$ at $t = 0$. The first term on the right-hand side describes binary interactions of the individuals modelling the exchange of knowledge, while the second term describes binary interactions of the agents modelling the exchange of wealth.

We focused on the Boltzmann equation and we proved the existence of weak solutions. In the numerical section we presented some interesting behaviour obtained by introducing thresholds for the collisional rules and studying the two operators independently.

2

ENTROPY AND BIFURCATION IN CROSS-DIFFUSION HERDING

The chapter is organised in the following way: in Section 2.1, we state our main results and provide an overview of the strategy for the proofs respectively the numerical methods employed. In particular, the entropy method results are considered in Section 2.1.1, the analytical local bifurcation in Section 2.1.2, and the numerical global bifurcation results in Section 2.1.3. The following sections contain the full details for the main results. The proofs using the entropy method are contained in Section 2.2, where the weak solution construction is carried out in Section 3.2.1 and the global decay is proved in Section 2.2.2. Section 2.3 proves the existence of local bifurcation points to non-trivial solutions upon decreasing δ. The details for the global numerical continuation results are reported in Section 2.4.

2.1 MAIN RESULTS

We describe the main results, obtained by either the entropy method or local analytical and global numerical bifurcation analysis.

2.1.1 *Entropy Method*

First, we show the global existence of weak solutions and their large-time decay to equilibrium. We observe that the diffusion matrix of system (1.1)-(1.2) is neither symmetric nor positive definite which complicates the analysis. Local existence of (smooth) solutions follows from Amann's results [Ama89] if the system is parabolic in the sense of Petrovskii, i.e., if the real parts of the eigenvalues of the diffusion matrix are positive. A sufficient condition for this statement is $\delta \geq \delta_d = -\kappa/\gamma$. The challenge here is to prove the existence of *global* (weak) solutions.

The main challenge of (1.1)-(1.2) is that the diffusion matrix of the system is neither symmetric nor positive definite. The key idea of our analysis, similar as in [HJ11], is to define a suitable entropy functional. The entropy is a special Lyapunov functional which provides suitable gradient estimates. Compared to Lyapunov functional techniques like in [Hor11, Wol02] (used for the case $\delta = 0$), the entropy method provides explicit decay rates and, in our case, L^∞ bounds without the use of a maximum principle. (Note that in the system at hand, the L^∞ bounds can be obtained by the standard maximum principle but there are systems where this can be achieved by using the entropy method only; see [Jün15].) For this, we introduce the entropy density

$$h(u) = h_0(u_1) + \frac{u_2^2}{2\delta_0}, \quad u = (u_1, u_2)^\top \in [0, 1] \times \mathbb{R},$$

where h_0 is defined as the second anti-derivative of $1/g$,

$$h_0(s) := \int_m^s \int_m^\sigma \frac{1}{g(t)} \, dt \, d\sigma, \quad s \in (0, 1), \tag{2.1}$$

where $0 < m < 1$ is a fixed number, and

$$\delta_0 := \delta \quad \text{if } \delta > 0, \quad \delta_0 := \kappa/\gamma \quad \text{if } -\kappa/\gamma < \delta < 0.$$

It turns out that the so-called entropy variables $w = (w_1, w_2)^\top$ with $w_1 = h_0'(u_1)$ and $w_2 = u_2/\delta_0$ make the diffusion matrix positive semi-definite for all $\delta > \delta^* := -\kappa/\gamma$, $\delta \neq 0$. We remark that for $\delta = 0$ the method does not work and we do not cover this case. In the w-variables, we can formulate (1.1)-(1.2) equivalently as

$$\partial_t u = \operatorname{div}(B(w)\nabla w) + F(u),$$

where $u = u(w)$, $F(u) = (0, f(u_1) - \alpha u_2)^\top$ and

$$B(w) = \begin{pmatrix} g(u_1) & -\delta_0 g(u_1) \\ \delta g(u_1) & \delta_0 \kappa \end{pmatrix}. \tag{2.2}$$

The invertibility of the mapping $w \mapsto u(w)$ is guaranteed by Hypothesis (H3) below. We show in Lemma 4 below that $B(w)$ is positive semi-definite if $\delta > \delta^*$, $\delta \neq 0$. The global existence is based on the fact that the entropy

$$H(u(t)) = \int_\Omega \left(h_0(u_1(t)) + \frac{u_2(t)^2}{2\delta_0} \right) \mathrm{d}x \tag{2.3}$$

is bounded on $[0, T]$ for any $T > 0$; note that we write $u = u(t)$ here to emphasize the time dependence of H. A formal computation, which is made rigorous in Section 3.2.1, shows that

$$\frac{\mathrm{d}H}{\mathrm{d}t} = -\int_\Omega \left(\frac{|\nabla u_1|^2}{g(u_1)} + \left(\frac{\delta}{\delta_0} - 1 \right) \nabla u_1 \cdot \nabla u_2 + \frac{\kappa}{\delta_0} |\nabla u_2|^2 \right) \mathrm{d}x \tag{2.4}$$
$$+ \frac{1}{\delta_0} \int_\Omega (f(u_1) - \alpha u_2) u_2 \, \mathrm{d}x.$$

The terms in the first bracket define a positive definite quadratic form if and only if $\delta > \delta^*$. The second integral is bounded since $f(u_1)$ is bounded. This shows that for some $\varepsilon_1(\delta) > 0$,

$$\frac{\mathrm{d}H}{\mathrm{d}t} \leq -\varepsilon_1(\delta) \int_\Omega \left(\frac{|\nabla u_1|^2}{g(u_1)} + \frac{|\nabla u_2|^2}{\delta_0^2} \right) \mathrm{d}x + c, \tag{2.5}$$

where the constant $c > 0$ depends on Ω, f, and α. These gradient bounds are essential for the existence analysis.

Before we state the existence theorem, we make our assumptions precise:

(H1) $\Omega \subset \mathbb{R}^d$ with $\partial\Omega \in C^2$, $\alpha > 0$, $\kappa > 0$, $h(u^0) \in L^1(\Omega)$ with $u_1^0 \in (0, 1)$ a.e.

(H2) $f \in C^0([0, 1])$ is nonnegative.

(H3) $g \in C^2([0, 1])$ is positive on $(0, 1)$, $g(0) = g(1) = 0$, $g(u) \leq \gamma$ for $u \in [0, 1]$, where $\gamma > 0$, and $\int_0^m \mathrm{d}s/g(s) = \int_m^1 \mathrm{d}s/g(s) = +\infty$ for some $0 < m < 1$.

The condition $g(u) \leq \gamma$ in $[0,1]$ in (H3) implies that $(u_1^0 - m)^2/(2\gamma) \leq h_0(u_1^0)$ and hence, $h(u^0) \in L^1(\Omega)$ in (H1) yields $u_1^0 \in L^2(\Omega)$ and $u_2^0 \in L^2(\Omega)$. Hypothesis (H3) ensures that the function h_0 defined in (2.1) is well defined and of class C^4 (needed in Lemma 5). Its derivative h_0' is strictly increasing on $(0,1)$ with range $\mathbb{R}$, thus being invertible with inverse $(h_0')^{-1} : \mathbb{R} \to (0,1)$. For instance, the function $g(s) = s(1-s)$, $s \in [0,1]$, satisfies (H3) and $h_0(s) = s \log s + (1-s) \log(1-s)$, where log denotes the natural logarithm. A more general class of functions fulfilling (H3) is $g(s) = s^a(1-s)^b$ with $a, b \geq 1$.

Theorem 1 (Global existence). *Let assumptions (H1)-(H3) hold and let $\delta > -\kappa/\gamma$. Then there exists a weak solution to (1.1)-(1.3) satisfying $0 \leq u_1 \leq 1$ in Ω, $t > 0$ and*

$$u_1, \, u_2 \in L^2_{\mathrm{loc}}(0,\infty; H^1(\Omega)), \quad \partial_t u_1, \, \partial_t u_2 \in L^2_{\mathrm{loc}}(0,\infty; H^1(\Omega)').$$

The initial datum is satisfied in the sense of $H^1(\Omega; \mathbb{R}^2)'$.

We provide a brief overview of the proof. First, we discretize the equations in time using the implicit Euler scheme, which keeps the entropy structure. Since we are working in the entropy-variable formulation, we need to regularize the equations in order to be able to apply the Lax-Milgram lemma for the linearised problem. The existence of solutions to the nonlinear problem then follows from the Leray-Schauder theorem, where the uniform estimate is a consequence of the entropy inequality (2.5). This estimate also provides bounds uniform in the approximation parameters. A discrete Aubin lemma in the version of [DJ12] provides compactness, which allows us to perform the limit of vanishing approximation parameters.

Although the proof is similar to the existence proofs in [HJ11, Jün15], the results presented here are not directly applicable since our situation is more general than in [HJ11, Jün15]. The main novelties of our existence analysis are the new entropy (2.3) and the treatment of destabilizing cross diffusion ($\delta < 0$).

For the analysis of the large-time asymptotics, we introduce the constant steady state $u^* = (u_1^*, u_2^*)$, where

$$u_1^* = \overline{u}_1^0, \quad u_2^* = \frac{f(u_1^*)}{\alpha}, \qquad \text{with } \overline{u}_j^0 := \frac{1}{\mathrm{m}(\Omega)} \int_\Omega u_j^0(x) \, \mathrm{d}x, \ j \in \{1,2\},$$

and $\mathrm{m}(\Omega)$ denotes the Lebesgue measure of Ω. Furthermore, we define the relative entropy

$$H(u|u^*) = \int_\Omega h(u|u^*) \, \mathrm{d}x$$

with the entropy density

$$h(u|u^*) = h_0(u_1|u_1^*) + \frac{1}{2\delta_0}(u_2 - u_2^*)^2, \tag{2.6}$$

$$\text{where} \quad h_0(u_1|u_1^*) = h_0(u_1) - h_0(u_1^*).$$

Note that u_1 conserves mass, i.e. $\overline{u}_1(t) := \mathrm{m}(\Omega)^{-1} \int_\Omega u_1(t) \, \mathrm{d}x$ is constant in time and $\overline{u}_1(t) = u_1^*$ for all $t > 0$. Thus, by Jensen's inequality, $h_0(u_1|u_1^*) \geq 0$.

Theorem 2 (Exponential decay). *Let assumptions (H1)-(H3) hold, let Ω be convex, let f be Lipschitz continuous with constant $c_L > 0$, and let*

$$\delta_0 \varepsilon_1(\delta) > \frac{\gamma}{\alpha} c_L^2 c_S, \tag{2.7}$$

where $\varepsilon_1(\delta) > 0$ and $c_S > 0$ are defined in Lemmas 4 and 5, respectively. Then, for $t > 0$,

$$H(u(t)|u^*) \leq e^{-\chi(\delta)t} H(u^0|u^*), \tag{2.8}$$

$$\text{where} \quad \chi(\delta) := \min\left\{ \frac{\varepsilon_1(\delta)}{c_S} - \frac{\gamma c_L^2}{\alpha \delta_0}, \alpha \right\} > 0.$$

Moreover, it holds for $t > 0$,

$$\|u_1(t) - u_1^*\|_{L^2(\Omega)} + \|u_2(t) - u_2^*\|_{L^2(\Omega)} \leq 2\sqrt{\max\{\gamma, \delta\} H(u^0|u^*)} e^{-\chi(\delta)t/2}. \tag{2.9}$$

Recall that $\delta_0 = \kappa/\gamma$ if $\delta < 0$ and $\delta_0 = \delta$ if $\delta > 0$. The values for $\delta_0 \varepsilon_1(\delta)$ are illustrated in Figure 2. It turns out that (2.7) is fulfilled if either the additional diffusion $\delta > 0$ is sufficiently large or if γ/α is sufficiently small. The latter condition means that the influence of the drift term $g(u_1)\nabla u_2$ is "small" or that the relaxation $-\alpha u_2$ is "strong". The theorem states that in all these cases, the diffusion is sufficiently strong to lead to exponential decay to equilibrium. For all parameters fixed, except δ, we conclude from the condition (2.7) that there exists a δ_e such that exponential decay holds for $\delta > \delta_e$ ($\delta \neq 0$) and we see that

$$\lim_{\alpha \to +\infty} \delta_e = \delta^* = -\kappa/\gamma$$

as a singular limit already discussed above. We remark that the exclusion of the decay for $\delta = 0$ seems to be purely technical and we conjecture that exponential decay also holds for $\delta = 0$. On the contrary, extensions to $\alpha \to 0$ are highly nontrivial and we can currently not cover this degenerate limiting case using entropy methods.
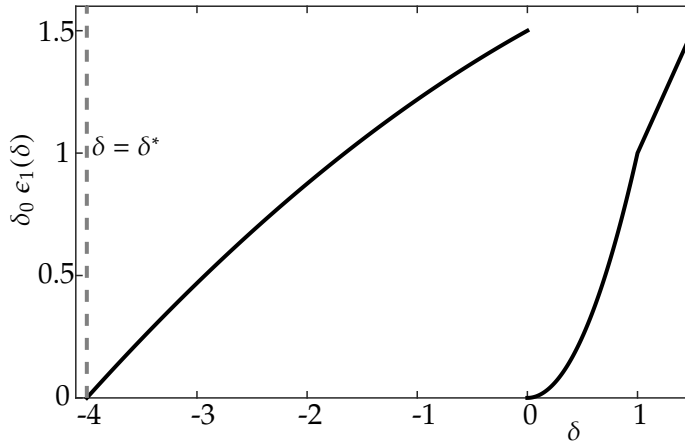
Figure 2: Illustration of $\delta_0 \varepsilon_1(\delta)$ for $\kappa = 1$ and $\delta = \frac{1}{4}$ (black curves). The corresponding singular limit $\delta^* = -\kappa/\gamma = -4$ is also marked (grey dashed vertical line).

Theorem 2 is proved by differentiating the relative entropy $H(u|u^*)$ with respect to time, similar as in (2.4). We wish to estimate the gradient terms from below by a multiple of $H(u|u^*)$. The convex Sobolev

inequality from Lemma 5 shows that the L^2-norm of $g(u_1)^{1/2}\nabla u_1$ is estimated from below by $\int_\Omega h_0(u_1|u_1^*)\,\mathrm{d}x$, up to a factor. The L^2-norm of ∇u_2 is estimated from below by a multiple of $\int_\Omega (u_2 - \overline{u}_2)^2\,\mathrm{d}x$, using the Poincaré inequality. However, the variable u_2 generally does not conserve mass and in particular, $\overline{u}_2 \neq u_2^*$. We exploit instead the relaxation term in (1.2) to achieve the estimate

$$H(u(t)|u^*) + \chi(\delta) \int_0^t H(u(s)|u^*)\,\mathrm{d}s \leq 0.$$

Then Gronwall's lemma gives the result. The difficulty is the estimate of the source term $f(u_1)$. This problem is overcome by controlling the expression involving $f(u_1)$ by taking into account the contribution coming from the convex Sobolev inequality. However, we need that δ is sufficiently large, i.e., cross diffusion has to dominate reaction.

The above arguments hold on a formal level only. A second difficulty is to make these arguments rigorous since we need the test function $h_0'(u_1) - h_0'(u_1^*)$, which is undefined if $u_1 = 0$ or $u_1 = 1$ (since $h_0'(0) = -\infty$ and $h_0'(1) = +\infty$ by Hypothesis (H3)). The idea is to perform a transformation of variables in terms of so-called entropy variables which ensure that $0 < u_1 < 1$ in a time-discrete setting. Passing from the semi-discrete to the continuous case, the variable u_1 may satisfy $0 \leq u_1 \leq 1$ in the limit.

2.1.2 *Analytical Bifurcation Analysis*

As outlined in the introduction, the first natural conjecture for the failure of the entropy method is to study bifurcations of the homogeneous steady states $u^* = (u_1^*, u_2^*)$, which solve

$$\begin{aligned}
0 &= \mathrm{div}(\nabla u_1 - g(u_1)\nabla u_2), \\
0 &= \mathrm{div}(\delta\nabla u_1 + \kappa\nabla u_2) + f(u_1) - \alpha u_2,
\end{aligned} \tag{2.10}$$

with the no-flux boundary conditions (1.3). To study the bifurcations of u^* under variation of δ we use the right-hand side of (2.10) to define a bifurcation function and apply the theory of Crandall-Rabinowitz [CR71, Kie04]. The problem is that u^* is not an *isolated* bifurcation branch as a function of δ since fixing any initial mass yields a different one-dimensional family of homogeneous steady states with

$$u_1^* = \frac{1}{\mathrm{m}(\Omega)} \int_\Omega u_1(x)\,\mathrm{d}x \geq 0. \tag{2.11}$$

Hence, the standard approach has to be modified and we follow arguments that can be found in [CKWW12, SW09, WX13]. It is helpful to introduce some notations first. For $p > d$, let

$$\begin{aligned}
\mathcal{X} &:= \{u \in W^{2,p}(\Omega) : \nabla u \cdot \nu = 0 \text{ on } \partial\Omega\}, \\
\mathcal{Y} &:= L^p(\Omega), \\
\mathcal{Y}_0 &:= \left\{u_1 \in L^p(\Omega) : \int_\Omega u_1(x)\,\mathrm{d}x = 0\right\}
\end{aligned} \tag{2.12}$$

where the space $\mathcal{X}$ includes standard Neumann boundary conditions. Due to the Sobolev embedding theorem we know that $W^{2,p}(\Omega)$ is continuously embedded in $C^{(1+\theta)}(\overline{\Omega})$ for some $\theta \in (0,1)$. If Neumann boundary conditions hold, then our original boundary conditions (1.3)

hold as well. However, the converse is only true if we can invert the diffusion matrix, i.e., as long as $\delta \neq \delta_d = -\frac{\kappa}{g(u_1)}$. In particular, we shall always assume for the local bifurcation analysis of homogeneous steady states that

$$\delta \neq \delta_{\mathrm{d}} = -\frac{\kappa}{g(u_1^*)}. \tag{2.13}$$

This implies that we may not find all possible bifurcations and the single point when the diffusion matrix vanishes has to be treated separately; we leave this as a goal for future work.

Next, we define the mapping $\mathcal{F} : \mathcal{X} \times \mathcal{X} \times \mathbb{R} \longrightarrow \mathcal{Y}_0 \times \mathcal{Y} \times \mathbb{R}$ by

$$\mathcal{F}(u_1, u_2, \delta) := \begin{pmatrix} \operatorname{div}(\nabla u_1 - g(u_1)\nabla u_2) \\ \delta\Delta u_1 + \kappa\Delta u_2 - \alpha u_2 + f(u_1) \\ \int_\Omega u_1(x)\,\mathrm{d}x - \mathrm{m}(\Omega)u_1^* \end{pmatrix}. \tag{2.14}$$

The first two terms are the usual bifurcation functions one would naturally define, the third term is used to isolate the bifurcation branch for the mapping $\mathcal{F}$, i.e., to avoid the problem with mass conservation, while the last two terms take into account the boundary conditions. We know that there exists a family of homogeneous steady state solutions

$$\mathcal{F}(u_1^*, u_2^*, \delta) = 0$$

for each $\delta \in \mathbb{R}$. The goal is to find the parameter values δ_{b} such that at $\delta = \delta_{\mathrm{b}}$ a non-trivial (or non-homogeneous) branch of steady states is generated at the bifurcation point; see also Figure 1. We are going to check that $\mathcal{F}$ is C^1-smooth and the Fréchet derivative $\mathrm{D}_u\mathcal{F}$ with respect to u at a point $\tilde{u} = (\tilde{u}_1, \tilde{u}_2)$ is given by

$$
\begin{aligned}
\mathcal{A}_\delta(\tilde{u})\begin{pmatrix} U_1 \\ U_2 \end{pmatrix} :=& \mathrm{D}_u\mathcal{F}(\tilde{u}, \delta)\begin{pmatrix} U_1 \\ U_2 \end{pmatrix} \\
=& \begin{pmatrix} \Delta U_1 - \operatorname{div}[g'(\tilde{u}_1)(\nabla\tilde{u}_2)U_1 + g(\tilde{u}_1)\nabla U_2] \\ \delta\Delta U_1 + \kappa\Delta U_2 - \alpha U_2 + f'(\tilde{u}_1)U_1 \\ \int_\Omega U_1(x)\,\mathrm{d}x \end{pmatrix}
\end{aligned} \tag{2.15}
$$

where $(U_1, U_2)^\top \in \mathcal{X} \times \mathcal{X}$ and $\mathcal{A}_\delta : \mathcal{X} \times \mathcal{X} \to \mathcal{Y}_0 \times \mathcal{Y} \times \mathbb{R}$. We already know from Theorem 2 that for all $\delta > \delta_{\mathrm{e}}$ ($\delta \neq 0$), the homogeneous steady state u^* is globally stable. Clearly this implies local stability as well and this fact can also be checked by studying the spectrum of $\mathcal{A}_\delta(u^*)$. From the structure of the cross-diffusion equations (1.1)-(1.2) one does expect destabilization of the homogeneous state upon decreasing δ.

Theorem 3. *Let $u^* = (u_1^*, u_2^*)$ be a homogeneous steady state, consider the generic parameter case with $-\kappa \neq \delta g(u_1^*)$ and suppose all eigenvalues μ_n of the negative Neumann Laplacian on Ω are simple. Then the following hold:*

(R1) $\mathrm{D}_u\mathcal{F}(\tilde{u}, \delta) : \mathcal{X} \times \mathcal{X} \to \mathcal{Y}_0 \times \mathcal{Y} \times \mathbb{R}$ *is a Fredholm operator with index zero;*

(R2) *there exists a sequence of bifurcation points $\delta = \delta_{\mathrm{b}}^n$ such that* $\dim\left(\mathcal{N}[\mathrm{D}_u\mathcal{F}(u^*, \delta_{\mathrm{b}}^n)]\right) = 1$, *where $\mathcal{N}[\cdot]$ denotes the nullspace;*

(R3) *there exist simple real eigenvalues $\lambda_n(\delta)$ of $\mathcal{A}_\delta(u^*)$, which satisfy $\lambda_n(\delta_b^n) = 0$. Furthermore, $\lambda_n(\delta)$ crosses the imaginary axis at δ_b^n with non-zero speed, i.e., $D_{\delta u}F(u^*, \delta_b^n)e_b^n \notin \mathcal{R}[\mathcal{A}_{\delta_b^n}]$, where $\mathcal{R}[\cdot]$ denotes the range and $\mathrm{span}[e_b^n] = \mathcal{N}[\mathcal{A}_{\delta_b^n}]$.*

The results from (R1)-(R3) hold quite generically (i.e., for $\delta \neq \delta_d$ and for generic domains [Uhl72]) and yield, upon applying a standard result by Crandall-Rabinowitz [CR71, CR73, Kie04], the existence of branches of non-trivial solutions

$$(u_1[s], u_2[s], \delta[s]) \in X \times X \times \mathbb{R}, \qquad (u_1[0], u_2[0], \delta[0]) = (u_1^*, u_2^*, \delta_b^n),$$

where $s \in [-s_0, s_0]$ parametrizes the steady-state branch locally for some small $s_0 > 0$, and $(u_1[s], u_2[s], \delta[s]) \neq (u_1^*, u_2^*, \delta_b^n)$ for $s \in [-s_0, 0) \cup (0, s_0]$. Slightly more precise information about the branch can be obtained using the eigenfunction e_b and we refer to Section 2.3 for the details. The main conclusion of the bifurcation theorem is that we know that the entropy method cannot show the decay to steady state for all parameter regions. However, to track the non-trivial solution branches in parameter space, it is usually not possible to compute the global shape of all bifurcation branches analytically. In this case, numerical bifurcation analysis is extremely helpful.

2.1.3 *Numerical Bifurcation Analysis*

The results from Section 2.1.1-2.1.2 do not provide a full exploration of the dynamical structure of the solutions for the parameter regime $\delta < \delta^*$. To understand this regime better we study the bifurcations of (2.10) numerically for

$$f(s) = s(1-s), \qquad g(s) = s(1-s), \qquad s \in \Omega = [0, l] \subset \mathbb{R}. \quad (2.16)$$

for some interval length $l > 0$. Note that this yields a boundary-value problem (BVP) involving two second-order ordinary differential equations (ODEs)

$$0 = \frac{d}{dx}\left(\frac{du_1}{dx} - g(u_1)\frac{du_2}{dx}\right), \tag{2.17}$$

$$0 = \delta\frac{d^2u_1}{dx^2} + \kappa\frac{d^2u_2}{dx^2} - \alpha u_2 + f(u_1). \tag{2.18}$$

with boundary conditions

$$0 = \frac{du_1}{dx}(0) - g(u_1(0))\frac{du_2}{dx}(0), \quad 0 = \delta\frac{du_1}{dx}(0) + \kappa\frac{du_2}{dx}(0), \tag{2.19}$$

$$0 = \frac{du_1}{dx}(1) - g(u_1(1))\frac{du_2}{dx}(1), \quad 0 = \delta\frac{du_1}{dx}(1) + \kappa\frac{du_2}{dx}(1). \tag{2.20}$$

An excellent available tool to study the problem (2.17)-(2.20) is the software AUTO [DCD+07] for numerical continuation of BVPs; for other possible options and extensions we refer to the discussion in Chapter 5. AUTO is precisely designed to deal with BVPs for ODEs of the form

$$\frac{dz}{dx} = F(z; p), \qquad x \in [0, 1], \quad G(w(0), w(1)) = 0 \tag{2.21}$$

where $F : \mathbb{R}^N \times \mathbb{R}^P \to \mathbb{R}^N$, $G : \mathbb{R}^N \times \mathbb{R}^N \to \mathbb{R}^N$ and $p \in \mathbb{R}^P$ are parameters and $z = z(x) \in \mathbb{R}^N$ is the unknown vector. It is easy to re-write (2.17)-(2.20) as a system in the form (2.21) of four first-order ODEs, i.e., we get

$N = 4$, consider the scaling $\tilde{x} = x/l$ to normalize the interval length to one, then drop the tilde for x again, and let

$$p_1 := \delta, \quad p_2 := \kappa, \quad p_3 := \alpha, \quad p_4 := l,$$

so $P = 4$ with primary bifurcation parameter δ. For more background on AUTO and on numerical continuation we refer to [KOGV07, Kel77, Gov87]. In the setup (2.21) one can numerically continue the family of homogeneous solutions

$$(u^*, \delta) = (u_1^*, u_2^*, \delta)$$

as a function of δ, i.e., to compute $u^* = u^*(\cdot; \delta)$ for δ in some specified parameter interval. Although this calculation yields bifurcation points for some δ values, it is not straightforward to use the formulation (2.17)-(2.18) to switch onto the non-homogeneous solution branches generated at the bifurcation point. The problem is due to the mass conservation since

$$\overline{u}_1 = m(\Omega)^{-1} \int_\Omega u_1 \, dx = u_1^*, \qquad u_2^* = \frac{f(u_1^*)}{\alpha}$$

is a solution for every positive initial mass $\overline{u}_1^0$. In particular, the branch of solutions is not isolated and there exist parametric two-dimensional families of solutions. There are multiple ways to deal with this problem; see also Chapter 5. One possibility is to resolve the degeneracy of the problem via a small parameter $0 < \rho \ll 1$ and consider

$$0 \;=\; \frac{d}{dx}\left(\frac{du_1}{dx} - g(u_1)\frac{du_2}{dx}\right) - \rho(u_1 - \overline{u}_1), \tag{2.22}$$

$$0 \;=\; \delta\frac{d^2 u_1}{dx^2} + \kappa\frac{d^2 u_2}{dx^2} - \alpha u_2 + f(u_1). \tag{2.23}$$

for a fixed positive parameter $\overline{u}_1 > 0$. In particular, upon setting

$$z_1 := u_1, \qquad z_2 := u_2, \qquad z_3 := \frac{du_1}{dx}, \qquad z_4 := \frac{du_2}{dx},$$

as well as

$$p_5 := \overline{u}_1, \qquad p_6 := \rho, \qquad P = 6,$$

we end up with a problem of the form (2.21) by transforming the two second-order ODEs to four first-order ODEs and re-labelling parameters. The vector field for the ODE-BVP we study numerically is then given by

$$F(z; p) = \begin{pmatrix} p_4 z_3 \\ p_4 z_4 \\ \frac{p_4}{\mathcal{D}_g}[-g(z_1)f(z_1) + p_3 g(z_1)z_2 + p_2 g'(z_1)z_3 z_4 + p_2 p_6(z_1 - p_5)] \\ \frac{p_4}{\mathcal{D}_g}[-f(z_1) + p_3 z_2 - p_1 g'(z_1)z_3 z_4 - p_1(z_1 - p_5)p_6] \end{pmatrix} \tag{2.24}$$

where $\mathcal{D}_g := p_2 + p_1 g(z_1)$ and the detailed choices for the free parameters are discussed in Section 2.4. Observe that the system (2.24) becomes singular if $\mathcal{D}_g = 0$, which is precisely the condition $\delta \neq -\kappa/g(u_1)$ already discovered above. Therefore, we would need also for the numerical analysis a re-formulation (or de-singularization) of the problem to deal with this singularity and we postpone this problem to future

work. As mentioned above, the primary bifurcation parameter we are going to be interested in is $\delta = p_1$. The main results of the numerical bifurcation analysis, which are presented in full detail in Section 2.4, are the following:

(B1) As predicted by the analytical results, we find the existence of local bifurcation points on the branch of homogeneous steady states in the parameter region with $\delta < \delta_d$ for the case of sufficiently large α and for $\delta > \delta_d$ for the case of sufficiently small α. At each bifurcation point on the homogeneous branch, a simple eigenvalue crosses the imaginary axis.

(B2) The non-trivial (i.e. non-homogeneous) solution branches consist of solutions of multiple 'interfaces' or 'layers'; branches originating further away from δ_d contain less layers. The branches can acquire sharper layers upon variation of further parameters which is important for information herding.

(B3) At the local bifurcation points, we observe the emergence of two symmetric branches of solutions for the case when the nonlinearities are identical quadratic nonlinearities of the form $s \mapsto s(1-s)$.

(B4) We also construct non-homogeneous solutions for $\rho = 0$ by a homotopy continuation step first continuing onto the non-trivial branches in δ and then decreasing ρ to zero in a second continuation step.

(B5) Furthermore, we also study the shape deformation of non-trivial solutions upon variation of κ and the domain length l. The numerical results show that the main interesting structures of the problem have already been obtained by just varying δ and α.

2.2 ENTROPY METHOD − PROOFS

2.2.1 *Proof of Theorem 9*

First, we prove that the new diffusion matrix $B(w)$, defined in (2.2), is positive semi-definite if δ is not too negative.

Lemma 4. *Assume (H3) and $\delta > -\kappa/\gamma$, $\delta \neq 0$. Then the matrix $B(w)$ is positive semi-definite, and there exists $\varepsilon_1(\delta) > 0$ such that for all $z = (z_1, z_2)^\top \in \mathbb{R}^2$, $w \in \mathbb{R}^2$:*
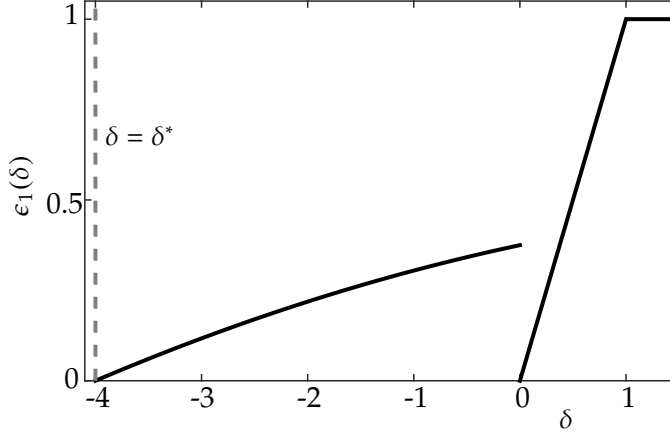
$$z^\top B(w)z \geq \varepsilon_1(\delta)(g(u_1)z_1^2 + z_2^2).$$

It holds $\varepsilon_1(\delta) \to 0$ as $\delta \searrow 0$ and $\delta \searrow -\kappa/\gamma$ (see Figure 3).

For later use, we note that the lemma implies that

$$\nabla w : B(w)\nabla w \geq \varepsilon_1(\delta)\left(\frac{|\nabla u_1|^2}{g(u_1)} + \frac{|\nabla u_2|^2}{\delta_0^2}\right), \tag{2.25}$$

where $w = (w_1, w_2) = (h_0'(u_1), u_2/\delta_0)$ are the entropy variables introduced in the introduction and $A : B = \sum_{i,j} A_{ij}B_{ij}$ for two matrices $A = (A_{ij})$, $B = (B_{ij})$.

Figure 3: Illustration of $\varepsilon_1(\delta)$ for $\kappa = 1$ and $\delta = \frac{1}{4}$ (black curves). The corresponding singular limit $\delta^* = -\kappa/\gamma = -4$ is also marked (grey dashed vertical line).

Proof. Let $z = (z_1, z_2)^\top \in \mathbb{R}^2$. Then

$$z^\top B(w)z = g(u_1)z_1^2 - (\delta_0 - \delta)g(u_1)z_1 z_2 + \delta_0 \kappa z_2^2.$$

If $\delta > 0$, then $\delta_0 = \delta$ and the mixed term vanishes, showing the claim for $\varepsilon_1(\delta) = \min\{1, \delta\kappa\}$. If $-\kappa/\gamma < \delta < 0$, we have $\delta_0 = \kappa/\gamma$. We make the (non-optimal) choice

$$\varepsilon_0 = \varepsilon_0(\delta) = \frac{1}{2}\left[1 - \frac{1}{4}\left(1 - \frac{\gamma\delta}{\kappa}\right)^2\right] > 0.$$

Then $\varepsilon_0 < 1 - (1 - \gamma\delta/\kappa)^2/4$, which is equivalent to $(\kappa - \gamma\delta)^2 < 4(1 - \varepsilon_0)\kappa^2$. Thus, using $g(u_1) \leq \gamma$ (see assumption (H3)),

$$z^\top B(w)z = g(u_1)z_1^2 - \left(\frac{\kappa}{\gamma} - \delta\right)g(u_1)z_1 z_2 + \frac{\kappa^2}{\gamma}z_2^2$$

$$= \varepsilon_0 g(u_1)z_1^2 + (1 - \varepsilon_0)g(u_1)\left(z_1 - \frac{(\kappa - \gamma\delta)z_2}{2\gamma(1 - \varepsilon_0)}\right)^2$$

$$+ \frac{1}{\gamma}\left(\kappa^2 - \frac{(\kappa - \gamma\delta)^2}{4\gamma(1 - \varepsilon_0)}g(u_1)\right)z_2^2$$

$$\geq \varepsilon_0 g(u_1)z_1^2 + \frac{1}{\gamma}\left(\kappa^2 - \frac{(\kappa - \gamma\delta)^2}{4(1 - \varepsilon_0)}\right)z_2^2.$$

In view of the choice of ε_0, the bracket on the right-hand side is positive, and the claim follows after choosing $\varepsilon_1(\delta) = \min\{\varepsilon_0(\delta), [\kappa^2 - (\kappa - \gamma\delta)^2/(4(1 - \varepsilon_0(\delta)))]/\gamma\} > 0$ for $-\kappa/\gamma < \delta < 0$. $\square$

The proof of Theorem 9 is based on the solution of a time-discrete and regularized problem.

Step 1: Solution of an approximate problem. Let $T > 0$, $N \in \mathbb{N}$, $\tau = T/N$, $\varepsilon > 0$, and $n \in \mathbb{N}$ such that $n > d/2$. Then $H^n(\Omega; \mathbb{R}^2) \hookrightarrow L^\infty(\Omega; \mathbb{R}^2)$. Let $w^{k-1} \in L^\infty(\Omega; \mathbb{R}^2)$ be given. If $k = 1$, we define $w^0 = h'(u^0)$. We wish to find $w^k \in H^n(\Omega; \mathbb{R}^2)$ such that

$$\frac{1}{\tau}\int_\Omega (u(w^k) - u(w^{k-1})) \cdot \phi \, dx + \int_\Omega \nabla\phi : B(w^k)\nabla w^k \, dx \quad (2.26)$$

$$+ \varepsilon \int_\Omega \left(\sum_{|\beta|=n} D^\beta w^k \cdot D^\beta \phi + w^k \cdot \phi\right) dx = \int_\Omega F(u(w^k)) \cdot \phi \, dx$$

for all $\phi \in H^n(\Omega; \mathbb{R}^2)$, where $\beta \in \mathbb{N}_0^n$ is a multi-index, D^β is the corresponding partial derivative, $u(w) = (h')^{-1}(w)$ for $w \in \mathbb{R}$, and we recall that $F(u) = (0, f(u_1) - \alpha u_2)^\top$. By definition of h_0, we find that $u_1(w) \in (0, 1)$, thus avoiding any degeneracy at $u_1 = 0$ or $u_1 = 1$.

The existence of a solution to (2.26) will be shown by a fixed-point argument. In order to define the fixed-point operator, let $y \in L^\infty(\Omega; \mathbb{R}^2)$ and $\eta \in [0, 1]$ be given. We solve the linear problem

$$a(w, \phi) = G(\phi) \quad \text{for all } \phi \in H^n(\Omega; \mathbb{R}^2), \tag{2.27}$$

where

$$a(w, \phi) = \int_\Omega \nabla \phi : B(y) \nabla w \, dx + \varepsilon \int_\Omega \left(\sum_{|\beta|=n} D^\beta w \cdot D^\beta \phi + w \cdot \phi \right) dx,$$

$$G(\phi) = -\frac{\eta}{\tau} \int_\Omega (u(y) - u(w^{k-1})) \, dx + \eta \int_\Omega F(u(y)) \cdot \phi \, dx.$$

The forms a and G are bounded on $H^n(\Omega; \mathbb{R}^2)$. Moreover, in view of the positive semi-definiteness of $B(y)$ and the generalized Poincaré inequality (see Chap. II.1.4 in [Tem97]), the bilinear form a is coercive:

$$a(w, w) \geq \varepsilon \int_\Omega \left(\sum_{|\beta|=n} |D^\beta w|^2 + |w|^2 \right) dx \geq \varepsilon c \|w\|_{H^n(\Omega)}$$

for $w \in H^n(\Omega; \mathbb{R}^2)$. By the Lax-Milgram lemma, there exists a unique solution $w \in H^n(\Omega; \mathbb{R}^2) \hookrightarrow L^\infty(\Omega; \mathbb{R}^2)$ to (2.27). This defines the fixed-point operator $S : L^\infty(\Omega; \mathbb{R}^2) \times [0, 1] \to L^\infty(\Omega; \mathbb{R}^2)$, $S(y, \eta) = w$.

By construction, $S(y, 0) = 0$ for all $y \in L^\infty(\Omega; \mathbb{R}^2)$, and standard arguments show that S is continuous and compact, observing that the embedding $H^n(\Omega; \mathbb{R}^2) \hookrightarrow L^\infty(\Omega; \mathbb{R}^2)$ is compact. It remains to prove a uniform bound for all fixed points of $S(\cdot, \eta)$. Let $w \in L^\infty(\Omega; \mathbb{R}^2)$ be such a fixed point. Then w solves (2.27) with y replaced by w. With the test function $\phi = w$, we find that

$$\frac{\eta}{\tau} \int_\Omega (u(w) - u(w^{k-1})) \cdot w \, dx + \int_\Omega \nabla w : B(w) \nabla w \, dx \tag{2.28}$$

$$+ \varepsilon \int_\Omega \left(\sum_{|\beta|=n} |D^\beta w|^2 + |w|^2 \right) dx = \eta \int_\Omega F(u(w)) \cdot w \, dx.$$

Since $h_0'' = 1/g > 0$ on $(0, 1)$, h_0 is convex. Consequently, $h_0(x) - h_0(y) \leq h_0'(x)(x - y)$ for all $x, y \in [0, 1]$. Choosing $x = u(w)$ and $y = u(w^{k-1})$ and using $h_0'(u(w)) = w$, this gives

$$\frac{\eta}{\tau} \int_\Omega (u(w) - u(w^{k-1})) \cdot w \, dx \geq \frac{\eta}{\tau} \int_\Omega (h(u(w)) - h(u(w^{k-1}))) \, dx.$$

Since $u_1 = u_1(w) \in (0, 1)$ and f is continuous, there exists $f_M = \max_{s \in [0,1]} f(s)$ and thus,

$$\int_\Omega F(u(w)) \cdot w \, dx \leq \int_\Omega (f_M - \alpha u_2) u_2 \, dx \leq c_f,$$

where $c_f > 0$ only depends on f_M and α. Hence, (3.20) can be estimated as follows:

$$\eta \int_\Omega h(u(w)) \, dx + \tau \int_\Omega \nabla w : B(w) \nabla w \, dx \tag{2.29}$$

$$+ \varepsilon \tau \int_\Omega \Big(\sum_{|\beta|=n} |D^\beta w|^2 + |w|^2 \Big) \, \mathrm{d}x \le \eta \tau c_f + \eta \int_\Omega h(u(w^{k-1})) \, \mathrm{d}x.$$

This yields an H^n bound for w uniform in η (but not uniform in τ or ε). The Leray-Schauder fixed-point theorem shows the existence of a solution $w \in H^n(\Omega; \mathbb{R}^2)$ to (2.27) with y replaced by w and with $\eta = 1$, which is a solution to (2.26).

Step 2: Uniform bounds. Let w^k be a solution to (2.26). Set $w^{(\tau)}(x,t) = w^k(x)$ and $u^{(\tau)}(x,t) = u(w^k(x))$ for $x \in \Omega$ and $t \in ((k-1)\tau, k\tau]$, $k = 1, \ldots, N$. At time $t = 0$, we set $w^{(\tau)}(\cdot, 0) = h_0'(u^0)$ and $u^{(\tau)}(0) = u^0$. We introduce the shift operator $(\sigma_\tau u^{(\tau)})(t) = u(w^{k-1})$ for $t \in ((k-1)\tau, k\tau]$, $k = 1, \ldots, N$. Then $u^{(\tau)}$ solves

$$\frac{1}{\tau} \int_0^T \int_\Omega (u^{(\tau)} - \sigma_\tau u^{(\tau)}) \cdot \phi \, \mathrm{d}x \, \mathrm{d}t + \int_0^T \int_\Omega \nabla \phi : B(w^{(\tau)}) \nabla w^{(\tau)} \, \mathrm{d}x \, \mathrm{d}t$$

$$+ \varepsilon \int_0^T \int_\Omega \Big(\sum_{|\beta|=n} D^\beta w^{(\tau)} \cdot D^\beta \phi + w^{(\tau)} \cdot \phi \Big) \, \mathrm{d}x \, \mathrm{d}t$$

$$= \int_0^T \int_\Omega F(u^{(\tau)}) \cdot \phi \, \mathrm{d}x \, \mathrm{d}t \tag{2.30}$$

for piecewise constant functions $\phi : (0,T) \to H^n(\Omega; \mathbb{R}^2)$. By density, the weak formulation also holds for all $L^2(0, T; H^n(\Omega; \mathbb{R}^2))$.

We have shown in Step 1 that the solution $w = w^k$ satisfies the entropy estimate (2.29). By (2.25), we obtain the gradient estimate

$$\int_\Omega \nabla w^k : B(w^k) \nabla w^k \, \mathrm{d}x \ge \varepsilon_1(\delta) \min\{\gamma^{-1}, \delta_0^{-2}\} \int_\Omega (|\nabla u_1^k|^2 + |\nabla u_2^k|^2) \, \mathrm{d}x,$$

since $g(u_1^k) \le \gamma$. Thus, we obtain from (2.29) the following entropy inequality:

$$\int_\Omega h(u^k) \, \mathrm{d}x + c_0 \tau \int_\Omega (|\nabla u_1^k|^2 + |\nabla u_2^k|^2) \, \mathrm{d}x \tag{2.31}$$

$$+ \varepsilon \tau \int_\Omega \Big(\sum_{|\beta|=n} |D^\beta w^k|^2 + |w^k|^2 \Big) \, \mathrm{d}x$$

$$\le c_f \tau + \int_\Omega h(u^{k-1}) \, \mathrm{d}x,$$

where $c_0 = \varepsilon_1(\delta) \min\{\gamma^{-1}, \delta_0^{-2}\}$. Adding these inequalities leads to

$$\int_\Omega h(u^k) \, \mathrm{d}x + c_0 \tau \sum_{j=1}^k \int_\Omega (|\nabla u_1^j|^2 + |\nabla u_2^j|^2) \, \mathrm{d}x$$

$$+ \varepsilon \tau \sum_{j=1}^k \int_\Omega \Big(\sum_{|\beta|=n} |D^\beta w^k|^2 + |w^k|^2 \Big) \, \mathrm{d}x$$

$$\le c_f k \tau + \int_\Omega h(u^0) \, \mathrm{d}x.$$

Since

$$\int_\Omega h(u^k) \, \mathrm{d}x = \int_\Omega \Big(h_0(u_1^k) + \frac{(u_2^k)^2}{2\delta_0} \Big) \, \mathrm{d}x \ge \frac{1}{2\delta_0} \int_\Omega (u_2^k)^2 \, \mathrm{d}x,$$

the above estimate shows the following uniform bounds:

$$\|u_1^{(\tau)}\|_{L^\infty(0,T;L^\infty(\Omega))} + \|u_2^{(\tau)}\|_{L^\infty(0,T;L^2(\Omega))} \le c, \tag{2.32}$$

$$\|u_1^{(\tau)}\|_{L^2(0,T;H^1(\Omega))} + \|u_2^{(\tau)}\|_{L^2(0,T;H^1(\Omega))} \leq c, \tag{2.33}$$

$$\sqrt{\varepsilon}\|w^{(\tau)}\|_{L^2(0,T;H^n(\Omega))} \leq c, \tag{2.34}$$

where $c > 0$ denotes here and in the following a constant which is independent of ε or τ (but possibly depending on T).

In order to derive a uniform estimate for the discrete time derivative, let $\phi \in L^2(0,T;H^n(\Omega))$. Then, setting $Q_T = \Omega \times (0,T)$,

$$\frac{1}{\tau}\left|\int_\tau^T \int_\Omega (u_1^{(\tau)} - \sigma_\tau u_1^{(\tau)})\phi \, dx \, dt\right|$$

$$\leq (\|\nabla u_1^{(\tau)}\|_{L^2(Q_T)} + \|g(u_1^{(\tau)})\|_{L^\infty(Q_T)}\|\nabla u_2^{(\tau)}\|_{L^2(Q_T)})$$

$$\times \|\nabla\phi\|_{L^2(Q_T)} + \varepsilon\|w_1^{(\tau)}\|_{L^2(0,T;H^n(\Omega))}\|\phi\|_{L^2(0,T;H^n(\Omega))}$$

$$\leq c\sqrt{\varepsilon}\|\phi\|_{L^2(0,T;H^n(\Omega))} + c\|\phi\|_{L^2(0,T;H^1(\Omega))},$$

$$\frac{1}{\tau}\left|\int_\tau^T \int_\Omega (u_2^{(\tau)} - \sigma_\tau u_2^{(\tau)})\phi \, dx \, dt\right|$$

$$\leq (\delta\|\nabla u_1^{(\tau)}\|_{L^2(Q_T)} + \kappa\|\nabla u_2^{(\tau)}\|_{L^2(Q_T)})\|\nabla\phi\|_{L^2(Q_T)} \tag{2.35}$$

$$+ \varepsilon\|w_1^{(\tau)}\|_{L^2(0,T;H^n(\Omega))}\|\phi\|_{L^2(0,T;H^n(\Omega))}$$

$$+ (\|f(u_1^{(\tau)})\|_{L^2(Q_T)} + \alpha\|u_2^{(\tau)}\|_{L^2(Q_T)})\|\phi\|_{L^2(Q_T)}$$

$$\leq c\sqrt{\varepsilon}\|\phi\|_{L^2(0,T;H^n(\Omega))} + c\|\phi\|_{L^2(0,T;H^1(\Omega))},$$

which shows that

$$\tau^{-1}\|u^{(\tau)} - \sigma_\tau u^{(\tau)}\|_{L^2(0,T;(H^n(\Omega))')} \leq c. \tag{2.36}$$

Step 3: The limit $(\varepsilon, \tau) \to 0$. The uniform estimates (2.33) and (2.36) allow us to apply the discrete Aubin lemma in the version of [DJ12], showing that, up to a subsequence which is not relabelled, as $(\varepsilon, \tau) \to 0$,

$$u^{(\tau)} \to u \quad \text{strongly in } L^2(0,T;L^2(\Omega)) \text{ and a.e. in } Q_T, \tag{2.37}$$

$$u^{(\tau)} \rightharpoonup u \quad \text{weakly in } L^2(0,T;H^1(\Omega)),$$

$$\tau^{-1}(u^{(\tau)} - \sigma_\tau u^{(\tau)}) \rightharpoonup \partial_t u \quad \text{weakly in } L^2(0,T;(H^n(\Omega))'),$$

$$\varepsilon w^{(\tau)} \to 0 \quad \text{strongly in } L^2(0,T;H^n(\Omega)).$$

Because of the L^∞ bound (2.32) for $(u_1^{(\tau)})$, we have

$$g(u_1^{(\tau)}) \rightharpoonup^* g(u_1), \quad f(u_1^{(\tau)}) \rightharpoonup^* f(u_1) \quad \text{weakly* in } L^\infty(0,T;L^\infty(\Omega))$$

(and even strongly in $L^p(Q_T)$ for any $p < \infty$). Thus, we can pass to the limit $(\varepsilon, \tau) \to 0$ in (2.30) to obtain a solution to

$$\int_0^T \langle\partial_t u_1, \phi\rangle \, dt + \int_0^T \int_\Omega (\nabla u_1 - g(u_1)\nabla u_2)\phi \, dx \, dt = 0,$$

$$\int_0^T \langle\partial_t u_2, \phi\rangle \, dt + \int_0^T \int_\Omega (\delta\nabla u_1 + \kappa\nabla u_2)\phi \, dx \, dt$$

$$= \int_0^T \int_\Omega (f(u_1) - \alpha u_2)\phi \, dx \, dt$$

for all $\phi \in L^2(0,T;H^n(\Omega))$. In fact, performing the limit $\varepsilon \to 0$ and then $\tau \to 0$, we see from (2.35) that $\partial_t u \in L^2(0,T;(H^1(\Omega))')$ and hence, the weak formulation also holds for all $\phi \in L^2(0,T;H^1(\Omega))$. It contains the no-flux boundary conditions (1.3). Moreover, the initial conditions are satisfied in the sense of $(H^1(\Omega;\mathbb{R}^2))'$; see Step 3 of the proof of Theorem 2 in [Jün15]. This finishes the proof.

2.2.2 *Proof of Theorem 2*

We recall first the following convex Sobolev inequality which is used to estimate the gradient terms in the entropy inequality.

Lemma 5. *Let $\Omega \subset \mathbb{R}^d$ ($d \geq 1$) be a convex domain and let $\phi \in C^4$ be a convex function such that $1/\phi''$ is concave. Then there exists $c_S > 0$ such that for all integrable functions u with integrable $\phi(u)$ and $\phi''(u)|\nabla u|^2$,*

$$\frac{1}{m(\Omega)} \int_\Omega \phi(u) \, dx - \phi\Big(\frac{1}{m(\Omega)} \int_\Omega u \, dx\Big) \leq \frac{c_S}{m(\Omega)} \int_\Omega \phi''(u)|\nabla u|^2 \, dx,$$

where $m(\Omega)$ denotes the measure of Ω.

Proof. The lemma is a consequence of Prop. 7.6.1 in [BGL14] after choosing the probability measure $d\mu = dx/m(\Omega)$ on Ω and the differential operator $L = \Delta - x \cdot \nabla$, which satisfies the curvature condition $CD(1, \infty)$ since $\Gamma_2(u) = \frac{1}{2}(|\nabla^2 u|^2 + |\nabla u|^2) \geq \frac{1}{2}|\nabla u|^2 = \Gamma(u)$. Another proof can be found in [AMTU01, Section 3.4]. □

Step 1: Uniform bound for the L^1 norm of u_1^k. The L^1 norm of u_1^k is not conserved but we are able to control its L^1 norm. For this, let $w^k \in H^n(\Omega; \mathbb{R}^2)$ be a solution to (2.26) and set $u_1^k = u_1(w^k)$. We introduce the notation $\overline{v} = m(\Omega)^{-1} \int_\Omega v(x) \, dx$ for any integrable function v. This implies that $u_1^* = \overline{u}_1^0$. Employing the test function $\phi = (1, 0)$ in (2.26), we find that $\overline{u}_1^k = \overline{u}_1^{k-1} - \varepsilon\tau\overline{w}_1^k$. Solving the recursion gives

$$\overline{u}_1^k = \overline{u}_1^0 - \varepsilon\tau \sum_{j=1}^k \overline{w}_1^j = u_1^* - \varepsilon\tau \sum_{j=1}^k \overline{w}_1^j,$$

and by (2.34), we conclude that

$$|\overline{u}_1^{(\tau)}(t) - u_1^*| \leq \varepsilon\|w_1^{(\tau)}\|_{L^1(0,t;L^1(\Omega))} \leq \sqrt{\varepsilon}c,$$

where $\overline{u}_1^{(\tau)}(t) = \overline{u}_1^k$ for $t \in ((k-1)\tau, k\tau]$. Consequently, as $(\varepsilon, \tau) \to 0$, the convergence (2.37) shows that $\overline{u}_1(t) = u_1^*$ for $t > 0$.

Step 2: Estimate of the relative entropy. We employ the test function

$$\phi = (h_0'(u_1^k) - h_0'(u_1^*), (u_2^k - u_2^*)/\delta_0) = (w_1^k - h_0'(u_1^*), w_2^k - u_2^*/\delta_0)$$

in (2.26) to obtain

$$0 = \frac{1}{\tau} \int_\Omega \Big((u_1^k - u_1^{k-1})(h_0'(u_1^k) - h_0'(u_1^*)) + \frac{1}{\delta_0}(u_2^k - u_2^{k-1})(u_2^k - u_2^*)\Big) \, dx$$
$$+ \int_\Omega \nabla w^k : B(w^k)\nabla w^k \, dx + \varepsilon \int_\Omega \Big(\sum_{|\beta|=n} |D^\beta w^k|^2 + w_1^k(w_1^k - h_0'(u_1^*))$$

$$\text{(2.38)}$$

$$+ w_2^k(w_2^k - u_2^*)/\delta_0\Big) \, dx - \frac{1}{\delta_0} \int_\Omega (f(u_1^k) - \alpha u_2^k)(u_2^k - u_2^*) \, dx$$
$$=: I_1 + \cdots + I_4.$$

For the first integral, we employ the convexity of h_0:

$$(u_1^k - u_1^{k-1})(h_0'(u_1^k) - h_0'(u_1^*)) \geq (h_0(u_1^k) - h_0(u_1^{k-1})) - h_0'(u_1^*)(u_1^k - u_1^{k-1}),$$
$$(u_2^k - u_2^{k-1})(u_2^k - u_2^*) \geq \frac{1}{2}((u_2^k - u_2^*)^2 - (u_2^{k-1} - u_2^*)^2),$$

which yields

$$I_1 \geq \frac{1}{\tau} \int_\Omega (h_0(u_1^k) - h_0(u_1^{k-1}))\,\mathrm{d}x - \frac{h_0'(u_1^*)}{\tau} \int_\Omega (u_1^k - u_1^{k-1})\,\mathrm{d}x$$
$$+ \frac{1}{2\delta_0\tau} \int_\Omega ((u_2^k - u_2^*)^2 - (u_2^{k-1} - u_2^*)^2)\,\mathrm{d}x.$$

By (2.25), it follows that

$$I_2 \geq \varepsilon_1(\delta) \int_\Omega \left(\frac{|\nabla u_1^k|^2}{g(u_1^k)} + \frac{|\nabla u_2^k|^2}{\delta_0^2} \right)\,\mathrm{d}x$$
$$= \varepsilon_1(\delta) \int_\Omega \left(h_0''(u_1^k)|\nabla u_1^k|^2 + \frac{|\nabla u_2^k|^2}{\delta_0^2} \right)\,\mathrm{d}x.$$

Lemma 5 then shows that

$$I_2 \geq \frac{\varepsilon_1(\delta)}{c_S} \int_\Omega (h_0(u_1^k) - h_0(\overline{u}_1^k))\,\mathrm{d}x + \frac{\varepsilon_1(\delta)}{\delta_0^2} \int_\Omega |\nabla u_2^k|^2\,\mathrm{d}x.$$

The third integral in (2.38) is estimated by using Young's inequality:

$$I_3 \geq \frac{\varepsilon}{2} \int_\Omega ((w_1^k)^2 + (w_2^k)^2 - h_0'(u_1^*)^2 - \delta_0^{-2}(u_2^*)^2)\,\mathrm{d}x$$
$$\geq -\frac{\varepsilon}{2} \int_\Omega (h_0'(u_1^*)^2 + \delta_0^{-2}(u_2^*)^2)\,\mathrm{d}x.$$

Summarizing these estimates, we infer from (2.38) that

$$\int_\Omega (h_0(u_1^k) - h_0(u_1^{k-1}))\,\mathrm{d}x - h_0'(u_1^*) \int_\Omega (u_1^k - u_1^{k-1})\,\mathrm{d}x$$
$$+ \frac{1}{2\delta_0} \int_\Omega ((u_2^k - u_2^*)^2 - (u_2^{k-1} - u_2^*)^2)\,\mathrm{d}x$$
$$+ \frac{\varepsilon_1(\delta)\tau}{c_S} \int_\Omega (h_0(u_1^k) - h_0(\overline{u}_1^k))\,\mathrm{d}x + \frac{\varepsilon_1(\delta)\tau}{\delta_0^2} \int_\Omega |\nabla u_2^k|^2\,\mathrm{d}x$$
$$\leq \frac{\varepsilon\tau}{2} \int_\Omega (h_0'(\overline{u}_1^k)^2 + \delta_0^{-2}(u_2^*)^2)\,\mathrm{d}x$$
$$+ \frac{\tau}{\delta_0} \int_\Omega (f(u_1^k) - \alpha u_2^k)(u_2^k - u_2^*)\,\mathrm{d}x.$$

Adding these equations over k and using the notation as in the proof of Theorem 9 for $u_i^{(\tau)}$, we obtain

$$\int_\Omega (h_0(u_1^{(\tau)}(t)) - h_0(u_1^0))\,\mathrm{d}x - h_0'(u_1^*) \int_\Omega (u_1^{(\tau)}(t) - u_1^0)\,\mathrm{d}x$$
$$+ \frac{1}{2\delta_0} \int_\Omega ((u_2^{(\tau)}(t) - u_2^*)^2 - (u_2^0 - u_2^*)^2)\,\mathrm{d}x \qquad (2.39)$$
$$+ \frac{\varepsilon_1(\delta)}{c_S} \int_0^t \int_\Omega (h_0(u_1^{(\tau)}) - h_0(\overline{u}_1^{(\tau)}))\,\mathrm{d}x\,\mathrm{d}s$$
$$+ \frac{\varepsilon_1(\delta)}{\delta_0^2} \int_0^t \int_\Omega |\nabla u_2^{(\tau)}|^2\,\mathrm{d}x\,\mathrm{d}s$$
$$\leq \frac{\varepsilon}{2} \int_0^t \int_\Omega (h_0'(\overline{u}_1^{(\tau)})^2 + \delta_0^{-2}(u_2^*)^2)\,\mathrm{d}x\,\mathrm{d}s$$
$$+ \frac{1}{\delta_0} \int_0^t \int_\Omega (f(u_1^{(\tau)}) - \alpha u_2^{(\tau)})(u_2^{(\tau)} - u_2^*)\,\mathrm{d}x\,\mathrm{d}s.$$

Step 3: The limit $(\varepsilon, \tau) \to 0$. Because of the L^∞ bound for $(u_1^{(\tau)})$, it follows that, for a subsequence, $u_1^{(\tau)} \rightharpoonup^* u_1$ weakly* in $L^\infty(0, T; L^1(\Omega))$ and thus, as $(\varepsilon, \tau) \to 0$,

$$\int_\Omega (u_1^{(\tau)}(t) - u_1^0) \, dx = \int_\Omega (u_1^{(\tau)}(t) - u_1^*) \, dx \to \int_\Omega (u_1(t) - u_1^*) \, dx = 0,$$

since $\overline{u}_1(t) = u_1^*$ for $t > 0$, by Step 1. The weak convergence of $(\nabla u_2^{(\tau)})$ to ∇u_2 in $L^2(0, T; L^2(\Omega))$ implies that

$$\liminf_{\tau \to 0} \int_0^t \int_\Omega |\nabla u_2^{(\tau)}|^2 \, dx \, ds \leq \int_0^t \int_\Omega |\nabla u_2|^2 \, dx \, ds.$$

Furthermore, by the strong convergence $u_1^{(\tau)} \to u_1$ in $L^2(0, T; L^2(\Omega))$, up to a subsequence, $u_1^{(\tau)} \to u_1$ a.e. in $Q_T = \Omega \times (0, T)$ and $h_0(u_1^{(\tau)}) \to h_0(u_1)$ a.e. in Q_T. Then the L^∞ bound of $(u_1^{(\tau)})$ implies that $h_0(u_1^{(\tau)}) \to h_0(u_1)$ strongly in $L^p(0, T; L^p(\Omega))$ for any $p < \infty$. Furthermore, we know that $u_2^{(\tau)} \to u_2$ strongly in $L^2(0, T; L^2(\Omega))$, see (2.37). Therefore, the limit $(\varepsilon, \tau) \to 0$ in (2.39) leads to

$$\int_\Omega (h_0(u_1(t)) - h_0(u_1^0)) \, dx + \frac{1}{2\delta_0} \int_\Omega ((u_2(t) - u_2^*)^2 - (u_2^0 - u_2^*)^2) \, dx$$

$$+ \frac{\varepsilon_1(\delta)}{c_S} \int_0^t \int_\Omega (h_0(u_1) - h_0(u_1^*)) \, dx \, ds + \frac{\varepsilon_1(\delta)}{\delta_0^2} \int_0^t \int_\Omega |\nabla u_2|^2 \, dx \, ds$$

$$\leq \frac{1}{\delta_0} \int_0^t \int_\Omega (f(u_1) - \alpha u_2)(u_2 - u_2^*) \, dx \, ds.$$

Now, we estimate the right-hand side. Because of $f(u_1^*) = \alpha u_2^*$ and the Lipschitz continuity of f with Lipschitz constant $c_L > 0$, we infer that (recall (2.6) for the definition of $h_0(u_1|u_1^*)$)

$$\int_\Omega (h_0(u_1(t)|u_1^*) \, dx - h_0(u_1(0)|u_1^*)) \, dx$$

$$+ \frac{1}{2\delta_0} \int_\Omega ((u_2(t) - u_2^*)^2 - (u_2(0) - u_2^*)^2) \, dx$$

$$+ \frac{\varepsilon_1(\delta)}{c_S} \int_0^t \int_\Omega h_0(u_1(s)|u_1^*) \, dx \, ds$$

$$\leq \frac{1}{\delta_0} \int_0^t \int_\Omega (f(u_1) - f(u_1^*))(u_2 - u_2^*) \, dx \, ds$$

$$- \frac{\alpha}{\delta_0} \int_0^t \int_\Omega (u_2 - u_2^*)^2 \, dx \, ds$$

$$\leq \frac{1}{2\delta_0 \alpha} \int_0^t \int_\Omega (f(u_1) - f(u_1^*))^2 \, dx \, ds$$

$$- \frac{\alpha}{2\delta_0} \int_0^t \int_\Omega (u_2 - u_2^*)^2 \, dx \, ds$$

$$\leq \frac{c_L^2}{2\alpha\delta_0} \int_0^t \int_\Omega (u_1 - u_1^*)^2 \, dx \, ds$$

$$- \frac{\alpha}{2\delta_0} \int_0^t \int_\Omega (u_2 - u_2^*)^2 \, dx \, ds.$$

Since $\overline{u}_1 = u_1^*$, a Taylor expansion and the assumption $1/h_0''(u_1) = g(u_1) \leq \gamma$ give

$$\int_0^t \int_\Omega h_0(u_1|u_1^*) \, dx \, ds = \int_0^t \int_\Omega (h_0(u_1) - h_0(u_1^*) \, dx \, ds$$

$$= \int_0^t \int_\Omega \left(h_0'(u_1^*)(u_1 - u_1^*) + \frac{1}{2} h_0''(\xi)(u_1 - u_1^*)^2 \right) \mathrm{d}x \, \mathrm{d}s \qquad (2.40)$$

$$\geq \frac{1}{2\gamma} \int_0^t \int_\Omega (u_1 - u_1^*)^2 \, \mathrm{d}x \, \mathrm{d}s,$$

where ξ is a number between u_1 and u_1^*. We conclude that

$$\int_\Omega h_0(u_1(t)|u_1^*) \, \mathrm{d}x + \frac{1}{2\delta_0} \int_\Omega (u_2(t) - u_2^*)^2 \, \mathrm{d}x$$

$$+ \left(\frac{\varepsilon_1(\delta)}{c_S} - \frac{\gamma c_L^2}{\alpha \delta_0} \right) \int_0^t \int_\Omega h_0(u_1(s)|u_1^*) \, \mathrm{d}x \, \mathrm{d}s$$

$$+ \frac{\alpha}{2\delta_0} \int_0^t \int_\Omega (u_2 - u_2^*)^2 \, \mathrm{d}x \, \mathrm{d}s$$

$$\leq \int_\Omega h_0(u_1(0)|u_1^*) \, \mathrm{d}x + \frac{1}{2\delta_0} \int_\Omega (u_2(0) - u_2^*)^2 \, \mathrm{d}x,$$

and recalling the notation $h(u|U) = h_0(u_1|u_1^*) + (u_2 - u_2^*)^2/(2\delta_0)$,

$$\int_\Omega h(u(t)|U) \, \mathrm{d}x + \min \left\{ \frac{\varepsilon_1(\delta)}{c_S} - \frac{\gamma c_L^2}{\alpha \delta_0}, \alpha \right\} \int_0^t h(u|U) \, \mathrm{d}s \leq \int_\Omega h(u(0)|U) \, \mathrm{d}x.$$

Then Gronwall's lemma implies that

$$H(u(t)|U) = \int_\Omega h(u(t)|U) \, \mathrm{d}x \leq e^{-\chi(\delta)t} H(u(0)|U), \quad t \geq 0,$$

where $\chi(\delta)$ is defined in (2.8). Finally, taking into account (2.40), we estimate

$$h(u|U) \geq \frac{1}{2\gamma}(u_1 - u_1^*)^2 + \frac{1}{2\delta}(u_2 - u_2^*)^2,$$

which shows (2.9) and finishes the proof.

2.3 ANALYTICAL BIFURCATION ANALYSIS – PROOFS

In this section, we are going to prove Theorem 3. The proofs follow closely ideas presented for similar systems in [CKWW12, SW09, WX13], which are fundamentally based upon an application of results of Crandall and Rabinowitz [CR71, CR73]; see also [Kie04] for a detailed exposition of the these results. Recall that we defined the spaces $\mathcal{X}, \mathcal{Y}, \mathcal{Y}_0$ in (2.12) and the mapping

$$\mathcal{F} : \mathcal{X} \times \mathcal{X} \times \mathbb{R} \to \mathcal{Y}_0 \times \mathcal{Y} \times \mathbb{R}$$

in (2.14). A first step is to investigate the Fredholm and differentiability properties of $\mathcal{F}$.

Lemma 6. *The mapping $\mathcal{F}$ satisfies the following properties:*

(L1) $\mathcal{F}(u^*, \delta) = 0$ for all $\delta \in \mathbb{R}$.

(L2) $\mathcal{F}(u_1, u_2, \delta) = 0$ implies that (u_1, u_2) solves (2.10).

(L3) $\mathcal{F}$ is C^1-smooth with Fréchet derivative $\mathrm{D}_u \mathcal{F}$ given by (2.15).

(L4) If $\tilde{u}(x) \equiv (\tilde{u}_1, \tilde{u}_2)$ is a homogeneous state and $\delta g(\tilde{u}_1) \neq -\kappa$ then $\mathrm{D}_u \mathcal{F}(\tilde{u}_1, \tilde{u}_2, \delta)$ is a Fredholm operator with index zero.

Proof. For (L1) recall that $u^* = (u_1^*, u_2^*)$ was the notation for a homogeneous steady state. Regarding (L2), observe that the first two components of $\mathcal{F}$ are just the steady state equations (2.10). Statement (L3) follows from a direct calculation. The problem is to show (L4). We follow the argument given in [CKWW12, WX13] and consider

$$D_u \mathcal{F}(\tilde{u}_1, \tilde{u}_2, \delta)(U_1, U_2)^\top = \mathcal{B}_1(U_1, U_2)^\top + \mathcal{B}_2(U_1, U_2)^\top, \quad (2.41)$$

where $\mathcal{B}_1 : X \times X \to \mathcal{Y}_0 \times \mathcal{Y} \times \mathbb{R}$ is defined by

$$\mathcal{B}_1 \begin{pmatrix} U_1 \\ U_2 \end{pmatrix} = \begin{pmatrix} \Delta U_1 - \operatorname{div}[g'(\tilde{u}_1)(\nabla \tilde{u}_2)U_1 + g(\tilde{u}_1)\nabla U_2] \\ \delta \Delta U_1 + \kappa \Delta U_2 - \alpha U_2 + f'(\tilde{u}_1)U_1 \\ 0 \end{pmatrix}, \quad (2.42)$$

and the mapping $\mathcal{B}_2 : X \times X \to \mathcal{Y}_0 \times \mathcal{Y} \times \mathbb{R}$ is given by

$$\mathcal{B}_2 \begin{pmatrix} U_1 \\ U_2 \end{pmatrix} = \begin{pmatrix} 0 \\ 0 \\ \int_\Omega U_1(x) \, dx \end{pmatrix}. \quad (2.43)$$

We observe easily that $\mathcal{B}_2 : X \times X \to \mathcal{Y}_0 \times \mathcal{Y} \times \mathbb{R}$ is linear and compact. We need an ellipticity condition and $\mathcal{B}_1$ should satisfy Agmon's condition [SW09]. We have ellipticity for $\mathcal{B}_1$ (in the sense of Petrovskii [Jan98, SW09]) if

$$\det \left[\begin{pmatrix} 1 & -g(\tilde{u}_1) \\ \delta & \kappa \end{pmatrix} \xi \cdot \xi \right] \neq 0, \quad (2.44)$$

for all $\xi = (\xi_1, \xi_2, \ldots, \xi_d) \in \mathbb{R}^d \backslash \{0\}$. Computing the determinant this condition just yields

$$0 \neq (\xi_1^2 + \cdots + \xi_d^2)(\kappa + \delta g(\tilde{u}_1)) \quad \text{if and only if} \quad -\kappa \neq \delta g(\tilde{u}_1)$$

and ellipticity in the sense of Petrovskii follows. Moreover we need to verify Agmon's condition at a fixed angle $\theta \in [-\pi, \pi)$. Using [SW09, Remark 2.5] with $\theta = \pi/2$, one verifies computing a shifted determinant similar to the previously computed one in (2.44) that Agmon's condition holds for all values of κ. In particular, the ellipticity condition gives a restriction on the parameters for the bifurcation analysis and not Agmon's condition. By applying [SW09, Thm. 3.3] we infer that

$$\mathcal{B}_1 : X \times X \to \mathcal{Y} \times \mathcal{Y} \times \{0\}$$

is a Fredholm operator of index zero. Hence $\mathcal{Y}_0 \times \mathcal{Y} \times \{0\} = \mathcal{R}(\mathcal{B}_1) \oplus W$, where $\mathcal{R}(\mathcal{B}_1)$ is the range of $\mathcal{B}_1$ and W is a closed subspace of $\mathcal{Y} \times \mathcal{Y} \times \mathbb{R}$ with $\dim W = \dim \mathcal{N}(\mathcal{B}_1) < \infty$. Consequently, since the first component of $\mathcal{B}_1$ is in $\mathcal{Y}_0$, we have

$$\mathcal{Y}_0 \times \mathcal{Y} \times \mathbb{R} = \mathcal{R}(\mathcal{B}_1) \oplus W_0 \oplus \operatorname{span}\{(0, 0, 1)^\top\}$$

where $W_0 = \{(H_1, H_2, H_3) \in W | \int_0^L H_1(x)dx = 0\}$ and $W = W_0 + \operatorname{span}\{(1, 0, 0)\}$. Then $\dim W = \dim W_0 + 1$. Thus the codimension of $\mathcal{R}(\mathcal{B}_1)$ in $\mathcal{Y}_0 \times \mathcal{Y} \times \mathbb{R}$ is equal to $\dim W = \dim \mathcal{N}(\mathcal{B}_1)$. Hence, $\mathcal{B}_1 : X \times X \to \mathcal{Y}_0 \times \mathcal{Y} \times \mathbb{R}$ is a Fredholm operator of index zero for $\delta g(\tilde{u}_1) \neq -\kappa$. Therefore, $D_u \mathcal{F}$ is a Fredholm operator of index zero as $\mathcal{B}_2$ is a compact perturbation. Hence, the result (R1) in Theorem 3 follows. $\qquad\square$

It seems difficult to improve the result to include the degenerate cases when $\kappa = -\delta g(u_1^*)$ as this would require to deal with bifurcation problems with non-elliptic operators. The next goal is to apply [SW09, Thm. 4.3]. To do so, we need some additional properties of $\mathcal{F}$. In particular, in order that bifurcations occur from the homogeneous steady state $u^* = (u_1^*, u_2^*)$ we need that the implicit function theorem fails. For the following lemma we need to be in the case where each eigenvalue μ_n of the negative Neumann Laplacian on Ω eigenvalue is simple. For the one-dimensional case this always holds, while for generic d-dimensional domains the eigenvalues are also simple [Uhl72].

Lemma 7. *Suppose the eigenvalues of the negative Neumann Laplacian on $\Omega \subset \mathbb{R}^d$ are simple and $\delta g(u_1^*) \neq -\kappa$. Then there exist bifurcation points at $\delta = \delta_b^n$ such that the map $\mathcal{F}$ satisfies the following properties:*

(L5) the null space $\mathcal{N}[D_u \mathcal{F}(u^*, \delta_b^n)]$ is one-dimensional, i.e., $\mathrm{span}[e_b^n] = \mathcal{N}[D_u \mathcal{F}(u^*, \delta_b^n)]$;

(L6) the non-degenerate crossing condition holds, i.e.,

$$D_{\delta u}\mathcal{F}(u^*, \delta_b^n)e_b^n \notin \mathcal{R}[D_u \mathcal{F}(u^*, \delta_b^n)]. \tag{2.45}$$

Proof. We start by proving (L5). By (2.42), the null space of $D_u \mathcal{F}(u^*, \delta)$ consists of solutions for

$$\Delta U_1 - g(u_1^*)\Delta U_2 = 0,$$
$$\delta \Delta U_1 + \kappa \Delta U_2 - \alpha U_2 + f'(u_1^*)U_1 = 0, \tag{2.46}$$
$$\int_\Omega U_1(x)\,\mathrm{d}x = 0,$$

with no-flux conditions on $\partial\Omega$. For any pair $u = (u_1, u_2) \in X \times X$, we can expand u_1 and u_2 as a series of mutually orthogonal eigenfunctions of the following system

$$\begin{cases} -\Delta u = \mu u & \text{in } \Omega, \\ \frac{\partial u}{\partial \nu} = 0 & \text{on } \partial\Omega, \end{cases} \tag{2.47}$$

multiplied by constants vectors. Let $\mu_n > 0$ be a simple eigenvalue of (2.47) and e_{μ_n} is the eigenfunction corresponding to μ_n normalized by $\int_\Omega (e_{\mu_n})^2 \,\mathrm{d}x = 1$. Then we define

$$\bar{U}_1 := \int_\Omega u_1(x)e_{\mu_n}(x)\,\mathrm{d}x, \qquad \bar{U}_2 := \int_\Omega u_2(x)e_{\mu_n}(x)\,\mathrm{d}x.$$

We obtain

$$\int_\Omega e_{\mu_n}\Delta u_1 \,\mathrm{d}x = -\mu_n \int_\Omega u_1 e_{\mu_n}\,\mathrm{d}x = -\mu_n \bar{U}_1,$$
$$\int_\Omega e_{\mu_n}\Delta u_2 \,\mathrm{d}x = -\mu_n \int_\Omega u_2 e_{\mu_n}\,\mathrm{d}x = -\mu_n \bar{U}_2. \tag{2.48}$$

Now, by multiplying the first two equations of (2.46) by e_{μ_n} and integrating over Ω, using the boundary condition and (2.48), we arrive at the following algebraic system for $\bar{U}_1$ and $\bar{U}_2$:

$$\bar{U}_1 - g(u_1^*)\bar{U}_2 = 0,$$
$$(\kappa\mu_n + \alpha)\bar{U}_2 - (f'(u_1^*) - \delta\mu_n)\bar{U}_1 = 0. \tag{2.49}$$

If $\delta > f'(u_1^*)/\mu_n$ then the system (2.49) has only the zero solution. In this case, we would have $\mathcal{N}[D_u\mathcal{F}(u^*,\delta)] = 0$ for all δ. In order to have existence of a non-homogeneous solution we necessarily require $\delta \leq f'(u_1^*)/\mu_n$. In this case the system (2.49) has a non-zero solution if and only if

$$\delta =: \delta_b^n = -\frac{\kappa}{g(u_1^*)} + \frac{1}{\mu_n}\left[f'(u_1^*) - \frac{\alpha}{g(u_1^*)}\right] = \delta_d + \frac{1}{\mu_n}\left[f'(u_1^*) - \frac{\alpha}{g(u_1^*)}\right].$$
(2.50)

Taking $\delta = \delta_b^n$, we can rewrite the first two equations of (2.46) as the system:

$$\begin{pmatrix} \Delta U_1 \\ \Delta U_2 \end{pmatrix} = \frac{1}{\kappa + \delta_b^n g(u_1^*)} \begin{pmatrix} -g(u_1^*)f'(u_1^*) & g(u_1^*)\alpha \\ -f'(u_1^*) & \alpha \end{pmatrix} \begin{pmatrix} U_1 \\ U_2 \end{pmatrix} =: A \begin{pmatrix} U_1 \\ U_2 \end{pmatrix} \quad (2.51)$$

Using (2.50) and computing the determinant and the trace of the matrix A we find that its eigenvalues are $\lambda_1 = 0$ and $\lambda_2 = -\mu_n$, where $\mu_n > 0$ is a single eigenvalue of the problem (2.47). Let T be the matrix whose columns are the eigenvectors corresponding to λ_1 and λ_2 respectively:

$$T = \begin{pmatrix} \alpha & g(u_1^*) \\ f'(u_1^*) & 1 \end{pmatrix}.$$

We have

$$T^{-1}AT = \begin{pmatrix} 0 & 0 \\ 0 & \mu_n \end{pmatrix}.$$

Then, by considering the transformation

$$\begin{pmatrix} p \\ q \end{pmatrix} = T^{-1}\begin{pmatrix} U_1 \\ U_2 \end{pmatrix},$$
(2.52)

it follows that the first two equations of (2.46) can be uncoupled and we find that

$$\begin{aligned} &\Delta p = 0 && \text{in } \Omega, \\ &\Delta q = \mu_n q && \text{in } \Omega, \\ &\alpha \int_\Omega p(x)\,\mathrm{d}x + g(u_1^*)\int_\Omega q(x)\,\mathrm{d}x = 0, \\ &\nabla p \cdot \nu = \nabla q \cdot \nu = 0 && \text{on } \partial\Omega, \end{aligned}$$
(2.53)

where the genericity condition $-\kappa \neq \delta_b^n g(u_1^*)$ is used to obtain zero Neumann boundary conditions. Recall that μ_n is a simple eigenvalue of (2.47) with eigenfunction e_{μ_n}. Observe that $\int_\Omega e_{\mu_n}(x)\,\mathrm{d}x = 0$, which implies that $p = 0$ and $q = Ce_{\mu_n}$ for some constant C are the solutions of (2.53). Therefore, it follows that

$$(U_1, U_2)^\top = Ce_{\mu_n}(g(u_1^*), 1)^\top.$$
(2.54)

This shows that $\mathcal{N}[D_u\mathcal{F}(u^*,\delta_b^n)] = \mathrm{span}[e_{\mu_n}(g(u_1^*),1)^\top] =: \mathrm{span}[e_b^n]$. In particular, the nullspace is one-dimensional and the result (L5) follows.

To prove (L6), we argue by contradiction and suppose that (2.45) is not satisfied. Hence, by computing $D_{\delta u} \mathcal{F}(u^*, \delta_b^n)$, it follows there exists (p, q) such that

$$
\begin{aligned}
\Delta p - g(u_1^*) \Delta q &= \mu_n g(u_1^*) e_{\mu_n} \quad \text{in } \Omega, \\
\kappa \Delta q + \delta_b^n \Delta p - \alpha q + f'(u_1^*) p &= 0 \quad \text{in } \Omega, \\
\int_\Omega p(x) \, dx &= 0, \\
\nabla p \cdot \nu = \nabla q \cdot \nu &= 0 \quad \text{on } \partial\Omega.
\end{aligned}
\tag{2.55}
$$

As in the first part of the proof, it is helpful to consider a suitable projection and we define P and Q as

$$
P := \int_\Omega p(x) e_b^n(x) \, dx, \qquad Q := \int_\Omega q(x) e_b^n(x) \, dx.
$$

Multiplying the first two equations (2.55) by e_b^n and integrating over Ω and using boundary conditions one obtains an algebraic system for P and Q given by

$$
\left\{
\begin{array}{rcl}
P - g(u_1^*) Q &=& -g(u_1^*), \\
(f'(u_1^*) - \delta_b^n \mu_n) P - (\kappa \mu_n + \alpha) Q &=& 0.
\end{array}
\right.
\tag{2.56}
$$

By the definition of δ_b^n, the determinant of the matrix of coefficients on the left-hand side of the system (2.56) is zero. This implies that the inhomogeneous linear system has no solution. Hence the system (2.55) has no solutions and the result (2.45) in (L6) follows. $\qquad\square$

Note that (L5)-(L6) are just the results (R2)-(R3) claimed in Theorem 3. By applying [SW09, Thm. 4.3] we obtain the existence of a non-trivial branch of solutions. Therefore, the local dynamics of the problem already shows that the entropy method cannot provide exponential decay to a distinguished steady state for all parameter values.

2.4 NUMERICAL BIFURCATION ANALYSIS − CONTINUATION RESULTS

In Section 2.1.1 we proved the existence of a weak solution for $\delta > \delta^* = -\kappa/\delta$ as well as global convergence to a steady state for $\delta > \delta_e$ ($\delta \neq 0$); in addition, δ_e converges to $\delta^* = -\kappa/\gamma$ as $\alpha \to +\infty$ and δ_e converges to $+\infty$ as $\alpha \to 0$. In Section 2.1.2 we showed the existence of non-trivial solutions for $\delta = \delta_b^n$ where δ_b^n is defined in (2.50) and in particular δ_b^n could be bigger or smaller than $\delta_d = \kappa/g(u_1^*)$ depending on α.

The numerical continuation results presented in this section aim to augment and extend these results. To simplify the comparison to numerical results, we focus on the case

$$
\kappa = 1, \qquad g(s) = s(1 - s), \qquad f(s) = s(1 - s),
$$

which yields the condition $\delta > \delta^* = -4$ for the validity of the entropy method for $\alpha \to +\infty$. As already mentioned, the values for δ_b^n depend on α, so we are going to study a case with α sufficiently large (Section 2.4.2) and the case with α sufficiently small (Section 2.4.3). Below we are going to define the meaning of sufficiently large and sufficiently small. First, we want to compare the values that we obtain for δ_b^n with the numerical results. The analytical problem did not include the small parameter ρ and the introduction of this term has the effect of shifting the bifurcation points.

n	1	2	3	4	5	6	7	8
(2.50)	-45.38	-14.45	-8.73	-6.72	-5.80	-5.29	-4.99	-4.79
(2.57)	-121.89	-20.81	-10.50	-7.51	-6.24	-5.58	-5.19	-4.94
AUTO	-121.89	-20.81	-10.50	-7.51	-6.24	-5.58	-5.19	-4.94

Table 1: Comparison between the analytical and numerical bifurcation values. The last two rows compare the numerical and analytical solutions with $0 < \rho \ll 1$.

2.4.1 *Comparison between the values of δ_b^n*

The formula for δ_b^n given in the equation (2.50) does not consider the additional term ρ. Introducing this term, we get a new formula which reads

$$\delta_b^n = \frac{f'(u_1^*)}{\mu} - \frac{(\kappa\mu + \alpha)(\mu + \rho)}{g(u_1^*)\mu^2} = \delta_d + \frac{1}{\mu}\Big[f'(u_1^*) - \frac{\kappa\rho + \alpha}{g(u_1^*)} - \frac{\alpha\rho}{g(u_1^*)\mu}\Big].$$

$$(2.57)$$

We observe that the formulas (2.50) and (2.57), due to the presence of the term ρ, will not give the same values δ_b^n but the two equations correspond if we take $\rho = 0$. We fix the following parameter values

$$(\kappa, \alpha, l, \bar{u}_1, \rho) = (1, 0.2, 20, 0.594, 0.05).$$

We are interested in computing the values of δ_b^n and to observe how the parameter ρ shifts the bifurcation branches.

In Table 1 we reported the bifurcation points δ_b^n for $n \in \{1, 2, \dots, 8\}$ computed with the two formulas (2.50) and (2.57) in comparison to the numerical continuation results using AUTO. The values detected using AUTO precisely correspond to the values computed with the formula (2.57) as expected while the points are shifted in comparison to the values for $\rho = 0$.

2.4.2 *Case 1: α sufficiently large*

Recall the formula for δ_b^n given in (2.50):

$$\delta_b^n = \delta_d + \frac{1}{\mu_n}\Big[f'(u_1^*) - \frac{\alpha}{g(u_1^*)}\Big].$$

We observe that if $\alpha > f'(u_1^*)g(u_1^*)$ then $\delta_b^n < \delta_d$ and the branches will approach the limit value δ_d for $n \to \infty$. Since we are using (2.57), the condition on α is

$$\alpha > \mu_n\Big[\frac{f'(u_1^*)g(u_1^*) - \kappa\rho}{\rho + \mu_n}\Big]$$

and, in the case of an interval we can compute the eigenvalues μ. So, α sufficiently large means

$$\alpha > \Big(\frac{n\pi}{l}\Big)^2\Big[\frac{f'(u_1^*)g(u_1^*) - \kappa\rho}{\rho + (\frac{n\pi}{l})^2}\Big].$$
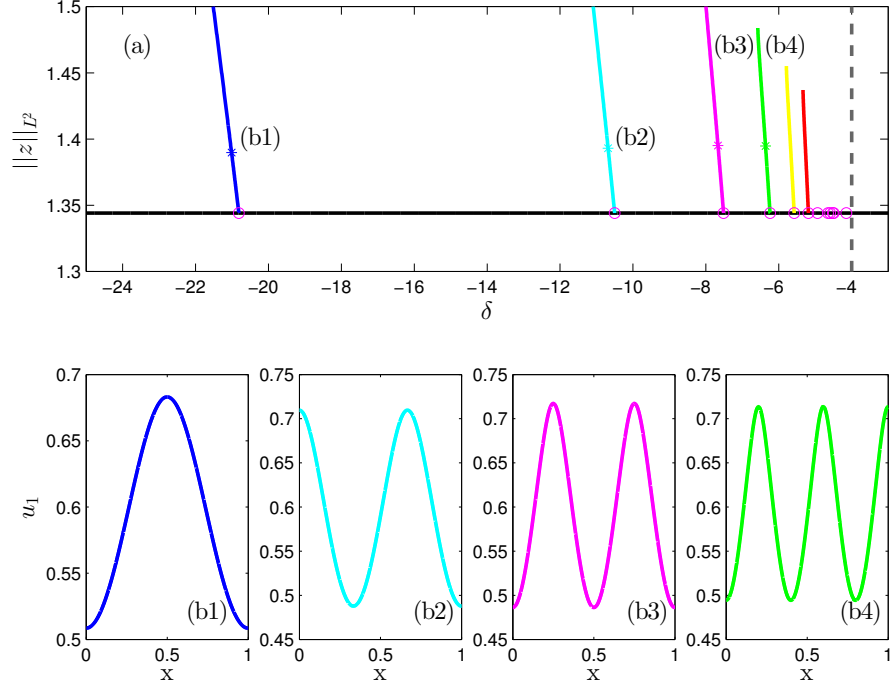
$$(2.58)$$

Figure 4 shows a continuation calculation for fixed parameters

$$(\kappa, \alpha, l, \bar{u}_1, \rho) = (p_2, p_3, p_4, p_5, p_6) = (1, 0.2, 12, 0.594, 0.05)$$

using δ as the primary bifurcation parameter. We observe that the condition on α is satisfied since the right-hand side of (2.58) is negative for all $n \in \mathbb{N}$ and $\alpha = 0.2$. The steady state we start the continuation with is given by

$$(u_1^*, u_2^*) = (\bar{u}_1, f(\bar{u}_1)/\alpha).$$

Figure 4: Continuation calculation for the system (2.21) with parameter values $(\kappa, \alpha, l, \bar{u}_1, \rho) = (p_2, p_3, p_4, p_5, p_6) = (1, 0.2, 20, 0.594, 0.05)$ and primary bifurcation parameter δ. (a) Bifurcation diagram in $(\delta, \|z\|_{L^2})$-space showing the parameter on the horizontal axis and the solution norm on the vertical axis. Some of the detected bifurcation points are marked as circles (magenta). The last branch point (blue circle) is not a true bifurcation point but results from the degeneracy $\delta = -\kappa/g(u_1^*) =: \delta_d$. At the other branches points (magenta, filled circles) non-homogeneous solution branches (blue, cyan, magenta, green...) bifurcate via single eigenvalue crossing. The value $\delta^* = -\kappa/\gamma = -4$ is marked by a vertical grey dashed line. (b) Solutions are plotted for $(x, u_1 = u_1(x))$ at certain points on the non-homogeneous branches; the solutions are marked in (a) using crosses.

We begin the continuation at $\delta = -25$ and we find only one bifurcation point when δ is decreasing, i.e. for $\delta < -25$. This result is expected since $\delta_b^1 = -121.889$ is the value corresponding to the first eigenvalue. Moreover, we do not detect any bifurcations for $\delta > -4 = \delta^*$. The interesting results in the bifurcation calculation in Figure 4 occur when we increase the primary bifurcation parameter δ. In this case, several branch points are detected, in particular the closer we are to the value δ_d, the more bifurcation points are found. In Figure 4, we have shown the first six branch points detected obtained upon increasing δ. The point detected at $\delta = -20.8116$ corresponds to the second non-trivial bifurcation branch. There are more and more points as we get closer to δ_d. The last point detected (in blue) is not a bifurcation point but corresponds to the degeneracy at

$$\kappa/g(u_1^*) = -1/(0.594(1 - 0.594)) \approx -4.1466.$$

The remaining detected branch points in Figure 4 are true bifurcation points. This numerical result is in accordance with the analytical results on the existence of bifurcations in Theorem 3. In fact, one can carry out the same calculation as in Section 2.3. At each bifurcation point, a simple eigenvalue crosses the imaginary axis. One can use the branch switching algorithm implemented in `AUTO` to compute the non-homogeneous families of solutions as shown for four points in Figure 4(a). In Figure 4(b), we show a representative solution $u_1 = u_1(x)$ on each of the four solution families. The solutions are non-homogeneous steady states and have interface-like behaviour in the spatial variable. Each family has a characteristic number of these interfaces. There are families with even more interfaces than the one shown in Figure 4(b4), which can be found upon increasing δ even further; we are not interested in these highly oscillatory solutions here.
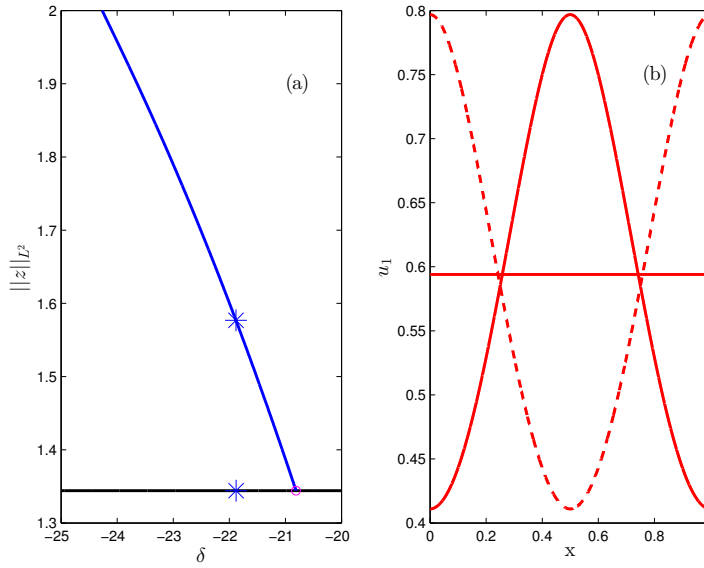
Figure 5: Continuation calculation for the system (2.21) as in Figure 4 with a focus on the second bifurcation point (filled circle, magenta). One can show that by using two different local branching directions that two different non-homogeneous solution branches (red) bifurcate via single eigenvalue crossing but the two branches contain solutions with identical L^2-norm for the same parameter value. This is a result of a symmetry in the problem. (b) Three different solutions plotted in $(x, u_1 = u_1(x))$-space at the parameter value $\delta = -21.8819$. The three solutions are marked in (a) using crosses.

Another observation regarding the continuation run in Figure 4 is reported in more detail in Figure 5 with a focus on the second bifurcation point. It is shown that there are actually two different branches bifurcating at the same point with families of non-homogeneous solutions that are symmetric. In particular, one non-trivial solution branch can be transformed into the other by considering $u \mapsto 1 - u$; as an illustration we refer to three representative numerical solutions on the three branches originating at the second bifurcation point as shown in Figure 5(b).

2.4.3 *Case 2: α sufficiently small*

As specified in (M7) in Chapter 1 when $\alpha < f'(u_1^*)g(u_1^*)$ then $\delta_b^n > \delta_d$ and this means that the branches will approach the limit value δ_d from
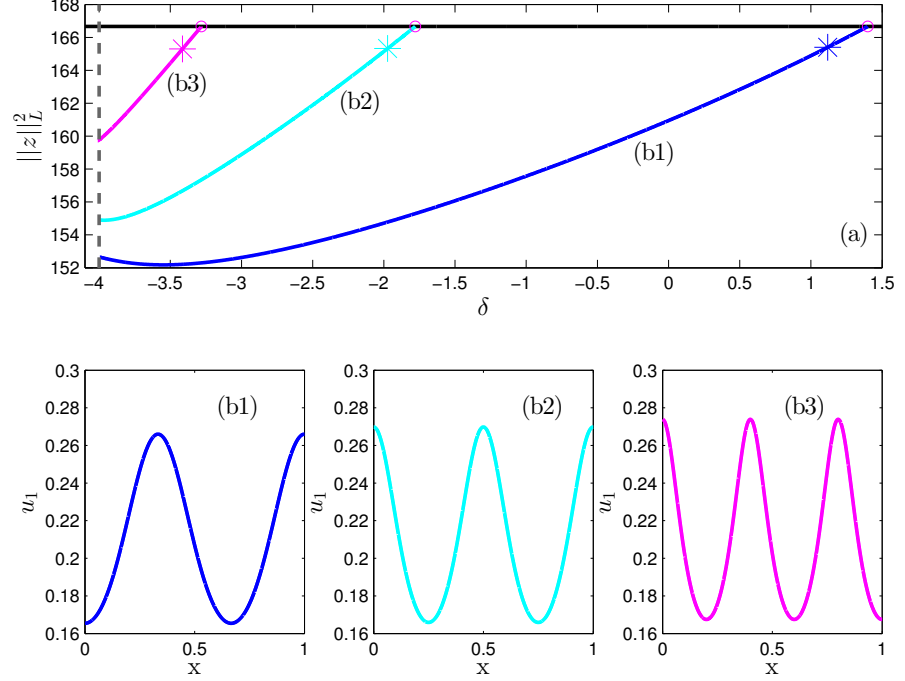
the right. As pointed out in Section 2.4.1, the condition on α is more complicated since our model contains ρ. The condition on α becomes

$$0 < \alpha < \mu_n \left[\frac{f'(u_1^*)g(u_1^*) - \kappa\rho}{\rho + \mu_n} \right],$$

i.e. we must choose an α which satisfied the inequality for each single μ_n. We fix

$$(\kappa, \alpha, l, \bar{u}_1, \rho) = (1, 0.001, 50, 0.211325, 0.05)$$

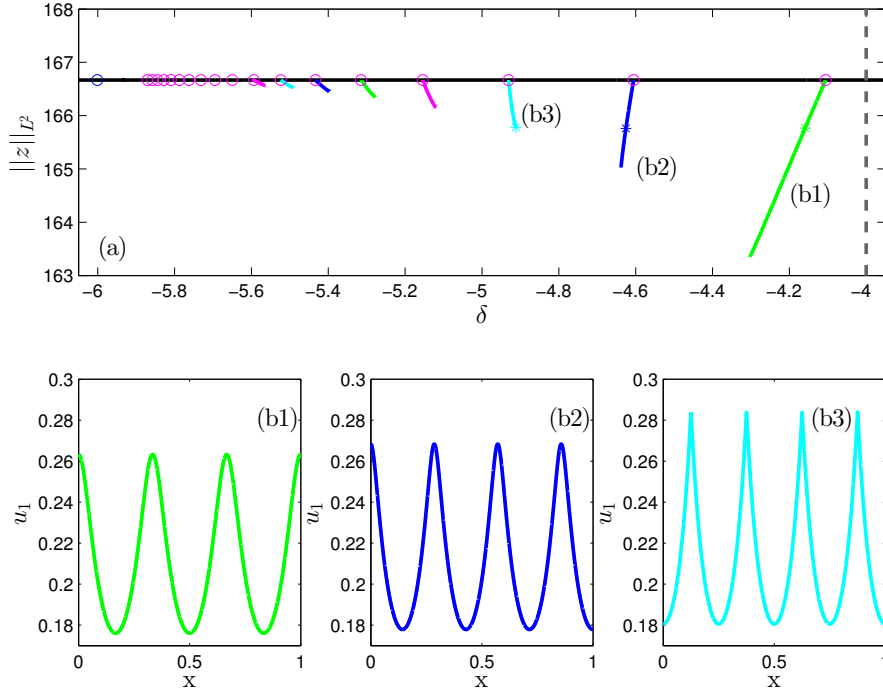for the numerical continuation in this section.

Figure 6: Continuation calculation for the system (2.21) with parameter values $(\kappa, \alpha, l, \bar{u}_1, \rho) = (p_2, p_3, p_4, p_5, p_6) = (1, 0.0001, 50, 0.211325, 0.05)$ and primary bifurcation parameter δ. (a) Bifurcation diagram in $(\delta, \|z\|_{L^2})$-space showing the parameter on the horizontal axis and the solution norm on the vertical axis. The detected bifurcation points are marked as circles (magenta). At the three branch points (magenta, filled circles) non-homogeneous solution branches (blue, cyan, magenta) corresponding to $\delta_b^3, \delta_b^4, \delta_b^5$ bifurcate via single eigenvalue crossing. The value $\delta^* = -\kappa/\gamma = -4$ is marked by a vertical grey dashed line. (b) Solutions are plotted for $(x, u_1 = u_1(x))$ at certain points on the non-homogeneous branches; the solutions are marked in (a) using crosses.

With these values the condition on α is given by $0 < \alpha < 0.0033827$ which is satisfied. We also find that with our choices

$$\delta_d < \delta_b^n < \delta^* < \delta_b^5 < \delta_b^4 < \delta_b^3 < \delta_b^2 < \delta_b^1 < \delta_e, \quad n \geq 6,$$

i.e. there are some bifurcation points which are bigger than δ^* and some which are smaller but all of them are bigger than δ_d. We begin the continuation at $\delta = 3$ and we detect only two more branches when we increase δ at $\delta = 43.4851$ and $\delta = 9.98041$ which correspond to δ_b^1 and δ_b^2. We focus on the branches for $n \in \{1, 2, 3, 4, 5\}$ such that $\delta_b^n > \delta^*$. This case is represented in Figure 6.

Numerically we observe that all the branches stop when they reach the critical value δ^*. Next, we consider $n \geq 6$ such that $\delta_d < \delta_b^n < \delta^*$ as
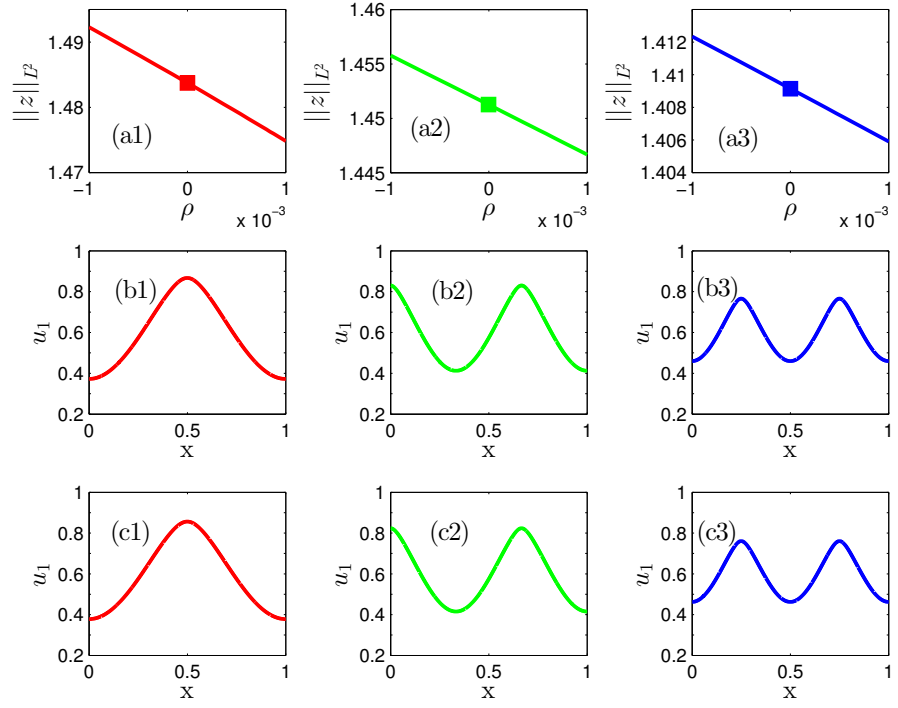
Figure 7: Continuation calculation for the system (2.21) with parameter values $(\kappa, \alpha, l, \bar{u}_1, \rho) = (p_2, p_3, p_4, p_5, p_6) = (1, 0.0001, 50, 0.211325, 0.05)$ and primary bifurcation parameter δ. (a) Bifurcation diagram in $(\delta, \|z\|_{L^2})$-space showing the parameter on the horizontal axis and the solution norm on the vertical axis. Some of the detected bifurcation points are marked as circles (magenta). The last branch point (blue circle) is not a true bifurcation point but results from the degeneracy $\delta = -\kappa/g(u_1^*) =: \delta_d$. At the other branch points (magenta, filled circles) non-homogeneous solution branches (green, blue, cyan) bifurcate via single eigenvalue crossing. The value $\delta^* = -\kappa/\gamma = -4$ is marked by a vertical grey dashed line. (b) Solutions are plotted for $(x, u_1 = u_1(x))$ at certain points on the non-homogeneous branches; the solutions are marked in (a) using crosses.

reported in Figure 7. In this case there are two critical values: $\delta^* = -4$ (dashed line) and $\delta_d = -6$ (blue circle). The branches detected for a δ close to δ^* have the same direction as the branches detected for $\delta > \delta^*$; but starting from a certain n, in this case $n = 8$, we notice that the branches change the direction. Probably this behaviour is due to the fact that the branches cannot cross the value $\delta = \delta_d$. We do no detect any branch for $\delta < \delta_d$.

In the range between δ_d and δ^* the branches do not seem to overlap. Numerically, one observes that the branches get shorter and shorter due to the numerical continuation breaking down as the branches approach δ_d. Looking at the shape of the solutions in the different branches we can observe that they have more and more interfaces as we approach the limiting value δ_d. Moreover, the solutions inside a fixed branch get sharper and sharper peaks along the branch (see for example the cyan branch).

2.4.4 *Continuation in ρ*

The next question is if we can find non-homogeneous steady states also for the original problem with $\rho = 0$. This can be achieved by using a homotopy-continuation idea.
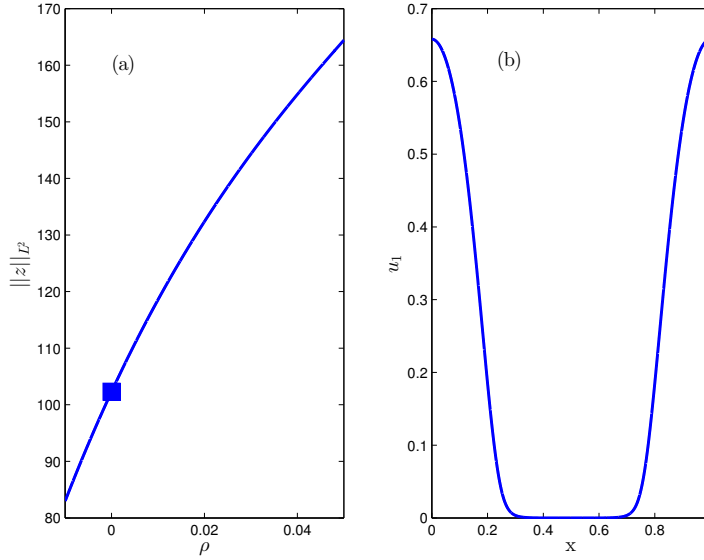
Figure 8: Continuation calculation for the system (2.21) starting with the same basic parameter values as in Figure 4 but with $\rho = 0.001$. We stop the continuation at the solution points for a certain δ (as done in Figure 4(a)) and change from δ as a primary continuation parameter to ρ as a primary parameter with the goal to decrease the parameter to $\rho = 0$. The values for δ are $\delta = -16$ for the red branch, $\delta = -9.4$ for the green branch and $\delta = -7$ for the blue one. (a1)-(a3) Bifurcation diagrams in $(\rho, \|z\|_{L^2})$-space. The starting point for the continuation is at the right boundary where $\rho = 0.001$ and then ρ is decreased. (b1)-(b3) Solutions obtained on the bifurcation branches above at the point $\rho = 0$ (points are marked with squares in (a1)-(a3)). (c1)-(c3) Solutions obtained on the bifurcation branches for the initial system with $\rho = 0.001$. We can observe that also for $\rho = 0$ the solutions have a non-trivial herding-type profile.

First, we continue the problem in δ and compute the non-homogeneous solution branches. Then we pick a steady state on the non-homogeneous branch and switch to continuation in ρ while keeping δ fixed. The results of this strategy are shown in Figure 8 (for $\alpha = 0.2$) and in Figure 9 (for $\alpha = 0.001$). For the first three solutions shown in Figure 4(b), this strategy works if we start from a very small ρ. Figure 8(c) shows the solution in the branch for a $\rho \neq 0$: we notice that the solutions for the case $\rho = 0$ keep the non-constant profile as for $\rho \neq 0$ yielding relevant herding solutions for applications.

In the case with α sufficiently small, the strategy works better and we indeed find non-homogeneous steady states for $\rho = 0$ as shown in Figure 9(b). Moreover we can also obtain herding solutions. We use the starting parameter values

$$(\kappa, \alpha, l, \bar{u}_1, \rho) = (1, 0.001, 50, 0.211325, 0.05).$$

We start from $\delta = 10$ and the first branch we detect is $\delta_b^2 = 9.98041$. Once we are in this branch, we continue in ρ for a fixed δ (in this case $\delta = -9$). For information herding models, solutions which are of particular importance are those with sharp interfaces between the endstates, i.e., the solution is near zero and near one in certain regions

Figure 9: Continuation calculation for the system (2.21) starting with the same parameter value and as in Figure 6. We stop the continuation at $\delta = -9$ (as done in Figure 6(a)) and change from δ as a primary continuation parameter to ρ as a primary parameter with the goal to decrease the parameter to $\rho = 0$. (a) Bifurcation diagram in $(\rho, \|z\|_{L^2})$-space. The starting point for the continuation is at the right boundary where $\rho = 0.05$ and then ρ is decreased. (b) Solution on the second branch δ_b^2 of non-homogeneous steady states at $\rho = 0$ (point is marked with squares in (a)).

with sharp interfaces in between. These solutions represent a herding effect in the sense of sharply split opinions. More precisely, they indicate for which values of the information variable x we observe a herding behaviour, i.e. a concentration of individuals ($u \approx 1$) at certain values of x. Figure 9(b) shows herding in the interval $[0, 0.2] \cup [0.8, 1]$, while only a few individuals adopt the information value in $[0.3, 0.7]$.

### 2.4.5 *Solutions and other parameters*

In this section we focus on the case with α sufficiently small. We are interested in studying, how the solutions change depending on the other parameters κ and l. We fix as starting parameters

$$(\kappa, \alpha, l, \bar{u}_1, \rho) = (1, 0.001, 50, 0.211325, 0.05)$$

and consider the branch δ_b^2. We study the solutions depending on the different parameters. In Figure 10 we show changes along the branch (which bifurcates at $\delta = 9.98041$). We observe that the shape is the same along the branch but the interfaces sharpen as δ is decreased.

In Figure 11 we show how the solution changes with the length of the domain. We consider $l = 20$, $l = 50$ and $l = 100$. The branch δ_b^2 is detected at $\delta = -3.28144, 9.98041, 43.4851$ respectively. Since we consider the same branch, the shape does not change and length of the domain shifts the bifurcation points and just scales the solution.

When we change the parameter κ the bifurcation points are also simply shifted. We consider $\kappa = 1$, $\kappa = 5$ and $\kappa = 10$. The branch δ_b^2 is detected at $\delta = 9.98041, -92.2877, -214.999$ respectively. Moreover, for the first case the branches approach the value δ_d from the right, while in the other two cases from the left. As for the previous case we
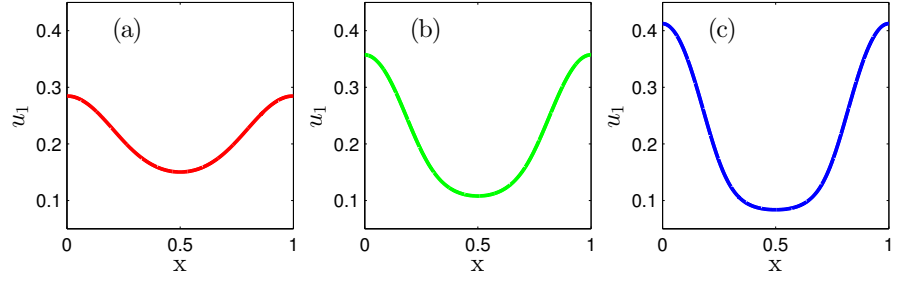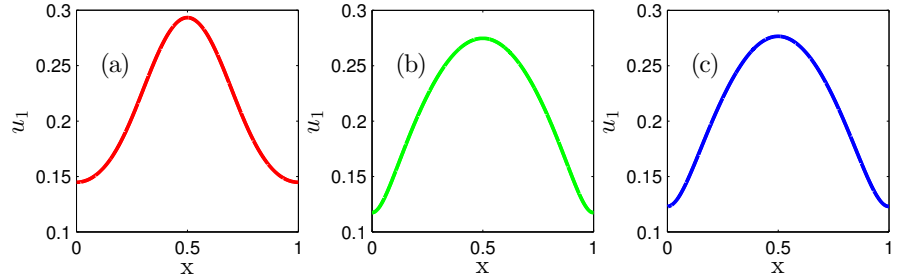
Figure 10: Solutions along the branch δ_b^2 for the system (2.21) with parameter values $(\kappa, \alpha, l, \bar{u}_1, \rho) = (p_2, p_3, p_4, p_5, p_6) = (1, 0.001, 50, 0.211325, 0.05)$. (a) Solution of non-homogeneous steady states at $\delta = 8.72901$. (b) Solution of non-homogeneous steady states at $\delta = 5.76477$. (c) Solution of non-homogeneous steady states at $\delta = 1.548$.
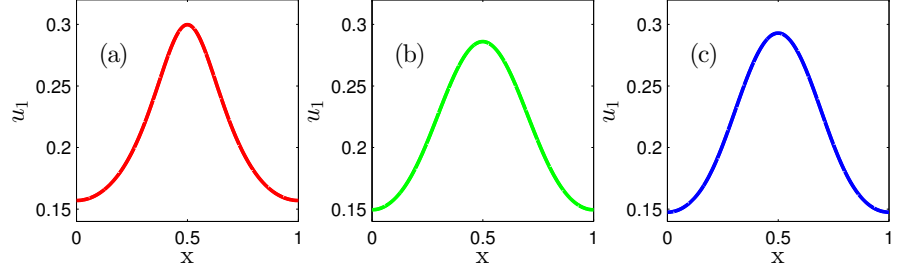
Figure 11: Solutions in the branch δ_b^2 for the system (2.21) with parameter values $(\kappa, \alpha, \bar{u}_1, \rho) = (p_2, p_3, p_5, p_6) = (1, 0.001, 0.211325, 0.05)$. (a) Solution of non-homogeneous steady states at $\delta = -3.5154$, $l = 20$. (b) Solution of non-homogeneous steady states at $\delta = 8.93964$, $l = 50$. (c) Solution of non-homogeneous steady states at $\delta = 37.9117$, $l = 100$.

consider three different solutions with (almost) the same norm (163.863 for the case (a), 163.872 for (b) and 163.911 for (c)).

Figure 12: Solutions in the branch δ_b^2 for the system (2.21) with parameter values $(\alpha, l, \bar{u}_1, \rho) = (p_3, p_4, p_5, p_6) = (0.001, 50, 0.211325, 0.05)$. (a) Solution of non-homogeneous steady states at $\delta = 8.72901$, $\kappa = 1$. (b) Solution of non-homogeneous steady states at $\delta = -92.2877$, $\kappa = 5$. (c) Solution of non-homogeneous steady states at $\delta = -220.578$, $\kappa = 10$.

In summary, we conclude that κ and l do not seem to be the parameters of primary importance in our context as we can re-obtain similar solutions and similar bifurcation structures for different values of κ and l upon varying δ, α as primary parameters.

A KINETIC EQUATION FOR ECONOMIC VALUE ESTIMATION WITH IRRATIONALITY AND HERDING

This chapter is organized as follows. In Section 3.1, the kinetic model is detailed and the grazing collision limit is performed. The resulting Fokker-Planck model (1.5)-(1.6) is analysed in Section 3.2. Furthermore, we discuss the time evolution of the moments of $g(x, w, t)$ in some specific examples. The numerical results are presented in Section 3.3.

3.1 MODELING

The aim of this chapter is to propose and investigate a kinetic model describing irrationality and herding of market agents, motivated by the works of Toscani [Tos06] and Delitala and Lorenzi [DL14], i. e. we model the evolution of the distribution of the number of agents in a large market using a kinetic approach.

3.1.1 *Public information and herding*

We describe the behaviour of the market agents by means of microscopic interactions among the agents. The state of the market is assumed to be characterized by two continuous variables: the estimated asset value $w \in \mathbb{R}^+ := [0, \infty)$ and the rationality $x \in \mathbb{R}$. We say that the agent has a rational behaviour if $x > 0$ and an irrational behaviour if $x < 0$. The changes in asset valuation are based on binary interactions. We take into account two different types: the interaction with public sources, which characterizes a rational agent, and the effect of herding, characterizing an irrational agent. In the following, we define the corresponding interaction rules.

Let w be the estimated asset value of an arbitrary agent before the interaction and w^* the asset value after exchanging information with the public source. Given the background $W = W(t)$, which may be interpreted as a "fair" value, the interaction is given, similarly as in [CDCT09], by

$$w^* = w - \alpha P(|w - W|)(w - W) + \eta d(w). \tag{3.1}$$

The function P measures the compromise propensity and takes values in $[0, 1]$, and the parameter $\alpha > 0$ is a measure of the strength of this effect. Furthermore, the function d with values in $[0, 1]$ describes the modification of the asset value due to diffusion, and η is a random variable with distribution μ with variance σ_I^2 and zero mean taking values on $\mathbb{R}$, i.e. $\langle w \rangle = \int_{\mathbb{R}} w d\mu(w) = 0$ and $\langle w^2 \rangle = \int_{\mathbb{R}} w^2 d\mu(w) = \sigma_I^2$. An example for P is [Tos06]

$$P(|w - W|) = 1_{\{|w-W|<r\}},$$

where $r > 0$ and 1_A denotes the characteristic function on the set A. Thus, if the estimated asset value is too far from the value available

from public sources (the "fair" value), the effect of public information will be discarded (selective perception). The idea behind (3.1) is that if a market agent trusts an information source, he/she will update his/her estimated asset value to make it closer to the one suggested by the public information. We expect that a rational investor follows such a strategy.

The interaction rule (3.1) has to ensure that the post-interaction value w^* remains in the interval $\mathbb{R}^+$. We have to require that diffusion vanishes at the border $w = 0$, i.e. $d(0) = 0$. In the absence of diffusion, it follows that $w^* = w - \alpha P(|w-W|)(w-W) \geq w - \alpha(w-W) = (1-\alpha)w + \alpha W \geq 0$ if $w > W$ and $w^* = w + \alpha P(|w-W|)(W-w) \geq w \geq 0$ if $w \leq W$. Therefore, the post-interaction value w^* stays in the domain $\mathbb{R}^+$.

The second interaction rule aims to model the effect of herding, i.e., we take into account the interaction between a market agent and other investors. We suggest the interaction rule, similarly as in [Tos06],

$$
\begin{aligned}
w^* &= w - \beta\gamma(v,w)(w-v) + \eta_1 d(w), \\
v^* &= v - \beta\gamma(v,w)(v-w) + \eta_2 d(v).
\end{aligned}
\tag{3.2}
$$

The pairs (w,v) and (w^*,v^*) denote the asset values of two arbitrary agents before and after the interaction, respectively. In (3.2), $\beta \in (0,1/2]$ is a constant which measures the attitude of the market participants to change their mind because of herding mechanisms. Furthermore, η_1, η_2 are random variables, modelling diffusion effects, with the same distribution with variance σ_H^2 and zero mean, and, to simplify, the function d is the same as in (3.1). The function γ with values in $[0,1]$ describes a socio-economic scenario where individuals are highly confident in the asset. An example, taken from [DL14], reads as

$$
\gamma(v,w) = 1_{\{w<v\}} v f(w),
\tag{3.3}
$$

where f is nonincreasing, $f(0) = 1$, and $\lim_{w\to\infty} f(w) = 0$. If an agent has an asset value w smaller than v, the function γ will push this agent to assume a higher value w^* than that one before the interaction. This means that the agent trusts other agents that assign a higher value. If w is larger than v, the agent hesitates to lower his asset value and nothing changes. Agents that assign a small value w tend to herd with a higher rate, i.e. f is nonincreasing. Another choice is given by $\gamma(v,w) = 1_{\{|w-v|<r_H\}}$ [DL14]. In this case, the interaction occurs only when the two interacting agents have asset values which are not too different from each other.

The interaction does not take place if w^*, v^* are negative. In the absence of diffusion, adding both equations in (3.2) gives $w^* + v^* = v + w$ which means that the total momentum is conserved. Subtracting both equations in (3.2) yields $w^* - v^* = (1 - 2\beta\gamma(v,w))(w-v)$. Since $1 - 2\beta\gamma(v,w) \in [0,1)$ (observe that $0 < \beta \leq 1/2$), the post-interaction difference $w^* - v^*$ in the asset values is smaller than the pre-interaction difference $w - v$. We infer that w^*, v^* remain nonnegative.

When diffusion is taken into account, we need to specify the range of values the random variables η_1, η_2 in (3.2) can assume. This clearly depends on the choice of $d(w)$, and we refer to [DMPW09, page 3691] for a more detailed discussion.

3.1.2 *The kinetic equation*

Instead of calculating the value x and w for each market agent, we prefer to investigate the evolution of the distribution $f(x, w, t)$ of the estimated value and the rationality of the market participants. The integral $\int_B f(x, w, t) dz$ with $z = (x, w)$ represents the number of agents with asset value and rationality in $B \subset \mathbb{R} \times \mathbb{R}^+$ at time $t \geq 0$. In analogy with classical kinetic theory of rarefied gases, we may identify the position variable with the rationality and the velocity with the asset value. Using standard methods of kinetic theory, $f(x, w, t)$ evolves according to the inhomogeneous Boltzmann equation

$$\partial_t f + [\Phi(x, w) f]_x = \frac{1}{\tau_I} Q_I(f) + \frac{1}{\tau_H} Q_H(f, f), \quad (x, w) \in \mathbb{R} \times \mathbb{R}^+, \ t > 0.$$

$$(3.4)$$

Here, $\Phi(x, w)$ is the drift term, Q_I and Q_H are interaction integrals modelling the public information and herding, respectively, and $1/\tau_I > 0$, $1/\tau_H > 0$ describe the interaction frequencies. This equation is supplemented by the boundary condition $f(x, 0, t) = 0$ (nobody believes that the asset has value zero) and the initial condition $f(x, w, 0) = f_0(x, w)$ for $(x, w) \in \mathbb{R} \times \mathbb{R}^+$.

A simple model for Φ can be introduced as follows. If an agent gives an asset value that is much larger than the "fair" value W, he/she will recognize that the value is overestimated and it is believed that he/she will become more rational. The same holds true when the estimated value is too low compared to W. In this regime, the drift function $\Phi(x, w)$ should be positive since agents drift towards higher rationality $x > 0$. When the estimated value is not too far from the value W, agents may behave more irrational and drift towards the region $x < 0$, so the drift function is negative. An example for such a function is

$$\Phi(x, w) = \begin{cases} -\delta\kappa & \text{for } |w - W| < R, \\ \kappa & \text{for } |w - W| \geq R, \end{cases} \qquad (3.5)$$

where $\delta, \kappa, R > 0$. The constant R fixes the range $|w - W| < R$ in which bubbles and crashes do not occur. More realistic models are obtained when R depends on time, and we consider such a case in Section 3.3. An alternative is to employ the mean asset value $\int_{\mathbb{R}} \int_{\mathbb{R}^+} f w \, dw \, dx$ instead of w in $|w - W| < R$ to distinguish the ranges.

Next, we detail the choice of the interaction integrals. As pointed out in [CDCT09], the existence of a pre-interaction pair which returns the post-interaction pair (w^*, v^*) through an interaction of the type (3.1) is not guaranteed, because of the boundary constraint. Therefore, we will give the interaction rule in the weak form. Let $\phi(w) := \phi(x, w)$ be a regular test function and set $\Omega = \mathbb{R} \times \mathbb{R}^+$, $z = (x, w)$. The weak form reads as

$$\int_\Omega Q_I(f) \phi(w) dz = \left\langle \int_{\mathbb{R}^+} \int_\Omega (\phi(w^*) - \phi(w)) M(W) f(x, w, t) dz \, dW \right\rangle,$$

$$(3.6)$$

where $\langle \cdot \rangle$ is the expectation value with respect to the random variable η in (3.1) and $M(W) \geq 0$ represents the fixed background satisfying

$\int_{\mathbb{R}^+} M(W)\mathrm{d}W = 1$. The Boltzmann equation for this operator, $\partial_t f = Q_I(f)/\tau_I$, becomes in the weak form

$$\partial_t \int_\Omega f(x,w,t)\phi(w)\mathrm{d}z = \frac{1}{\tau_I}\Big\langle \int_{\mathbb{R}^+} \int_\Omega (\phi(w^*)-\phi(w))M(W)f(x,w,t)\mathrm{d}z\mathrm{d}W\Big\rangle.$$

Choosing $\phi(w) = 1$, the right-hand side vanishes, which expresses conservation of the number of agents, $\partial_t \int_\Omega f(x,w,t)\mathrm{d}z = 0$. By taking $\phi(w) = w$, a computation shows that the mean asset value $m_w(f) = \int_\Omega f w\mathrm{d}z$ is nonincreasing.

The operator $Q_H(f,f)$ models the binary interaction of the agents and, similarly as in [Tos06], we define

$$\int_\Omega Q_H(f,f)\phi(w)\mathrm{d}z = \Big\langle \int_{\mathbb{R}^+} \int_\Omega (\phi(w^*)-\phi(w))f(x,w,t)f(x,v,t)\mathrm{d}z\mathrm{d}v\Big\rangle,$$
(3.7)

where (w,v) is the pre-interaction pair that generates via (3.2) the post-interaction pair (w^*,v^*). Choosing $\phi = 1$ in the Boltzmann equation $\partial_t f = Q_H(f,f)$, we see that this operator also conserves the number of agents. Taking $\phi(w) = w$ and using a symmetry argument, the interaction rule (3.2), and the fact that the random variables η_1 and η_2 have zero mean, a computation shows that $\partial_t m_w(f) = 0$., i.e., mean asset value is conserved. This is reasonable as the crowd may tend to any direction depending on the herding.

3.1.3 *Grazing collision limit*

The analysis of the Boltzmann equation (3.4) is rather involved, and it is common in kinetic theory to investigate certain asymptotic leading to simplified models of Fokker-Planck type. Our aim is to perform the formal limit $(\alpha, \beta, \sigma_H^2, \sigma_I^2) \to 0$ (in a certain sense made precise below), where α, β appear in the interaction rules (3.1) and (3.2) and σ_H^2, σ_I^2 are the variances of the random variables in these rules. Since the formal limit is very similar to that one in [CPT05, Tos06], we sketch it only.

Set $k = \beta/\alpha$, $t_s = \alpha t$, $x_s = \alpha x$, and introduce the functions $g(x_s,w,t_s) = f(x,w,t)$, $\Phi_s(x_s,w) = \Phi(x,w)$. After the change of variables $(x,w) \mapsto (x_s,t_s)$ and setting $z_s = (x_s,w)$, the weak form of (3.4) reads as

$$\frac{\partial}{\partial t_s} \int_\Omega g(x_s,w,t_s)\phi(w)\mathrm{d}z_s + \int_\Omega \frac{\partial}{\partial x_s}(\Phi_s(x_s,w)g(x_s,w,t_s))\phi(w)\mathrm{d}z_s$$

$$= \frac{1}{\alpha\tau_I} \int_\Omega Q_{I,s}(g)\phi(w)\mathrm{d}z_s + \frac{1}{\alpha\tau_H} \int_\Omega Q_{H,s}(g,g)\phi(w)\mathrm{d}z_s, \quad (3.8)$$

where $Q_{I,s}(g) = Q_I(f)$, $Q_{H,s}(g,g) = Q_H(f,f)$ are defined in weak form in (3.6), (3.7), respectively. In the following, we omit the index s.

Now, we rewrite the collision integrals in (3.8) using a Taylor expansion of $\phi(w^*) - \phi(w)$ and the properties $\langle\eta\rangle = 0$, $\langle\eta^2\rangle = \sigma_I^2$, leading to

$$\frac{1}{\alpha\tau_I} \int_\Omega Q_I(g)\phi(w)\mathrm{d}z$$

$$= -\frac{1}{\tau_I} \int_{\mathbb{R}^+} \int_\Omega \phi'(w)P(|w-W|)(w-W)M(W)g(x,w,t)\mathrm{d}z\mathrm{d}W$$

$$+ \frac{1}{2\tau_I} \int_{\mathbb{R}^+} \int_\Omega \phi''(\widetilde{w})\Big(\alpha P(|w-W|)^2(w-W)^2 + \frac{\sigma_I^2}{\alpha}d(w)^2\Big)$$

$$M(W)g(x,w,t)\mathrm{d}z\mathrm{d}W$$

$$= -\frac{1}{\tau_I}\int_\Omega \phi'(w)H(w)g(x,w,t)\mathrm{d}z + R(\alpha,\sigma_I)$$

$$+ \frac{1}{2\tau_I}\int_{\mathbb{R}^+}\int_\Omega \phi''(w)\left(\alpha P(|w-W|)^2(w-W)^2 + \frac{\sigma_I^2}{\alpha}d(w)^2\right)$$

$$M(W)g(x,w,t)\mathrm{d}z\mathrm{d}W,$$

where $R(\alpha,\sigma_I)$ is some remainder term with the property $R(\alpha,\sigma_I) \to 0$ as $(\alpha,\sigma_I) \to 0$ [Tos06, Section 4.1], and

$$H(w) = \frac{1}{\tau_I}\int_{\mathbb{R}^+} P(|w-W|)(w-W)M(W)\mathrm{d}W. \tag{3.9}$$

Then, in the limit $\alpha \to 0$ and $\sigma_I \to 0$ such that $\lambda_I := \sigma_I^2/\alpha$ is fixed,

$$\lim_{(\alpha,\sigma_I)\to 0}\frac{1}{\alpha\tau_I}\int_\Omega Q_I(g)\phi(w)\mathrm{d}z$$

$$= \frac{1}{\tau_I}\int_\Omega\left(-\phi'(w)H(w) + \frac{\lambda_I}{2}d(w)^2\phi''(w)\right)g(x,w,t)\mathrm{d}z$$

$$= \int_\Omega\left((H(w)g)_w + \frac{\lambda_I}{2\tau_I}(d(w)^2 g)_{ww}\right)\phi(w)\mathrm{d}z,$$

where in the last step we integrated by parts. The boundary integrals vanish since $g = 0$ at $w = 0$ and $d(0) = 0$ imply that $(d(w)^2 g)_w|_{w=0} = d'(0)g|_{w=0} + d(0)g_w|_{w=0} = 0$.

The limit $(\alpha,\sigma_H) \to 0$ in the last term of (3.8) is performed in a similar way. Using a Taylor expansion and (3.2), we can show that

$$\frac{1}{\alpha\tau_H}\int_\Omega Q_H(g,g)\mathrm{d}z$$

$$= \int_\Omega\left(-K[g](x,w,t)\phi'(w) + \frac{\sigma_H^2}{2\alpha\tau_H}d(w)^2\rho\phi''(w)\right)g(x,w,t)\mathrm{d}z$$

$$+ \frac{\alpha k^2}{2\tau_H}\int_{\mathbb{R}^+}\int_\Omega \gamma(v,w)^2(v-w)^2 g(x,v,t)g(x,w,t)\phi''(w)\mathrm{d}z\mathrm{d}w$$

$$+ R(\alpha,\sigma_H),$$

where $R(\alpha,\sigma_H)$ is another remainder term, $\rho = \int_\Omega f\mathrm{d}z$, and

$$K[g](x,w,t) = \frac{k}{\tau_H}\int_0^\infty \gamma(v,w)(v.w)g(x,v,t)\mathrm{d}v.$$

Keeping $\lambda_H = \sigma_H^2/\alpha$ fixed, the limit $(\alpha,\sigma_H) \to 0$ gives

$$\lim_{(\alpha,\sigma_H)\to 0}\frac{1}{\alpha\tau_H}\int_\Omega Q_H(g,g)\mathrm{d}z = \int_\Omega\left((K[g]g)_w + \frac{\lambda_H\rho}{2\tau_H}(d(w)^2 g)_{ww}\right)\phi(w)\mathrm{d}z.$$

Summarizing, we obtain in the limit the weak form of the Fokker-Planck-type equation

$$\partial_t g + (\Phi(x,w)g)_x = (K[g]g + H(w))_w + \frac{1}{2}\left(\frac{\lambda_I}{\tau_I} + \frac{\lambda_H\rho}{\tau_H}\right)(d(w)^2 g)_{ww} \tag{3.10}$$

for $(x,w) \in \mathbb{R}\times\mathbb{R}^+$, $t > 0$. This equation is supplemented by the boundary condition $g = 0$ at $w = 0$ and the initial condition $g(0) = g_0$ in Ω.

3.2   ANALYSIS

The aim of this section is to analyse the Fokker-Planck-type equation derived in the previous section. To this end, we set

$$\Gamma(v, w) := \frac{k}{\tau_H} \gamma(v, w)(v - w), \ D(w) := \frac{1}{2}\left(\frac{\lambda_I}{\tau_I} + \frac{\lambda_H \rho}{\tau_H}\right)d(w)^2, \ \Omega = \mathbb{R} \times \mathbb{R}^+.$$

Then (3.10) simplifies to

$$\partial_t g + [\Phi(x, w)g]_x = (K[g]g + H(w)g)_w + [D(w)g]_{ww} \qquad (3.11)$$

with

$$K[g] = \int_0^\infty \Gamma(v, w)g(v)\mathrm{d}v.$$

3.2.1   *Existence of weak solutions*

We wish to show the existence of weak solutions to (3.11)–(1.6) under the following hypotheses:

(H1) $\Phi \in W^{2,\infty}(\Omega)$, $H \in W^{1,\infty}(\mathbb{R}^+)$, $D \in W^{2,\infty}(\mathbb{R}^+)$, and there exists $\delta > 0$ such that $D(w) \geq \delta > 0$ for $w \in (0, \infty)$.

(H2) $\Gamma \in L^2((\mathbb{R}^+)^2)$, $\Gamma \geq 0$, and $\Gamma_w(v, w) \leq 0$ for all $v, w \geq 0$.

(H3) $g_0 \in H^1(\Omega)$ and $0 \leq g_0 \leq M_0$ for some $M_0 > 0$.

Remark 8. We discuss the above assumptions. The strict positivity of $D(w)$ (and consequently of $d(w)$) is needed for technical reasons since we cannot handle the degeneracy $d(0) = 0$ which was assumed in the modelling part. One may interpret our assumption as a regularization for "small" $\delta > 0$. Condition $\Gamma_w(v, w) \leq 0$ is satisfied for regularized versions of (3.3) since both $w \mapsto \gamma(v, w)$ and $w \mapsto v - w$ are nonincreasing functions on $\mathbb{R}^+$. The remaining hypotheses are regularity conditions needed for the mathematical analysis.   □

Then the main result reads as follows.

Theorem 9. *Let Hypotheses H1-H3 hold. Then there exists a weak solution g to (1.5)-(1.6) satisfying $0 \leq g(x, w, t) \leq M_0 e^{\lambda t}$ for $(x, w) \in \Omega$, $t > 0$, where $\lambda > 0$ depends on Φ, H and D, and it holds $g \in L^2(0, T; H^1(\Omega))$, $\partial_t g \in L^2(0, T; H^1(\Omega)')$.*

The idea of the proof is to regularize equation (1.5) by adding a second-order derivative with respect to x, to truncate the nonlinearity, and to solve the equation in the finite interval $w \in (0, \rho)$. Then we pass to the deregularization limit. The key step of the proof is the derivation of uniform H^1 estimates allowing for the compactness argument. These estimates are derived by analysing the differential equation satisfied by $h := g_x$ and by making crucial use of the boundary conditions.

Proof of Theorem 9. Let $\rho > 0$, $0 < \varepsilon < 1$, $M > 0$, set

$$K_M[g](x, w, t) = \int_0^\rho \Gamma(v, w)(g)_M(x, v, t)\mathrm{d}v$$

$$(g)_M = \max\{0, \min\{M, g\}\},$$

where g is an integrable function, and introduce $\Omega_\rho = (-\rho, \rho) \times (0, \rho)$. We split the boundary $\partial\Omega_R$ into two parts:

$$\partial\Omega_\rho = \partial\Omega_D \cup \partial\Omega_N, \quad \text{where}$$
$$\partial\Omega_D = \{(x, w) : x \in [-\rho, \rho], \, w = 0, \rho\},$$
$$\partial\Omega_N = \{(x, w) : x = \pm\rho, \, w \in (0, \rho)\}.$$

Finally, we set $g^+ = \max\{0, g\}$. Consider the approximated nonlinear problem

$$\partial_t g + [\Phi(x, w) g^+]_x \tag{3.12}$$
$$= [(K_M[g] + H(w) + D'(w)) g^+]_w + [D(w) g_w]_w + \varepsilon g_{xx},$$
$$g = 0 \quad \text{on } \partial\Omega_D, \quad g_x = 0 \quad \text{on } \partial\Omega_N, \quad g(x, w, 0) = 0 \quad \text{in } \Omega_\rho. \tag{3.13}$$

We introduce the space $H_D^1(\Omega_\rho)$ consisting of those functions $v \in H^1(\Omega_\rho)$ which satisfy $v = 0$ on $\partial\Omega_D$, and we set $H_D^{-1}(\Omega_\rho) = (H_D^1(\Omega_\rho))'$.

The weak formulation of (3.12)-(3.13) reads as: for all $v \in L^2(0, T; H_D^1(\Omega_\rho))$,

$$\int_0^T \langle \partial_t g, v \rangle \mathrm{d}t \tag{3.14}$$
$$= -\int_0^T \int_{\Omega_\rho} \Big((\Phi_x(x, w) g^+ + \Phi(x, w) g_x^+) v$$
$$+ (K_M[g] + H(w) + D'(w)) g^+ v_w + d(w) g_w v_w + \varepsilon g_x v_x \Big) \mathrm{d}z \mathrm{d}t,$$

where $\langle \cdot, \cdot \rangle$ is the dual product between $H_D^{-1}(\Omega_\rho)$ and $H_D^1(\Omega_\rho)$.

We wish to apply the Leray-Schauder fixed-point theorem. For this, we split the proof in several steps.

Lemma 10. *Given $T > 0$, $\widetilde{g} \in L^2(0, T; L^2(\Omega))$, and $\eta \in [0, 1]$, there exists a weak solution to the linearised problem*

$$\partial_t g + \eta(\Phi(x, w)_x \widetilde{g}^+ + \Phi(x, w) g_x)$$
$$= \eta((K_M[\widetilde{g}] + H(w) + D'(w)) \widetilde{g}^+)_w + (D(w) g_w)_w + \varepsilon g_{xx},$$
$$g = 0 \quad \text{on } \partial\Omega_D, \quad g_x = 0 \quad \text{on } \partial\Omega_N, \quad g(x, w, 0) = 0 \quad \text{in } \Omega_R.$$

Proof. We introduce the forms

$$a(g, v) = \int_{\Omega_\rho} (\eta \Phi(x, w) g_x v + D(w) g_w v_w + \varepsilon g_x v_x) \mathrm{d}z, \tag{3.15}$$
$$g, v \in H_D^1(\Omega_\rho),$$
$$F(v) = -\eta \int_{\Omega_\rho} (\Phi_x(x, w) \widetilde{g}^+ v + (K_M[\widetilde{g}] + H(w) + D'(w)) \widetilde{g}^+ v_w) \mathrm{d}z. \tag{3.16}$$

Since $K_M[\widetilde{g}]$ is bounded, it is not difficult to see that a is bilinear and continuous on $H_D^1(\Omega_\rho)^2$ and F is linear and continuous on $H_D^1(\Omega_\rho)$. Furthermore, using Young's inequality and $D(w) \geq \delta > 0$, it follows that, for some $C_\varepsilon > 0$,

$$a(g, g) \geq \frac{1}{2} \int_{\Omega_\rho} (\delta g_w^2 \mathrm{d}z + \varepsilon(g_x^2 + g^2)) \mathrm{d}z - (C_\varepsilon + \varepsilon) \int_{\Omega_\rho} g^2 \mathrm{d}z$$
$$\geq \min\{\delta, \varepsilon\} \|g\|_{H^1(\Omega_\rho)}^2 - (C_\varepsilon + \varepsilon) \|g\|_{L^2(\Omega_\rho)}^2.$$

By Corollary 23.26 in [Zei90], there exists a unique solution $g \in L^2(0, T; H^1_D(\Omega_\rho)) \cap H^1(0, T; H^{-1}_D(\Omega_\rho))$ to

$$\langle \partial_t g, v \rangle + a(g, v) = F(v), \quad t > 0, \quad g(0) = \eta g_0. \qquad (3.17)$$

finishing the proof. □

This defines the fixed-point operator $S : L^2(0, T; L^2(\Omega_\rho)) \times [0, 1] \to L^2(0, T; L^2(\Omega_\rho))$, $S(\widetilde{g}, \eta) = g$, where g solves (3.17). This operator satisfies $S(\widetilde{g}, 0) = 0$. Standard arguments show that S is continuous (employing H^1 estimates depending on ε). Since $L^2(0, T; H^1_D(\Omega_\rho)) \cap H^1(0, T; H^{-1}_D(\Omega_\rho))$ is compactly embedded in $L^2(0, T; L^2(\Omega_\rho))$, the operator is also compact. In order to apply the fixed-point theorem of Leray-Schauder, we need to show uniform estimates, which are provided by the following lemma.

Lemma 11. *Let g be a fixed point of $S(\cdot, \eta)$, i.e., g solves (3.17) with $\widetilde{g} = g$. Then, for some $\lambda > 0$ independent of ε and R, it holds that $0 \le g \le M_0 e^{\lambda t}$ in $(0, T)$*

Proof. We choose $v = g^- := \min\{0, g\} \in L^2(0, T; H^1_D(\Omega_R))$ as a test function in (3.17) and integrate over $(0, t)$. Since $g^+ g^- = 0$ and $g^-(0) = g_0^- = 0$, we have

$$a(g, g^-) = \int_{\Omega_R} (D(w)(g^-_w)^2 + \varepsilon(g^-_x)^2) dz \ge 0, \quad F(g^-) = 0,$$

which shows that

$$\frac{1}{2} \int_{\Omega_\rho} g^-(t)^2 dz = \frac{1}{2} \int_{\Omega_\rho} g^-(0)^2 dz - \int_0^t a(g, g^-) ds \le 0.$$

This yields $g^- = 0$ and $g \ge 0$ in Ω_ρ, $t > 0$. In particular, we may write g instead of g^+ in (3.15)-(3.16).

For the upper bound, we choose the test function $v = (g - M)^+ \in L^2(0, T; H^1_D(\Omega_\rho))$ in (3.14), where $M = M_0 e^{\lambda t}$ for some $\lambda > 0$ which will be determined later. By Hypothesis H3, $(g - M)^+(0) = (g_0 - M_0)^+ = 0$. Observing that $\partial_t M = \lambda M$, $(g - M)(g - M)^+_w = \frac{1}{2}[((g - M)^+)^2]_w$ and integrating by parts in the integrals involving $K_M[g] + H(w) + D'(w)$, we find that

$$\frac{1}{2} \int_{\Omega_\rho} (g - M)^+(t)^2 dz = -\lambda \int_0^t \int_{\Omega_\rho} M(g - M)^+ dz ds$$

$$- \eta \int_0^t \int_{\Omega_\rho} (\Phi_x(x, w)((g - M) + M) + \Phi(x, w)(g - M)^+_x)(g - M)^+ dz ds$$

$$- \eta \int_0^t \int_{\Omega_\rho} (K_M[g] + H(w) + D'(w))((g - M) + M)(g - M)^+_w dz ds$$

$$- \int_0^t \int_{\Omega_\rho} (D(w)((g - M)^+_w)^2 + \varepsilon((g - M)^+_x)^2) dz ds$$

$$= -\eta \int_0^t \int_{\Omega_\rho} (\Phi_x(x, w) + \lambda) M(g - M)^+ dz ds$$

$$- \eta \int_0^t \int_{\Omega_\rho} \Phi_x(x, w)((g - M)^+)^2 dz ds$$

$$- \eta \int_0^t \int_{\Omega_\rho} \Phi(x, w)(g - M)^+_x(g - M)^+ dz ds$$

$$+ \frac{\eta}{2} \int_0^t \int_{\Omega_\rho} (K_M[g]_w + H'(w) + D''(w))((g - M)^+)^2 \mathrm{d}z \mathrm{d}s$$

$$+ \eta \int_0^t \int_{\Omega_\rho} (K_M[g]_w + H'(w) + D''(w))M(g - M)^+ \mathrm{d}z \mathrm{d}s$$

$$- \int_0^t \int_{\Omega_\rho} (D(w)((g - M)_w^+)^2 + \varepsilon((g - M)_x^+)^2) \mathrm{d}z \mathrm{d}s.$$

The third integral on the right-hand side can be estimated by Young's inequality,

$$- \eta \int_0^t \int_{\Omega_\rho} \Phi(x, w)(g - M)_x^+(g - M)^+ \mathrm{d}z \mathrm{d}s$$

$$\leq \frac{\eta}{2\varepsilon} \|\Phi\|_{L^\infty(\Omega)}^2 \int_0^t \int_{\Omega_\rho} ((g - M)^+)^2 \mathrm{d}z \mathrm{d}s + \frac{\varepsilon}{2} \int_0^t \int_{\Omega_\rho} ((g - M)_x^+)^2 \mathrm{d}z \mathrm{d}s.$$

Then, collecting the integrals involving $M(g - M)^+$ and $((g - M)^+)^2$ and observing that $\Gamma_w \leq 0$ implies that $K_M[g]_w \leq 0$, it follows that

$$\frac{1}{2} \int_{\Omega_\rho} (g - M)^+(t)^2 \mathrm{d}z$$

$$\leq \eta \int_0^t \int_{\Omega_\rho} (-\Phi_x(x, w) + H'(w) + D''(w) - \lambda)M(g - M)^+ \mathrm{d}z \mathrm{d}s$$

$$+ \frac{\eta}{2} \int_0^t \int_{\Omega_\rho} \left(\frac{1}{\varepsilon} \|\Phi\|_{L^\infty(\Omega)}^2 - 2\Phi_x(x, w) + H'(w) + D''(w) \right)((g - M)^+)^2 \mathrm{d}z \mathrm{d}s$$

$$- \int_0^t \int_{\Omega_\rho} \left(D(w)((g - M)_w^+)^2 + \frac{\varepsilon}{2}((g - M)_x^+)^2 \right) \mathrm{d}z \mathrm{d}s.$$

Choosing $\lambda \geq \|\Phi_x\|_{L^\infty(\Omega)} + \|H'\|_{L^\infty(0,\infty)} + \|D''\|_{L^\infty(0,\infty)}$, the first integral on the right-hand side is nonpositive. The last integral is nonpositive too, and the second integral can be estimated by some constant $C_\varepsilon > 0$. We conclude that

$$\int_{\Omega_\rho} (g - M)^+(t)^2 \mathrm{d}z \leq C_\varepsilon \int_0^t \int_{\Omega_\rho} ((g - M)^+)^2 \mathrm{d}z \mathrm{d}s.$$

Then Gronwall's lemma implies that $(g - M)^+ = 0$ and $g \leq M$ in Ω_ρ, $t > 0$. $\qquad\square$

In particular, we can write $K[g]$ instead of $K_M[g]$ in (3.14). The L^∞ bound provides the desired bound for the fixed-point operator in $L^2(0, T; L^2(\Omega_R))$, yielding the existence of a weak solution to (3.14). We need more a priori estimates. The following lemma is the key step in the proof.

Lemma 12. *Let g be a weak solution to (3.14). Then there exists $C > 0$ independent of ε and R such that $\|g\|_{L^2(0,T;H^1(\Omega_R))} \leq C$.*

Proof. We choose first the test function $v = g \in L^2(0, T; H_D^1(\Omega_\rho))$ in (3.14) (replacing T by $t \in (0, T)$):

$$\frac{1}{2} \int_{\Omega_\rho} g(t)^2 \mathrm{d}z$$

$$= - \int_0^t \int_{\Omega_\rho} \Phi_x(x, w)g^2 \mathrm{d}z \mathrm{d}s - \int_0^t \int_{\Omega_\rho} \Phi(x, w)g_x g \mathrm{d}z \mathrm{d}s$$

$$- \frac{1}{2} \int_0^t \int_{\Omega_\rho} (K[g] + H(w) + D'(w))(g^2)_w \mathrm{d}z\mathrm{d}s$$

$$- \int_0^t \int_{\Omega_\rho} (D(w)g_w^2 + \varepsilon g_x^2)\mathrm{d}z\mathrm{d}s + \frac{1}{2} \int_{\Omega_\rho} g_0^2 \mathrm{d}z.$$

Applying Young's inequality to the second integral on the right-hand side, integrating by parts in the third integral, and observing that $g = 0$ at $w \in \{0, \rho\}$ yields, for some constant $C_1 > 0$ which depends on the L^∞ norms of Φ_x, H', and D'' (we use again that $K[g]_w \leq 0$),

$$\frac{1}{2} \int_{\Omega_\rho} g(t)^2 \mathrm{d}z\mathrm{d}t \tag{3.18}$$

$$\leq C_1 \int_0^t \int_{\Omega_\rho} g^2 \mathrm{d}z\mathrm{d}s + C_1 \int_0^T \int_{\Omega_\rho} g_x^2 \mathrm{d}z\mathrm{d}s$$

$$- \int_0^T \int_{\Omega_\rho} (\delta g_w^2 + \varepsilon g_x^2)\mathrm{d}z\mathrm{d}s + \frac{1}{2} \int_{\Omega_\rho} g_0^2 \mathrm{d}z.$$

Since $C_1 > \varepsilon$ is possible, this does not give an estimate, and we need a further argument.

Next, we differentiate (3.12) with respect to x in the sense of distributions and set $h := g_x$:

$$\partial_t h + [\Phi_x(x,w)g + \Phi(x,w)h]_x \tag{3.19}$$
$$= (K[h]g)_w + [(K[g] + H(w) + D'(w))h]_w$$
$$+ (D(w)h_w)_w + \varepsilon h_{xx} \quad \text{in } \Omega_\rho, \ t > 0.$$

We observe that the boundary condition $g = 0$ on $\partial\Omega_D$ implies that also $g_x = 0$ holds on $\partial\Omega_D$ and so, $g_x = 0$ on $\partial\Omega_\rho$. Hence, equation (3.19) is complemented with homogeneous Dirichlet boundary conditions. Furthermore, $h(x,w,0) = g_{0,x}(x,w)$. The weak formulation of (3.19) reads as

$$\int_0^T \langle \partial_t h, v \rangle \mathrm{d}t$$

$$= -\int_0^T \int_{\Omega_\rho} \Big((\Phi_{xx}(x,w)g + 2\Phi_x(x,w)h + \Phi(x,w)h_x)v$$

$$+ K[h]g v_w + (K[g] + H(w) + D'(w))h v_w + D(w)h_w v_w + \varepsilon h_x v_x \Big) \mathrm{d}z\mathrm{d}t$$

for all $v \in L^2(0,T;H_0^1(\Omega_\rho))$. This is a linear nonlocal problem for h, with given g, and we verify that there exists a solution $h \in L^2(0,T;H_0^1(\Omega_\rho)) \cap H^1(0,T;H^{-1}(\Omega_\rho))$, using similar arguments as above. Therefore, we can choose $v = h$ as a test function in (3.19):

$$\frac{1}{2} \int_{\Omega_\rho} h(t)^2 \mathrm{d}z$$

$$= -\int_0^t \int_{\Omega_\rho} \Big((\Phi_{xx}(x,w)gh + 2\Phi_x(x,w)h^2 + \frac{1}{2}\Phi(x,w)(h^2)_x \Big) \mathrm{d}z\mathrm{d}s$$

$$- \int_0^t \int_{\Omega_\rho} \Big(K[h]g h_w$$

$$+ \frac{1}{2}(K[g] + H(w) + D'(w))(h^2)_w + D(w)h_w^2 + \varepsilon h_x^2 \Big) \mathrm{d}z\mathrm{d}s$$

$$+ \frac{1}{2} \int_{\Omega_\rho} g_x(0)^2 \mathrm{d}z.$$

We integrate by parts and employ the inequalities $K[g]_w \leq 0, D(w) \geq \delta$:

$$\frac{1}{2} \int_{\Omega_\rho} h(t)^2 dz ds \tag{3.20}$$

$$\leq -\int_0^t \int_{\Omega_\rho} \left(\Phi_{xx}(x,w)gh + \frac{3}{2}\Phi_x(x,w)h^2 \right) dz ds$$

$$- \int_0^t \int_{\Omega_\rho} K[h]gh_w dz ds + \frac{1}{2}\int_0^t \int_{\Omega_\rho} (H'(w) + D''(w))h^2 dz ds$$

$$- \int_0^t \int_{\Omega_\rho} (\delta h_w^2 + \varepsilon h_x^2) dz ds + \frac{1}{2}\int_{\Omega_\rho} g_x(0)^2 dz.$$

The first integral on the right-hand side is estimated by using Young's inequality:

$$\int_0^t \int_{\Omega_\rho} \left(\Phi_{xx}(x,w)gh + \frac{3}{2}\Phi_x(x,w)h^2 \right) dz ds$$

$$\leq \frac{1}{2}\|\Phi_{xx}\|_{L^\infty(\Omega)} \int_0^t \int_{\Omega_\rho} (g^2 + h^2) dz ds$$

$$+ \frac{3}{2}\|\Phi_x\|_{L^\infty(\Omega)} \int_0^t \int_{\Omega_\rho} h^2 dz ds.$$

For the second integral on the right-hand side of (3.20), we observe that $0 \leq g \leq M$ and $\|K[h]\|_{L^2(\Omega_\rho)} \leq C_\Gamma \|h\|_{L^2(\Omega_\rho)}$, where $C_\Gamma^2 = \int_0^\infty \int_0^\infty \Gamma(v,w)^2 dv dw$. Thus,

$$-\int_0^t \int_{\Omega_\rho} K[h]gh_w dz ds \leq M \int_0^t \|h\|_{L^2(\Omega_\rho)}\|h_w\|_{L^2(\Omega_\rho)} ds$$

$$\leq \frac{\delta}{2}\int_0^t \int_{\Omega_\rho} h_w^2 dz ds + \frac{M}{2\delta}\int_0^t \int_{\Omega_\rho} h^2 dz ds.$$

This shows that, for some $C_2(\delta) > 0$,

$$\frac{1}{2}\int_{\Omega_\rho} h(t)^2 dz \leq C_2(\delta)\int_0^t \int_{\Omega_\rho} (g^2 + h^2) dz ds - \frac{\delta}{2}\int_0^t \int_{\Omega_\rho} h_w^2 dz ds$$

$$- \varepsilon \int_0^t \int_{\Omega_\rho} h_x^2 dz ds + \frac{1}{2}\int_{\Omega_\rho} g_x(0)^2 dz. \tag{3.21}$$

We add (3.18) and (3.21) to find that, for some $C_3(\delta) > 0$,

$$\int_{\Omega_\rho} (g^2 + h^2)(t) dz + \int_0^t \int_{\Omega_\rho} (\delta g_w^2 + \varepsilon h^2 + \varepsilon h_x^2) dz ds$$

$$\leq C_3(\delta)\int_0^t \int_{\Omega_\rho} (g^2 + h^2) dz ds + \frac{1}{2}\int_{\Omega_\rho} (g_0^2 + g_{0,x}^2) dz.$$

Gronwall's lemma provides uniform estimates for g and $g_x = h$:

$$\|g\|_{L^\infty(0,T;L^2(\Omega_\rho))} + \|g_x\|_{L^\infty(0,T;L^2(\Omega_\rho))} + \|g_w\|_{L^2(0,T;L^2(\Omega_\rho))} \leq C, \tag{3.22}$$

where $C > 0$ depends on δ, M, and the L^∞ bounds for Φ, H, D' and their derivatives, but not on R and ε. $\qquad\square$

Lemma 13. *There exists a weak solution g to*

$$\partial_t g + \Phi_x(x,w)g + \Phi(x,w)g_x$$
$$= ((K_M[g] + H(w) + D'(w))g^+)_w + (D(w)g_w)_w,$$
$$g = 0 \quad \text{on } \partial\Omega_D, \quad g_x = 0 \quad \text{on } \partial\Omega_N, \quad g(x,w,0) = 0 \quad \text{in } \Omega_R.$$

Proof. The lemma follows after passing to the limit $\varepsilon \to 0$ in (3.12). Let $g_\varepsilon := g$ be a solution to (3.12)-(3.13) with $K[g] = K_M[g]$. First, we estimate $\partial_t g_\varepsilon$:

$$\|\partial_t g_\varepsilon\|_{L^2(0,T;H_D^{-1}(\Omega_\rho))} \tag{3.23}$$

$$\leq \|\Phi(x,w)g_\varepsilon\|_{L^2(0,T;L^2(\Omega_\rho))}$$

$$+ \|K[g_\varepsilon] + H(w) + D'(w)\|_{L^\infty(0,T;L^\infty(\Omega_\rho))} \|g_\varepsilon\|_{L^2(0,T;L^2(\Omega_\rho))}$$

$$+ (\|D\|_{L^\infty(0,T;L^\infty(\Omega_\rho))} + 1)\|g_\varepsilon\|_{L^2(0,T;H^1(\Omega_\rho))} \leq C,$$

where $C > 0$ does not depend on ε and ρ (since $K[g_\varepsilon]$ is uniformly bounded). Estimates (3.22) and (3.23) allow us to apply the Aubin-Lions lemma to conclude the existence of a subsequence of (g_ε), which is not relabelled, such that as $\varepsilon \to 0$,

$$g_\varepsilon \to g \quad \text{strongly in } L^2(0,T;L^2(\Omega_\rho)),$$

$$g_\varepsilon \rightharpoonup g \quad \text{weakly in } L^2(0,T;H^1(\Omega_\rho)),$$

$$\partial_t g_\varepsilon \rightharpoonup \partial_t g \quad \text{weakly in } L^2(0,T;H_D^{-1}(\Omega_\rho)).$$

By the Cauchy-Schwarz inequality, this shows that

$$\|K[g_\varepsilon] - K[g]\|_{L^2(0,T;L^2(\Omega_\rho))}$$

$$\leq \left(\int_0^\rho \int_0^\infty \Gamma(v,w)^2 dvdw\right) \int_0^T \int_0^\rho \int_{-\rho}^\rho (g_\varepsilon - g)^2(x,w,t)dxdwdt$$

$$\leq C_\Gamma \|g_\varepsilon - g\|_{L^2(0,T;L^2(\Omega_\rho))} \to 0 \quad \text{as } \varepsilon \to 0.$$

We infer that

$$K[g_\varepsilon]g_\varepsilon \to K[g]g \quad \text{strongly in } L^1(0,T;L^1(\Omega_\rho)).$$

Since $(K[g_\varepsilon]g_\varepsilon)$ is bounded, this convergence holds in L^p for any $p < \infty$. Consequently, we may perform the limit $\varepsilon \to 0$ in (3.14) (with $g^+ = g$ and $K_M[g] = K[g]$) to obtain for all $v \in L^2(0,T;H_D^1(\Omega_\rho))$,

$$\int_0^T \langle \partial_t g, v \rangle = -\int_0^T \int_{\Omega_\rho} \Big((\Phi_x(x,w)g + \Phi(x,w)g_x)v \tag{3.24}$$

$$+ (K[g] + H(w) + D'(w))gv_w + D(w)g_w v_w \Big) dzdt$$

which finishes the proof. $\qquad\square$

To finish the proof of Theorem 9, it remains to perform the limit $R \to \infty$. This limit is based on Cantor's diagonal argument. We have shown that there exists a weak solution g_n to (3.24) with $g_n(0) = g_0$ in the sense of $H_D^{-1}(\Omega_n)$, where $n \in \mathbb{N}$. In particular, (g_n) is bounded in $L^2(0,T;H^1(\Omega_m))$ for all $n \geq m$. We can extract a subsequence $(g_{n,m})$ of (g_n) that converges weakly in $L^2(0,T;H^1(\Omega_m))$ to some $g^{(m)}$ as $n \to \infty$. Observing that the estimates in Step 4 are independent of $\rho = n$, we obtain even the strong convergence $g_{n,m} \to g^{(m)}$ in $L^2(0,T;L^2(\Omega_m))$ and a.e. in $\Omega_m \times (0,T)$. This yields the diagonal scheme

$$g_{1,1}, \ g_{2,1}, \ g_{3,1}, \ \cdots \to g^{(1)} = u|_{\Omega_1 \times (0,T)},$$

$$g_{2,2}, \ g_{3,2}, \ \cdots \to g^{(2)} = u|_{\Omega_2 \times (0,T)},$$

$$g_{3,3}, \ \cdots \to g^{(3)} = u|_{\Omega_3 \times (0,T)},$$

$$\ddots \qquad \vdots$$

This means that there exists a subsequence $(g_{n,1})$ of (g_n) that converges strongly in $L^2(0, T; H^1(\Omega_1))$ to some $g^{(1)}$. From this subsequence, we can select a subsequence $(g_{n,2})$ that converges strongly in $L^2(0, T; H^1(\Omega_1))$ to some $g^{(2)}$ such that $g^{(2)}|_{\Omega_1 \times (0,T)} = g^{(1)}$, etc. The diagonal sequence $(g_{n,n})$ converges to some $g \in L^2(0, T; H^1(\Omega))$ which is a solution to (1.5)-(1.6). $\qquad\square$

3.2.2 *Asymptotic behaviour of the moments*

We analyse the time evolution of the macroscopic moments

$$m_w(g) = \int_\Omega g(x, w, t) w \, dz, \quad m_x(g) = \int_\Omega g(x, w, t) x \, dz,$$

where g is a (smooth) solution to (1.5)-(1.3), in the special situation that $P = 1$ and $\Phi(x, w)$ is given by (3.5). We assume that the number of agents is normalized, $\int_\Omega g \, dz = 1$.

Proposition 14 (Convergence of the first moment $m_w(g)$)**.** *Let $P = 1$ and let Φ be given by (3.5). Then $m_w(g(t)) \to W$ as $t \to \infty$, and the convergence is exponentially fast.*

Proof. Assumption $P = 1$ implies that (recall (3.9))

$$H(w) = w - W, \quad \text{where } W = \int_0^\infty \omega M(\omega) \, d\omega.$$

The parameter W may be the same as in the definition of $\Phi(x, w)$ in (3.5). Using $g = 0$ at $w = 0$ and integrating by parts with respect to w, we obtain

$$\partial_t m_w(g) = - \int_\Omega (K[g]g + H(w)g) \, dz \leq - \int_\Omega (w - W) g \, dz = -m_w(g) + W,$$

where we have taken into account that $K[g] \geq 0$. By Gronwall's lemma, $m_w(g(t))$ converges exponentially fast to the mean value W as $t \to \infty$. $\qquad\square$

Proposition 15 (Convergence of the variance)**.** *Let $P = 1$, $\Gamma(v, w) = \Gamma_0$, $D(w) = w$, and let Φ be given by (3.5). Then $V_w(g(t)) := \int_\Omega g(t)(w - W)^2 dz \to W$ as $t \to \infty$, and the convergence is exponentially fast.*

Proof. We compute

$$\partial_t V_w(g) = -2 \int_\Omega (K[g] + H(w))(w - W) g \, dz + 2 \int_\Omega D(w) g \, dz.$$

Since $\Gamma(v, w) = \Gamma_0$ and $D(w) = w$, we find that $K[g] = \Gamma_0 \rho$ and

$$\begin{aligned} \partial_t V_w(g) &= -2 \int_\Omega (\Gamma_0 \rho (w - W) g + (w - W)^2 g) \, dz + 2 \int_\Omega g w \, dz \\ &= 2(1 - \Gamma_0) m_w(g) + 2\Gamma_0 W - 2 V_w(g) \\ &= 2(m_w(g) - V_w(g)) + 2\Gamma_0 (W - m_w(g)). \end{aligned}$$

We infer from $m_w(g(t)) \to W$ that the variance $V_w(g(t))$ converges to W as $t \to \infty$. $\qquad\square$

Finally, we compute $\partial_t m_x(g)$. Then

$$\partial_t m_x(g) = \int_{\mathbb{R}} \Phi(x, w) g \, dw$$

$$= -\delta\kappa \int_{\mathbb{R}} \int_{\{|w-W|<R\}} g \, dw \, dx + \kappa \int_{\mathbb{R}} \int_{\{|w-W|\geq R\}} g \, dw \, dx.$$

This expression explains the role of the parameter δ. Indeed, assume that in some time interval, the number of agents with estimated asset value around W ($|w - W| < R$) is of the same order as those with asset value which differs significantly from W ($|w-W| \geq R$). Then, for $\delta \gg 1$, the mean rationality is decreasing, and if $\delta \ll 1$, it is increasing. Thus, δ is a measure for the expected mean rationality.

3.3   NUMERICAL SIMULATIONS

We illustrate the behaviour of the solution to the kinetic model derived in Section 3.1.2 by numerical simulations.

3.3.1   *The numerical scheme*

The kinetic equation (3.4) is originally posed in the unbounded spatial domain $(x, w) \in \mathbb{R} \times \mathbb{R}^+$. Numerically, we consider instead a bounded domain, similarly as for the approximate equation (3.12) in the existence analysis. Since the first moment with respect to w is conserved along the evolution, we can normalize the maximal possible asset value to one and thus consider $w \in I = [0, 1]$. For the rationality variable, we approximate the whole line $\mathbb{R}$ by a bounded interval $x \in [-1, 1]$. This means that agents with $x = -1$ are completely irrational and individuals with $x = 1$ are completely rational. A scaling argument shows that we may also choose $x \in [-R, R]$ for any $R > 0$. By our existence analysis, the solution on $[-R, R]$ for sufficiently large R converges to the solution on $\mathbb{R}$. Thus, the reduction to the finite interval $[-1, 1]$ will not destroy the qualitative behaviour of the solution. Thanks to the interaction rules (3.1)-(3.2), we do not need to impose any boundary conditions. Indeed, if we start with a value $w \in I$, the post-interaction value w^* stays in this interval. We choose uniform subdivisions $(x_0, \ldots, x_N)$ for the variable x and $(w_0, \ldots, w_M)$ for the variable w. We take $N = M = 70$ in the simulations. The function $f(x, w, t_k)$ is approximated by f_{ij}^k, where $x \in (x_i, x_{i+1})$, $w \in (w_j, w_{j+1})$, and $t_k = k \triangle t$, where $\triangle t$ is the time step size (we choose $\triangle t = 10^{-5}$).

For the numerical approximation, we make an operator splitting ansatz, i.e., we split the Boltzmann equation (3.4) into a collisional part and a drift part. The collisional part

$$\partial_t f = Q_I(f) \quad \text{or} \quad \partial_t f = Q_H(f, f)$$

is numerically solved by using the interaction rules (3.1) or (3.2), respectively, and a slightly modified Bird scheme [Bir95]. First, we describe the choice of the interaction rule. The stochastic process η is a point process with $\eta = \pm 0.06$ with probability 0.5. The total number of agents is normalized to one. We introduce the number of irrational agents $I_{\mathrm{irr}}(w, t) = \int_{-1}^{0} f(x, w, t) dx$ and the number of rational agents

$I_{\text{rat}}(w,t) = \int_0^1 f(x,w,t)\mathrm{d}x$. If for fixed (w,t), the majority of the agents is rational ($I_{\text{rat}} > 0.6$), we select the herding interaction rule (3.2). If the majority of the market participants is irrational ($I_{\text{rat}} < 0.4$), we choose the interaction rule (3.1). In the intermediate case, the choice of the interaction rule is random. Clearly, this choice could be refined by relating it to the value of the ratio $I_{\text{rat}}/I_{\text{irr}}$. The pairs of individuals that interact are chosen randomly and at each step all the agents interact with the background and with another randomly chosen agent, respectively.

After the interaction part, we need to distribute the function f on the grid. The distribution at w^* is defined by $f(w^*) = f(w) - f(v)$. Then the part $f(w^*)$ is distributed proportionally to the neighbouring grid points w_j and w_{j+1}. In order to avoid that the post-interaction values become negative, some restriction on the random variables are needed; we refer to [DW15, Section 2.1] for details.

At each time step, we solve the transport part

$$\partial_t f = (\Phi(x,w)f)_x$$

using a flux-limited Lax-Wendroff/upwind scheme. More precisely, let $\triangle x = 1/N$ be the step size for the rationality variable, and recall that $\triangle t = 10^{-5}$ is the time step size. The value $f(x_i, w_j, t_k)$ is approximated by f_i^k for a fixed w_j. We recall that the upwind scheme reads as

$$f_i^{k+1} = \begin{cases} f_i^k - \frac{\triangle t}{\triangle x}\Phi(x_i, w_j)(f_i^k - f_{i-1}^k) & \text{if } \Phi(x_i, w_j) > 0, \\ f_i^k - \frac{\triangle t}{\triangle x}\Phi(x_i, w_j)(f_{i+1}^k - f_i^k) & \text{if } \Phi(x_i, w_j) \leq 0, \end{cases}$$

and the Lax-Wendroff scheme is given by

$$f_i^{k+1} = f_i^k - \frac{\triangle t}{2\triangle x}\Phi(x_i, w_j)(f_{i+1}^k - f_{i-1}^k) + \frac{(\triangle t)^2}{2(\triangle x)^2}\Phi(x_i, w_j)^2(f_{i+1}^k - 2f_i^k + f_{i-1}^k).$$

The Lax-Wendroff scheme has the advantage that it is of second order, while the first-order upwind scheme is employed close to discontinuities. The choice of the scheme depends on the smoothness of the data. In order to measure the smoothness, we compute the ratio θ_i^k of the consecutive differences and introduce a smooth van-Leer limiter function $\Psi(\theta_i^k)$, defined by

$$\Psi(\theta_i^k) = \frac{|\theta_i^k| + \theta_i^k}{1 + |\theta_i^k|}, \quad \text{where } \theta_i^k = \frac{f_i^k - f_{i-1}^k}{f_{i+1}^k - f_i}.$$

Our final scheme is defined by

$$f_i^{k+1} = f_i^k - \frac{\triangle t}{\triangle x}\Phi(x_i, w_j)(F_{i+1}^k - F_i^k), \quad \text{where}$$

$$F_i^k = \frac{1}{2}(f_{i-1}^k - f_i^k)$$
$$- \frac{1}{2}\text{sgn}(\Phi(x_i, w_j))\left(1 - \Psi(\theta_i)\left(1 - \frac{\triangle t}{\triangle x}|\Phi(x_i, w_j)|\right)\right)(f_i^k - f_{i-1}^k).$$

3.3.2 *Choice of functions and parameters*

We still need to specify the functions used in the simulations. We take $\tau_H = \tau_I = 1$,

$$P(|w - W|) = 1, \quad d(w) = 4w(1 - w), \quad \gamma(v,w) = 1_{\{w<v\}}v(1 - w),$$

and $\Phi(x, w)$ is given by (3.5). The values of the parameters α, β, R, W, δ, and κ are specified below. With the simple setting $P = 1$, the interaction rule (3.1) becomes $w^* = (1 - \alpha)w + \alpha W + \eta d(w)$. This means that α measures the influence of the public source: if $\alpha = 1$, the agent adopts the asset value W, being the background value; if $\alpha = 0$, the agent is not influenced by the public source. The random variables η is normally distributed with zero mean and standard deviation 0.06.

The diffusion coefficient $d(w)$ is chosen such that it vanishes at the boundary of the domain of definition of w, i.e. at $w = 0$ and $w = 1$, and that its maximal value is one.

The choice of $\gamma(v, w)$ is similar to that one in [DL14, Formula (11)], and we explained its structure already in Section 3.1.1. In (3.3), we have chosen $f(w) = 1 - w$. This means that agents do not change their asset value due to herding when w is close to its maximal value. When the asset value is very low, $w \approx 0$, we have $w^* \approx \beta v + \eta_1 d(w)$, and the agent adopts the value βv.

3.3.3 *Numerical test 1: constant R, constant W*

We choose $R = 0.025$ and $W = 0.5$. The aim is to understand the occurrence of bubbles and crashes depending on the parameters α, β, and κ. We say that a bubble (crash) occurs at time t if the mean asset value $m_w(f(t))$ is larger than $W + R$ (smaller than $W - R$). This definition is certainly a strong simplification. However, there seems to be no commonly accepted scientific definition or classification of a bubble. Shiller [Shi00, page 2] defines "a speculative bubble as a situation in which news of price increases spurs investor enthusiasm, which spreads by psychological contagion from person to person". Our definition may be different from the usual perception of a bubble or crash in real markets.

Figure 13 (left) presents the percentage of bubbles and crashes for different values of α. More precisely, we count how often the mean asset value is larger than $W + R$ (smaller than $W - R$) and how often it lies in the range $[W - R, W + R]$. The quotient defines the percentage of bubbles (crashes). The simulations were performed 200 times and the mean asset value is then averaged. We observe that bubbles occur more frequently when α is close to zero. This may be explained by the fact that α represents the reliability of the public information, and when this quantity is small, the agents do not trust the public source. If α is close to one, all the market participants rely on the public information. This means that they assume an asset value close to the "fair" prize W. This corresponds to a herding behaviour, and the herding interaction rule, which tends to higher values, applies, leading to bubble formation. A market that does neither overestimate nor underestimate public information leads to the smallest bubble percentage, here with α being around 0.5. Interestingly, the results vary only slightly with respect to the parameter β.

The percentage of crashes is depicted in Figure 13 (right). Qualitatively, the percentage is small for values α not too far from 0.5, but the shape of the curves is more complex than those for bubbles. For instance, there is a local maximum at $\alpha = 0.1$ and a local minimum at
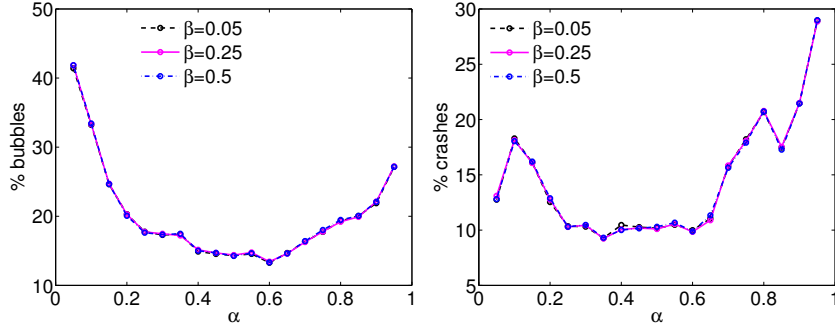
Figure 13: Left: Percentage of bubbles (left) and crashes (right) depending on the choice of α and β. The parameters are $R = 0.025$, $W = 0.5$, $\delta = \kappa = 1$.

$\alpha = 0.85$. The percentage of crashes is largest for α close to one. Again, the dependence on the parameter β is very weak.

In the above simulations, we have assumed a constant value for α, i.e., all market participants have the same attitude to change their mind when interacting with public sources. We wish to show that nonconstant values lead to similar conclusions. For this, we generate α from a normal distribution with standard deviation 0.45 and various means $\langle \alpha \rangle$. The result is shown in Figure 14 for $\beta = 0.25$ and $\beta = 0.5$. For comparison, the percentages for constant α and $\beta = 0.05$ are also shown. It turns out that the results for nonconstant or constant α are qualitatively similar which justifies the use of constant α.
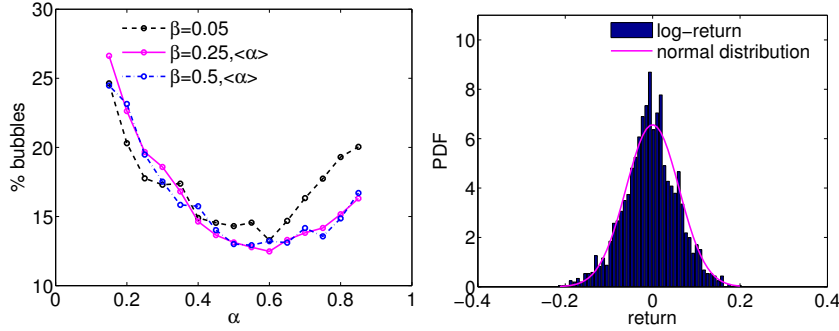
Figure 14: On the left: percentage of bubbles for varying α ($\beta = 0.25$) and constant α ($\beta = 0.5$ and $\beta = 0.05$); on the right: in blue is represented the probability distribution function for the logarithmic return, in magenta the normal distribution with same mean and variance as the return.

In Figure 14 (on the right) we show an empirical distribution function for the logarithmic return r_t which has been computed in the following way:

$$r_t = \ln\left(\frac{m_w(t)}{m_w(t - \Delta t)}\right), \quad \Delta t = 50, \quad t \in [0, 2500].$$

The first moment $m_w(t)$ has been computed choosing the parameters $\alpha = 0.35$, $\beta = 0.25$, and $\delta = 2$. The return distribution has a mean very close to zero and variance 0.0037. A normal distribution (in magenta) with the same mean and the same variance as the return is also shown for comparison. The returns are negatively skewed (skewness -0.1104) and leptokurtic (kurtosis 3.2743). These features are consistent with characteristics of real financial time series.
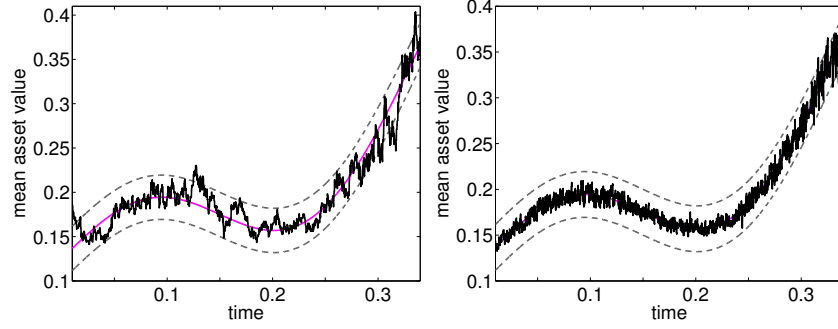
3.3.4   *Numerical test 2: constant R, time-dependent $W(t)$*

Now, we chose $R = 0.025$ and

$$W(t) = 0.1 + 0.05\left(\sin\frac{t}{500\triangle t} + \frac{1}{2}\exp\frac{t}{1500\triangle t}\right), \quad t \geq 0.$$

The time evolution of the first moment $m_w(f(t)) = \int_{\Omega_1} f(x, w, t)w\mathrm{d}z$ is shown in Figure 15. We see that the mean asset value stays within the range $[W(t) - R, W(t) + R]$ if α is small (except for increasing "fair" prices) and it has the tendency to take values larger than $W(t)$ if α is large.

Figure 15: Mean asset value $m_w(f(t))$ versus time t for $\alpha = 0.5$ (right) and $\alpha = 0.05$ (left). The function $W(t)$ is represented by the solid line in between the dashed lines which represent the functions $W(t) + R$ and $W(t) - R$. The parameters are $\beta = 0.25$, $R = 0.025$, $\delta = 2$, $\kappa = 1$.

Figure 16 illustrates the influence of the parameter δ which describes the strength of the drift in the region $|w - W(t)| < R$. The background value $W(t)$ models a crash: it increases up to time $t = 0.2$ then decreases abruptly, and stays constant for $t > 0.2$. For small values of δ, the mean asset value decreases slowly while it adapts to $W(t)$ more quickly when δ is large. Interestingly, we observe a (small) time delay for small δ although the equations do not contain any delay term. The delay is only caused by the slow drift term. The same phenomenon can be reproduced for abruptly increasing $W(t)$.
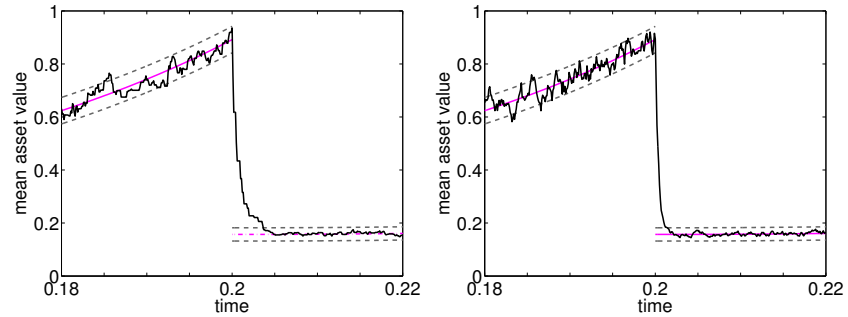
Figure 16: Mean asset value $m_w(f(t))$ versus time for $\delta = 0.01$ (left) and $\delta = 100$ (right) with $\alpha = 0.25$, $\beta = 0.2$, $R = 0.025$, $\kappa = 1$.

3.3.5   *Numerical test 3: time-dependent $R(t)$*

The final numerical test is concerned with time-dependent bounds $R(t)$. We distinguish the upper and lower bound and accordingly the

boundaries $w = W(t) + R^+(t)$ and $w = W(t) - R^-(t)$. The functions $R^\pm(t)$ are defined as the Bollinger bands which are volatility bands above and below a moving average. They are employed in technical chart analysis although its interpretation may be delicate. The definition reads as

$$R^\pm(t_k) = M_n(t_k) \pm k\sigma(t_k),$$

where $M_n(t_k)$ is the n-period moving average (we take $n = 30$), k is a factor (usually $k = 2$), and $\sigma(t_k)$ is the corrected sample standard deviation,

$$M_n(t_k) = \frac{1}{n} \sum_{\ell=1}^{n} m_w(f(t_{k-\ell})),$$

$$\sigma(t_k) = \left(\frac{1}{n-1} \sum_{\ell=1}^{n} \left(m_w(f(t_{k-\ell})) - M_n(t_{k-\ell}) \right)^2 \right)^{1/2}.$$

Figure 17 shows the time evolution of the mean asset value and the Bollinger bands for two different values of α and constant W. One may say that the market is overbought (or undersold) when the asset value is close to the upper (or lower) Bollinger band. For small values of α, the market participants are not much influenced by the public information and they tend to increase their estimated asset value due to herding.
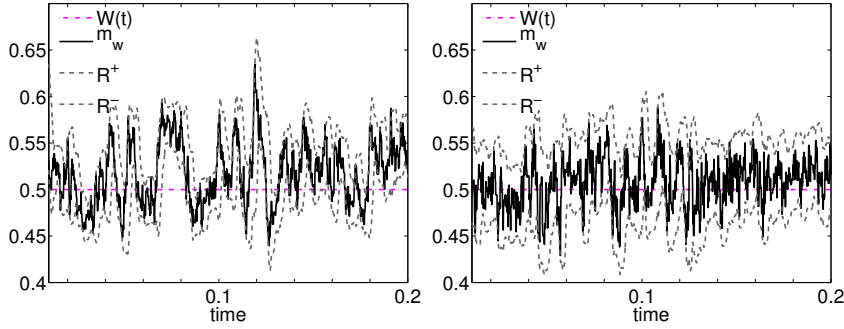
Figure 17: Mean asset value $m_w(f(t))$ and Bollinger bands $R^\pm(t)$ versus time for $\alpha = 0.2$ (right) and $\alpha = 0.05$ (left). The parameters are $\beta = 0.25$, $W = 0.5$, $\delta = 1$, $\kappa = 1$.

The mean asset value and the corresponding Bollinger bands for a discontinuous background value $W(t)$ is displayed in Figure 18 (left column). We have chosen $d(w) = w(1 - w)$ and $\eta = \pm 0.06$ (upper row) or $\eta = \pm 0.18$ (lower row).

The value $W(t)$ abruptly decreases at time $t = 0.2$. We are interested in the difference of the upper and lower Bollinger bands, more precisely in the Bollinger bandwidth $B(t) = 100(R^+(t) - R^-(t))/W(t)$, measuring the relative difference between the upper and lower Bollinger bands. According to chart analysts, falling (increasing) bandwidths reflect decreasing (increasing) volatility. In our simulation, the jump of $W(t)$ gives rise to a peak of the Bollinger bandwidth at $t = 0.2$; see Figure 18 (right column). Another small peak can be observed at $t \approx 0.38$ (upper right figure) when $\eta = \pm 0.06$. For larger values of η (lower right figure), the fluctuations in the Bollinger bandwidth are larger.
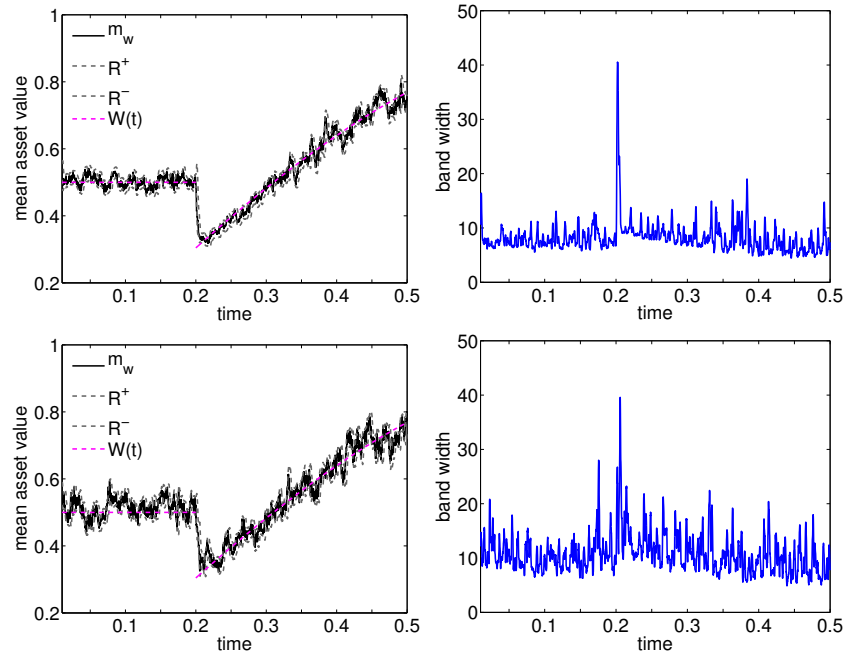
Figure 18: Mean asset value $m_w(f(t))$ (left column) and Bollinger bands $R^{\pm}(t)$ (right column) versus time. The function $W(t)$ has a jump at $t = 0.2$. The parameters are $\alpha = 0.05$, $\beta = 0.25$, $R = 0.025$, $\delta = \kappa = 1$. Upper row: $\eta = \pm 0.06$, lower row: $\eta = \pm 0.18$.

BOLTZMANN EQUATION FOR WEALTH AND KNOWLEDGE EXCHANGES

The chapter is organised as follow. Section 4.1 is dedicated to the presentation of the microscopic and kinetic models of wealth and knowledge exchange processes. Section 4.1.3 gives a proper mathematical framework of the model. In Section 4.2, we provide numerical experiments, including a study of the quasi-invariant knowledge case.

4.1 KINETIC MODEL

We want to foresee the time evolution of a population of agents who are described thanks to two characteristics: their wealth and their knowledge. Using the formalism of kinetic theory, we are led to introduce an unknown distribution function $f : \mathbb{R}_+ \times \mathbb{R}_+^* \times \mathbb{R}_+^* \to \mathbb{R}_+$, $(t, x, v) \mapsto f(t, x, v)$, where $t \geq 0$ is the time variable, $x > 0$ the knowledge and $v > 0$ the wealth. Then the quantity $f(t, x, v) \, \mathrm{d}x \, \mathrm{d}v$ can be understood as the fraction of agents of the population inside an elementary volume of the phase space (in both knowledge and wealth variables) centred at (x, v) and of measure $\mathrm{d}x \, \mathrm{d}v$.

We first need to describe the microscopic mechanisms between agents for both knowledge and wealth to be able to define the associated mesoscopic collision operators of Boltzmann type, and eventually write the kinetic equation governing the time evolution of f.

In what remains, for the sake of simplicity, when we write "agent (x, v)", that means that we deal with an agent of knowledge x and wealth v.

4.1.1 *Microscopic exchanges of knowledge and wealth*

An agent in the population can interact with any other one. We here assume that those interactions are of binary type, i.e. we suppose that the interactions involving three individuals or more can be seen as the "sum" of binary exchanges between agents. Moreover, the wealth and knowledge exchanges are chosen to be independent. That means that an agent does not interact with another one for both wealth and knowledge at the same time.

Let us first describe the knowledge binary exchange process, and consider two agents (x, v) and (y, w). Their knowledges x' and y' are updated thanks to the following collision (with the kinetic theory vocabulary) rule

$$\begin{cases} y' = y + \kappa(v)(x - y) = \kappa(v)x + [1 - \kappa(v)]y, \\ x' = x + \kappa(w)(y - x) = [1 - \kappa(w)]x + \kappa(w)y, \end{cases} \tag{4.1}$$

where $\kappa : \mathbb{R}_+^* \to [\alpha, 1/2)$ is a non-decreasing function of the wealth variable, with $0 < \alpha \ll 1/2$. For instance, we can choose κ constant or satisfying $\kappa(v) = [1 - (1 - 2\alpha)e^{-2v}]/2$. The previous mechanism (4.1) implies that the knowledge change for an individual depends on the

wealth of the other agent involved in the interaction. More precisely, κ can be considered as a *confidence* function, in the sense that the bigger v is with respect to w, the more agent (y, w) trusts agent (x, v). Let us point out that this rule is quite similar to the one presented in [Tos06]. As a matter of fact, the post-collisional knowledge x' is computed from x, contrary to [BS09] where the average opinion was used, by adding a quantity involving the relative knowledge $x - y$ and a coefficient $\kappa(w)$ depending on the wealth of the other agent. The dependence of this coefficient is a new feature, since it was previously related to x and not w in [Tos06]. We must also emphasize that the main difference with [PT14] lies in the fact that we allow interaction between agents for the exchange of information, whereas Pareschi and Toscani used the interaction a given background of information with a mean-field point of view.

Since x' and y' are clearly convex combinations of x and y, the knowledge bounds are preserved at the microscopic level, i.e. $[x', y'] \subset [x, y]$. There should eventually be a knowledge concentration effect inside the population, if there is no other phenomenon taken into account for the knowledge variable. Note that, nevertheless, there are no reasons for this concentration to go to the initial average knowledge. Indeed, the microscopic post-collisional total knowledge

$$x' + y' = x + y + (\kappa(v) - \kappa(w))(x - y)$$

can be larger than $x + y$ if we simultaneously have $x > y$ and $v > w$, ensuring that the exchange process is profitable to everyone when a wealthy well-informed agent interacts with the rest of the population.

As we can see, this whole behaviour remains quite simplistic from the modelling point of view, but it has the mathematical benefit that the collision rule (4.1) is invertible: both x and y can be expressed in terms of x' and y', since the Jacobian $J_K(v, w)$ of (4.1), which does not depend on x and y, writes $J_K(v, w) = \kappa(v) + \kappa(w) - 1$, and clearly remains negative for any v, w, by assumption on κ. We can also add to (4.1) a threshold effect, which is probably more realistic. The model then relies on a bounded-confidence assumption, i.e. the knowledge interaction is forbidden between agents (x, v) and (y, w) when $|v - w| \leq \omega$, where $\omega > 0$ is given. This assumption is very common in the literature of opinion dynamics, see [DNAW00, HK02] for instance.

Let us now focus on the wealth binary exchange process, and consider again two agents (x, v) and (y, w). Their wealth values v' and w' after interaction are given by the collision rule

$$\begin{cases} v' = [1 - \Psi(x)\gamma]v + \Psi(y)\gamma w, \\ w' = \Psi(x)\gamma v + [1 - \Psi(y)\gamma]w, \end{cases} \tag{4.2}$$

where $\gamma \in (0, 1)$ is fixed and $\Psi : \mathbb{R}_+^* \to (0, 1]$ is a non-increasing continuous function of the knowledge variable, for instance, $\Psi(x) = (1 + x)^{-\beta}$, with $\beta > 0$. The collision rule (4.2) is exactly the one used in [PT14] without the random risk parameter, and was first proposed in a simplified version in [CPT05]. This is a real modelling choice, since we believe that the saving and risk propensities of each agent are directly linked. That is why we choose, in this work, to treat them with the sole quantity $\gamma\Psi(x)$, which can then be understood as the saving/risk-taking propensity of agent (x, v). The monotonicity of Ψ implies that

the more an agent has knowledge, the less risky is the wealth exchange for him. Note that, for the well-posedness result detailed in Section 4.1.3, we need a stronger assumption on the lower bound of Ψ.

Moreover, it is clear that the microscopic total wealth is conserved during the exchange process: $v' + w' = v + w$. We also emphasize that v' and w' are not convex combinations of v and w, but satisfy some relevant properties, such as the following one. Assuming that $x > y$, which implies that $\Psi(x) \leq \Psi(y)$, we then have

$$v' \geq v + (w - v)\Psi(x)\gamma.$$

That ensures that the interaction of an agent with another one, richer but less informed, is profitable to the first one. Of course, there is an arguable situation when both y and w are respectively smaller than x and v. In such a case, agent (x, v) may not want to interact with (y, w), since he would have nothing to win in the wealth exchange. Consequently, a wealth threshold effect should also be investigated in the latter case. This will be more precisely discussed in the numerical experiments.

Eventually, we must point out a mathematical issue: the collision rule (4.2) may not be invertible. Indeed, we can check that the Jacobian J_W of (4.2), which does not depend on v and w, satisfies, for any x, y,

$$J_W(x, y) = 1 - \gamma(\Psi(x) + \Psi(y)) \in (1 - 2\gamma, 1).$$

Since Ψ is continuous, the previous bounding of $J_W(x, y)$ can be zero if $\gamma > 1/2$ for some values of x and y. This range of values of γ is realistic at the microscopic level, see [PT14] for more details. Nevertheless, for mathematical reasons, we choose $\gamma \leq 1/2$ to ensure the invertibility of (4.2).

Remark 16. *The microscopic property $[x', y'] \subset [x, y]$ clearly implies that, if f^{in} has a compact support in the knowledge variable, so has f at any time.*

4.1.2   Collision operators and governing equation

In order to take into account those microscopic collision rules (4.1)–(4.2) in the time evolution of the distribution function f, we need to write the related collision operators Q_K and Q_W. As we already stated, there is a possible issue on the non-invertibility of (4.2). Moreover, the rules may not diffeomorphisms from $\mathbb{R}_+^*$ onto itself. Then, to overcome those difficulties, as explained in [BS09, p.511], the natural framework consists in writing the collision operators under weak forms.

For a suitable test-function ϕ of (x, v), we write the weak form of the collision operator $Q_K(f, f)$, acting on the knowledge variable, as

$$\langle Q_K(f, f), \phi \rangle$$
$$= \nu_K \iint_{\mathbb{R}_+^{*4}} f(t, x, v)f(t, y, w)\left(\phi(x', v) - \phi(x, v)\right) \mathrm{d}x\,\mathrm{d}y\,\mathrm{d}v\,\mathrm{d}w$$
$$= \frac{\nu_K}{2} \iint_{\mathbb{R}_+^{*4}} f(t, x, v)f(t, y, w)$$
$$\left(\phi(x', v) + \phi(y', w) - \phi(x, v) - \phi(y, w)\right) \mathrm{d}x\,\mathrm{d}y\,\mathrm{d}v\,\mathrm{d}w, \quad (4.3)$$

where $\nu_K > 0$ denotes the interaction frequency in the population for the knowledge exchange. Both expressions of $Q_K(f, f)$ in (4.3) are equal, thanks to the change of variables $(x, y, v, w) \mapsto (y, x, w, v)$, whose Jacobian equals 1. In the same way, for the collision operator $Q_W(f, f)$, which acts on the wealth variable, we write, for any suitable test-function ϕ,

$$
\langle Q_W(f, f), \phi \rangle
$$
$$
= \nu_W \iint_{\mathbb{R}_+^{*4}} f(t, x, v) f(t, y, w) \left(\phi(x, v') - \phi(x, v) \right) dx\, dy\, dv\, dw
$$
$$
= \frac{\nu_W}{2} \iint_{\mathbb{R}_+^{*4}} f(t, x, v) f(t, y, w)
$$
$$
\left(\phi(x, v') + \phi(y, w') - \phi(x, v) - \phi(y, w) \right) dx\, dy\, dv\, dw, \quad (4.4)
$$

where $\nu_W > 0$ denotes the interaction frequency in the population for the wealth exchange.

Let us set, for any $w > 0$,

$$
D_K(w) = \{(x, x') \in \mathbb{R}^2 \mid 0 < (1 - \kappa(w))x < x'\} \subset \mathbb{R}_+^{*2}
$$

and, for any $x > 0$,

$$
D_W(x) = \{(v, v') \in \mathbb{R}^2 \mid 0 < (1 - \gamma\Psi(x))v < v'\} \subset \mathbb{R}_+^{*2}.
$$

It is then easy to check that the transformations $(x, y) \mapsto (x, x')$ for a fixed $w > 0$ and $(v, w) \mapsto (v, v')$ for a fixed $x > 0$ are bijections, respectively $D_K(w) \to \mathbb{R}_+^{*2}$ and $D_W(x) \to \mathbb{R}_+^{*2}$. Both weak forms (4.3)–(4.4) can be written as the difference between the weak form of gain terms $Q_K^+(f, f)$, $Q_W^+(f, f)$, and loss terms $Q_K^-(f, f)$, $Q_W^-(f, f)$, which do not use the post-collisional variables at all. More precisely, we have, for any test-function ϕ,

$$
\langle Q_K^+(f, f), \phi \rangle = \iint_{\mathbb{R}_+^{*4}} \frac{\nu_K \mathbb{1}_{D_K(w)}(x', x)}{\kappa(w)} \tag{4.5}
$$
$$
f(t, x', v) f\left(t, \frac{x - (1 - \kappa(w))x'}{\kappa(w)}, w \right) \phi(x, v)\, dx\, dx'\, dw\, dv,
$$

$$
\langle Q_W^+(f, f), \phi \rangle = \iint_{\mathbb{R}_+^{*4}} \frac{\nu_W \mathbb{1}_{D_W(x)}(v', v)}{\gamma\Psi(y)} \tag{4.6}
$$
$$
f(t, x, v') f\left(t, y, \frac{v - ((1 - \gamma\Psi(x)))v'}{\gamma\Psi(y)} \right) \phi(x, v)\, dv\, dv'\, dy\, dx,
$$

$$
\langle Q_K^-(f, f), \phi \rangle = \nu_K \iint_{\mathbb{R}_+^{*4}} f(t, x, v) f(t, y, w) \phi(x, v)\, dx\, dy\, dv\, dw,
$$
$$
\tag{4.7}
$$

$$
\langle Q_W^-(f, f), \phi \rangle = \nu_W \iint_{\mathbb{R}_+^{*4}} f(t, x, v) f(t, y, w) \phi(x, v)\, dx\, dy\, dv\, dw,
$$
$$
\tag{4.8}
$$

where $\mathbb{1}_E$ denotes the characteristic function of any subset E of $\mathbb{R}_+^{*2}$. The gain terms quantify the exchanges of knowledge/wealth between individuals which produce, after the interaction with another agent, an agent (x, v). The loss terms take into account the exchanges of knowledge/wealth where an agent (x, v) is involved before the collisional process.

Note that the collision rules and operators about the knowledge variable do not imply the possibility of a time delay in the learning

process. The way how the agents gather knowledge is an intricate process and modelling it remains difficult.

Let $T > 0$. The previous considerations allow to eventually write down the integro-differential equation of Boltzmann type, satisfied, in a weak sense, by the distribution function f, that is, for any suitable test-function ϕ of (x, v) and almost every $t \in [0, T]$,

$$\int_{\mathbb{R}_+^{*2}} \partial_t f(t, x, v) \phi(x, v) \, dx \, dv = \langle Q_K(f, f), \phi \rangle + \langle Q_W(f, f), \phi \rangle, \quad (4.9)$$

with initial condition $f(0, \cdot, \cdot) = f^{\text{in}}$, where the nonnegative function $f^{\text{in}} \in L^1(\mathbb{R}_+^{*2})$ is given.

The conservation of the total number of agents in the population is a straightforward consequence of the weak formulations (4.3)–(4.4). We have the following

Proposition 17. *Let* $f \in L^\infty(0, T; L^1(\mathbb{R}_+^{*2}))$ *solving (4.9). Then we have, for a.e.* t,

$$\|f(t, \cdot, \cdot)\|_{L^1(\mathbb{R}_+^{*2})} = \|f^{\text{in}}\|_{L^1(\mathbb{R}_+^{*2})}.$$

Proof. We just have to choose $\phi \equiv 1$ in (4.9) and use (4.3)–(4.4) for that test-function. □

Some a priori estimates on the collision operators and the well-posedness of the Boltzmann equation (4.9) is investigated in the following Section.

4.1.3 *Well-posedness of the problem*

We first need a priori estimates on the collision operators.

Lemma 18. *Assume that* Ψ *is lower-bounded by a constant* $\delta > 0$. *Let* $g \in L^1(\mathbb{R}_+^{*2})$. *Then* $Q_K^\pm(g, g)$ *and* $Q_W^\pm(g, g)$ *also lie in* $L^1(\mathbb{R}_+^{*2})$, *and the following estimates hold:*

$$\|Q_K^+(g, g)\|_{L^1(\mathbb{R}_+^{*2})} \leq \frac{\nu_K}{\alpha} \|g\|_{L^1(\mathbb{R}_+^{*2})}^2,$$

$$\|Q_K^-(g, g)\|_{L^1(\mathbb{R}_+^{*2})} \leq \nu_K \|g\|_{L^1(\mathbb{R}_+^{*2})}^2,$$

$$\|Q_W^+(g, g)\|_{L^1(\mathbb{R}_+^{*2})} \leq \frac{\nu_W}{\gamma \delta} \|g\|_{L^1(\mathbb{R}_+^{*2})}^2,$$

$$\|Q_W^-(g, g)\|_{L^1(\mathbb{R}_+^{*2})} \leq \nu_W \|g\|_{L^1(\mathbb{R}_+^{*2})}^2.$$

Proof. This lemma is a straightforward consequence of (4.5)–(4.8) with $\phi \equiv 1$ and Prop. 17. □

Remark 19. *The additional hypothesis on* Ψ *in Lemma 18 is not that limiting. It is enough, for instance, to replace it by an assumption stating that* g *is compactly supported in* x, *see Remark 16. That implies that* Ψ *is straightforwardly lower bounded by* δ *on that compact support, since* Ψ *is continuous.*

Theorem 20. *Assume again that* Ψ *is lower-bounded by a constant* $\delta > 0$. *Let* f^{in} *a nonnegative function in* $L^1(\mathbb{R}_+^{*2})$. *Then there exists a nonnegative* $f \in L^\infty(0, T; L^1(\mathbb{R}_+^{*2}))$ *which weakly solves (4.9) for almost every* t, *with initial datum* f^{in}.

Proof. We follow the same kind of strategy as in [BS09], but without any diffusion term. Set

$$\rho = \int_{\mathbb{R}_+^{*\,2}} f^{\text{in}}(x, v) \, dx \, dv.$$

and define $(f^n)_{n \in \mathbb{N}}$ by induction with $f^0 \equiv 0$, solving, for any $t \in [0, T]$,

$$\partial_t f^{n+1} + \sigma f^{n+1} = Q_K^+(f^n, f^n) + Q_W^+(f^n, f^n), \tag{4.10}$$

with the initial condition $f^{n+1}(0, \cdot, \cdot) = f^{\text{in}}$, where we set $\sigma = \rho(\nu_K + \nu_W) > 0$. Existence of solutions to (4.10) is straightforward, since f^{n+1} is not involved in the right-hand side of (4.10) (which we know is in $L^1(\mathbb{R}_+^{*\,2})$), and we also have $f^{n+1} \in C^0([0, T]; L^1(\mathbb{R}_+^{*\,2}))$.

Let us first prove by induction that f^n is nonnegative for any n. It is clear for $n = 0$. Assume now that $f^n \geq 0$. We want to prove that $f^{n+1} \geq 0$. From (4.10), we immediately get

$$\int_{\mathbb{R}_+^{*\,2}} \partial_t f^{n+1} \phi \, dx \, dv + \sigma \int_{\mathbb{R}_+^{*\,2}} f^{n+1} \phi \, dx \, dv \geq 0$$

for any nonnegative test-function ϕ. Multiplying by $e^{\sigma t}$ allows to prove that, for any nonnegative test-function ϕ,

$$\int_{\mathbb{R}_+^{*\,2}} f^{n+1} \phi \, dx \, dv \geq e^{-\sigma t} \int_{\mathbb{R}_+^{*\,2}} f^{\text{in}} \phi \, dx \, dv \geq 0,$$

which leads to the nonnegativity of f^{n+1}.

In the same way, we can prove that (f^n) is non-decreasing. We of course have $f^1 \geq f^0 \equiv 0$. Suppose that $f^n \geq f^{n-1}$, for a given $n \geq 0$. The difference $f^{n+1} - f^n$ satisfies the following equation, for any ϕ,

$$\int_{\mathbb{R}_+^{*\,2}} \partial_t (f^{n+1} - f^n) \phi \, dx \, dv + \sigma \int_{\mathbb{R}_+^{*\,2}} (f^{n+1} - f^n) \phi \, dx \, dv$$
$$= \langle Q_K^+(f^n, f^n), \phi \rangle - \langle Q_K^+(f^{n-1}, f^{n-1}), \phi \rangle$$
$$+ \langle Q_W^+(f^n, f^n), \phi \rangle - \langle Q_W^+(f^{n-1}, f^{n-1}), \phi \rangle.$$

The right-hand side of the previous equality is nonnegative because $f^n \geq f^{n-1}$. Consequently, we can write, for any nonnegative ϕ,

$$\frac{d}{dt} \left(e^{\sigma t} \int_{\mathbb{R}_+^{*\,2}} (f^{n+1} - f^n) \phi \, dx \, dv \right) \geq 0.$$

Noticing that the initial datum for $f^{n+1} - f^n$ is zero, that allows to conclude that (f^n) is non-decreasing. In particular, that ensures that

$$\int_{\mathbb{R}_+^{*\,2}} f^n \, dx \, dv \leq \int_{\mathbb{R}_+^{*\,2}} f^{n+1} \, dx \, dv. \tag{4.11}$$

We can then prove, by induction, that

$$\int_{\mathbb{R}_+^{*\,2}} f^n \, dx \, dv \leq \rho. \tag{4.12}$$

We can write, from (4.10), thanks to the invariance properties of $Q_K(f^n, f^n)$ and $Q_W(f^n, f^n)$,

$$\frac{\mathrm{d}}{\mathrm{d}t}\left(\int_{\mathbb{R}_+^{*2}} f^{n+1}\,\mathrm{d}x\,\mathrm{d}v\right) = (\nu_K + \nu_W)\left[\left(\int_{\mathbb{R}_+^{*2}} f^n\,\mathrm{d}x\,\mathrm{d}v\right)^2 - \rho \int_{\mathbb{R}_+^{*2}} f^{n+1}\,\mathrm{d}x\,\mathrm{d}v\right].$$

Using (4.11) and the inductive hypothesis, we observe that the right-hand side of the previous equality is non-positive, which allows to recover (4.12) for f^{n+1}.

Because of the monotonicity and the uniform bound (4.12) of (f^n), the monotone convergence theorem ensure the existence of $f \in L^\infty(0, T; L^1(\mathbb{R}_+^{*2}))$ such that (f^n) converges towards f almost everywhere, and in $L^1(\mathbb{R}_+^{*2})$, for almost every t.

We conclude that f solves (4.9) in the distributional sense in time and in a weak sense in $L^1(\mathbb{R}_+^{*2})$, exactly in the same way as in [BS09].

$\square$

Note that, in the numerical experiments, which are described in the next section, we endeavour to keep this conservation property true.

4.2 NUMERICAL EXPERIMENTS

In this section, we briefly discuss the numerical method and the computational tools. Then we present some numerical experiments on the model on various situations, including the quasi-invariant knowledge asymptotics.

4.2.1 *Numerical values, computational strategy*

The main issue here is to deal with both variables involved, wealth and knowledge, i.e. to discretize a two-dimensional model. We use a standard particle method [Bir95]. That means that f is approximated as a sum of Dirac masses:

$$f(t, x, v) \simeq \sum_{p=1}^{2N} \delta_{(x_p(t), v_p(t))}(x, v),$$

where $2N$ is the total number of agents in the numerical simulation, and $x_p(t)$, $v_p(t)$ are respectively the knowledge and wealth of an agent p at time t. The set of agents p with $1 \leq p \leq 2N$, is representative, from a statistical viewpoint, of the population. In what follows, N is chosen equal to 1000. As usual in a particle method, we have to compute afterwards an average between $M = 30$ different simulations. The final computational time T is chosen accordingly to the speed of convergence of each experiment.

To define the microscopic collision rules (4.2)–(4.1), we need κ, γ and Ψ: $\kappa(v) = [1 - (1 - 2\alpha)e^{-2v}]/2$ with $\alpha = 0.05$ or κ constant, $\gamma = 0.21$ and $\Psi(x) = (1 + x)^{-\beta}$ with $\beta = 1$.

The initial data we investigate are chosen with compact supports in both variables making a random selection from a uniform law.

For the knowledge variable, it is quite clear that it is possible to have a compact support, since the post-collisional knowledge values are bounded by the pre-collisional ones, as stated in 4.1.1. Therefore, we

assume that x lies in $[0, X]$ with $X = 1$. It is not a restrictive hypothesis from the computational viewpoint (although it is from the modelling one). Indeed, in principle, we just have to select the M populations and take the maximal possible value of x as the upper bound and renormalize the knowledge variables so that they all lie in $[0, 1]$. We proceed in the same way for the wealth variable, noticing that, this time, the wealth is only conserved at the whole population level. Hence, the initial data for v are chosen such that any wealth value lies in $[0, V]$, with $V = 10$. But in fact, at least after a few time steps, it is enough to choose the maximal value of v equal to 2. Consequently, most graphics presented below are shown for $(x, v) \in [0, 1] \times [0, 2]$. Moreover we do not need to impose any boundary conditions thanks to the collisional rules. We use a regular subdivision $(x_0, ..., x_H)$ for the variable x and $(v_0, ..., v_K)$ for the variable v. In the simulation we fix $H = K = 100$. Thus for each agent we get a certain value x_p and v_p for $p = 1, ..., 2N$ such that $x_p \in (x_i, x_{i+1})$ and $v_p \in (v_j, v_{j+1})$.

Since we normalised the total number of agents to one, the contribution of each individual is $1/(2NM)$ and we want to distribute the agents on the grid $[0, 1] \times [0, 2]$. For each time step t^n we check in which cell $(x_i, x_{i+1}) \times (v_j, v_{j+1})$ the value (x_p, v_p) is located and we add the quantity $1/(2NM)$ in the corresponding cell:

$$f(t^n, x_{i+1/2}, v_{j+1/2}) = \sum_{p=1}^{2N} \sum_{m=1}^{M} \frac{1}{2NM} \delta_{(x_i, x_{i+1}) \times (v_j, v_{j+1})}(x_p, v_p).$$

In particular the time $t^n = n\Delta t$, where Δt is the time step size (and we choose $\Delta t = \min(1/\nu_K, 1/\nu_W)$).

The collisions in x and v are independent, so the interactions for the wealth and the knowledge can simultaneously happen, but involve different agents, which are of course randomly chosen. Moreover, since we are interested in the case when there is no predominance of one kind of collision, we fix $\nu_K = \nu_W = 1$.

So, at each time step using a slightly modified Bird scheme [Bir95], we solve the two collisional parts

$$\partial_t f = Q_K(f, f), \text{ and } \partial_t f = Q_W(f, f)$$

according to the interaction rules (4.1)–(4.2).

After the collisions we obtain new values for the knowledge and the wealth and for each time step we can always reconstruct f as before.

The whole computational strategy is embedded in a numerical code written in C.

We can check that it exactly conserves the total number of agents, recovering the property from Proposition 17.

4.2.2   *Basic tests*

Let us first start with a constant $\kappa = 0.34$ and an initial datum which is uniform with respect to to (x, v) on $[0, 1] \times [0, 1]$, as seen on Figure 19a. The collision operators have a concentration effect which does not depend on the initial datum. Consequently, if t is large enough, $f(t, \cdot, \cdot)$
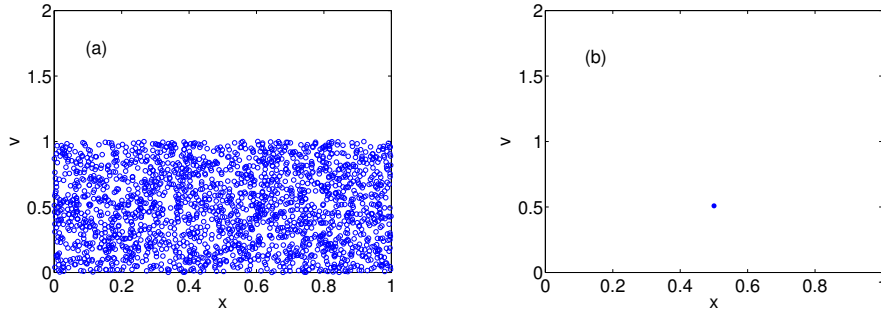
Figure 19: (a) Initial uniform distribution of 2000 agents on $[0,1] \times [0,1]$; (b) distribution at final time.

should behave like a Dirac mass. Since κ is constant, the concentration happens at the average values of x and v at initial time, which both equal 0.5, see Figure 19b. Note that if κ is not constant, the concentration also happens, but not necessarily at the average value of x, since the collision rule (4.1) for x does not conserve the total knowledge. It should be possible to prove that $f(t, \cdot, \cdot)$ converges to a Dirac mass exponentially fast in time, when t goes to $+\infty$. Nevertheless, this large-time result is not realistic from the modelling viewpoint: a society where all the individuals exactly share the same wealth and knowledge is utopian.
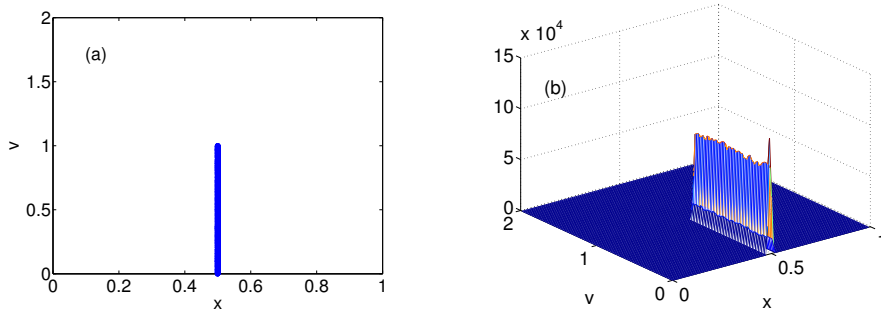
Figure 20: Profile of f at final time with only information exchanges: (a) agents distributed along a vertical line (one draw); (b) averaged result.

In the same way, if we only consider one type of collisions, we can observe the effect of the corresponding operator in the numerical simulations. For instance, we take again the same initial datum as in Figure 19a. The distribution at final time demonstrates a concentration effect, but on a line (since the other variable has no influence).

The knowledge collision rules (4.1) induce concentrating the agents at the average knowledge value, 0.5 on Figure 20, with no effect on the wealth distribution. The situation with the wealth collision rule (4.2) is different, as shown on Figure 21. When time grows, all the agents are on the same line, but they do not have the same wealth, because the less informed agents become poorer, and the more informed richer, which somehow seems more realistic.
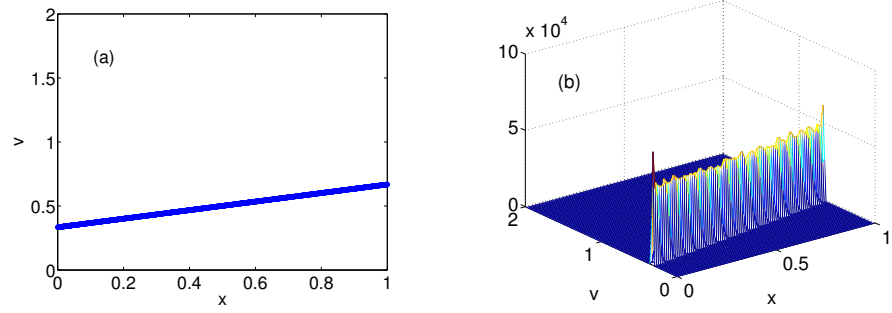
Figure 21: Profile of f at final time with only wealth exchanges: (a) agents distributed along a non-horizontal line (one draw); (b) averaged result.

4.2.3 *Thresholds and clusters*

Let us now some more realistic situations. As we already explained, interaction thresholds are often used in both knowledge and wealth exchanges, see [DNAW00, HK02, CCC07] for instance. Those thresholds usually induce cluster formations.

Let us take a smooth initial datum, with a lot of individuals with low values of knowledge and wealth, and a few agents with higher values of knowledge and/or wealth, as seen on Figure 22.
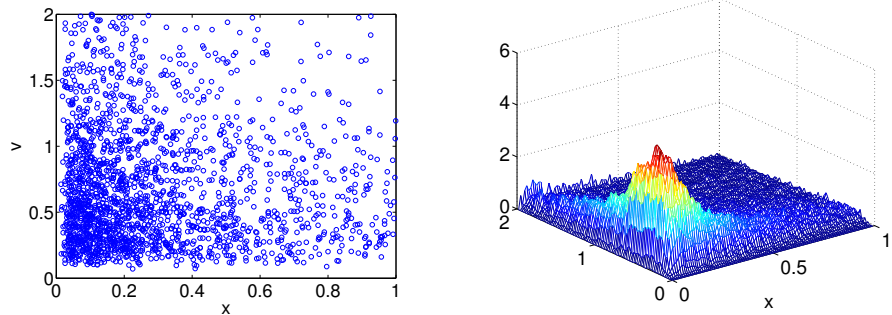

Figure 22: A more realistic initial datum for the distribution function.

For the threshold, we suppose that people usually interact with other agents which have more or less the same level of wealth and/or knowledge, for socio-professional networking reasons.

Hence, for this first experiment, we assume that a wealth exchange between agents (x, v) and (y, w) can only occur when $|v - w| \leq 0.5$, while the information exchange only occurs if both agents have the same level of knowledge and wealth. The first restriction has been introduced because the interaction takes place between people who have more or less the same cultural level, and the second one takes into account the fact that someone who owns a lot often does not want to share what he knows. The distribution obtained at final time with these thresholds is shown in Figure 23.

In the second experiment, with the same initial datum as in Figure 22, we provide a simpler threshold effect, which was already discussed
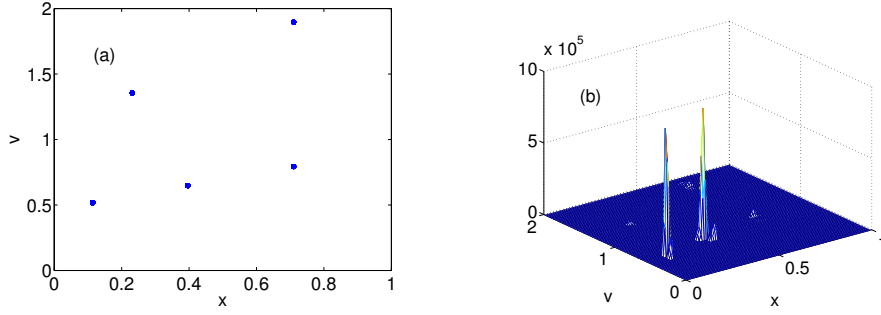
Figure 23: Experiment 1 (with thresholds): distribution at final time for one simulation (on the left), and averaged on 30 computations (on the right).

in Subsection 4.1.1. Two agents (x, v) and (y, w) can only exchange information when their respective wealth values are close, for instance $|v - w| < \omega$, with $\omega = 0.1$. The distribution function at final time is shown in Figure 24.
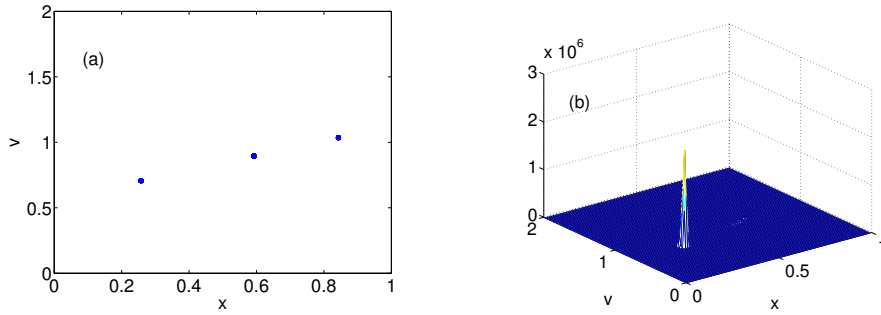

Figure 24: Experiment 2 (with thresholds): distribution at final time for one simulation (on the left), and averaged on 30 computations (on the right).
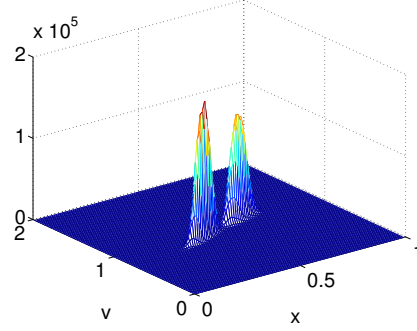
4.2.4 *Quasi-invariant knowledge*

The knowledge exchange seems to be the key mechanism of the whole process, in the sense that there is no way to get significantly richer without information. In this subsection, we consider the quasi-invariant knowledge case, i.e. we assume that the function κ which appears in the knowledge collision rule (4.1) is of order ε with $0 < \varepsilon \ll 1$. That means that κ is replaced in (4.1) by a function $\varepsilon \tilde{\kappa}$, where $\tilde{\kappa}$ is of order 1 and has the same form as κ.

Let us first perform an experiment with a piecewise constant initial datum f^{in}. We choose $\gamma = 0.21$, $\alpha = 0.05$ in the expression of $\tilde{\kappa}$, and $\varepsilon = 0.1$. Figure 25 shows the evolution of the the distribution function f for one numerical simulation.

The average on 30 simulations at time $t = 25$ is presented in Figure 26. We observe that f seems to be, when time grows, supported by a straight line, as in Figure 21.
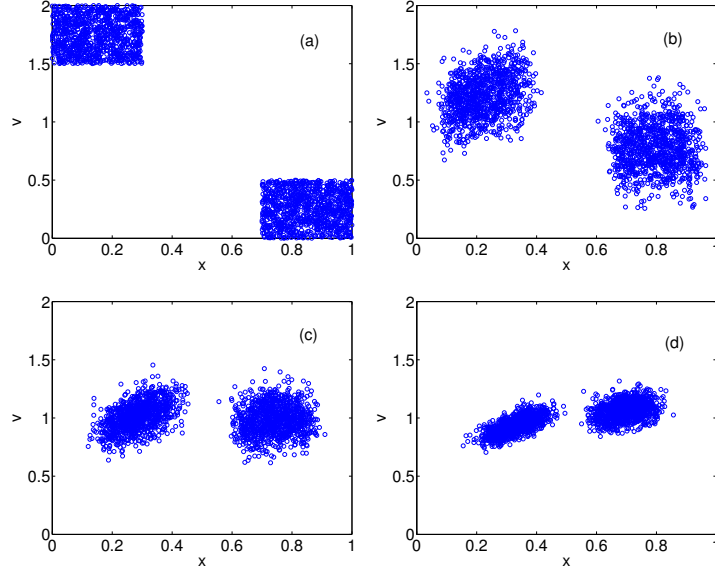
Figure 25: Quasi-invariant knowledge: time evolution of f at times (a) $t = 0$, (b) $t = 5$, (c) $t = 10$, (d) $t = 15$.

Figure 26: Quasi-invariant knowledge: distribution function at time $t = 25$ averaged on 30 simulations.

It is not really surprising. Indeed, when ε goes to 0, the term $Q_K(f, f)$ becomes negligible with respect to $Q_W(f, f)$. Choosing a test-function $\phi(x, v) = ax + bv$, where $a, b \in \mathbb{R}$, allows to state that

$$\frac{\mathrm{d}}{\mathrm{d}t} \int_{\mathbb{R}_+^{*2}} f(t, x, v)\phi(x, v) \,\mathrm{d}x\,\mathrm{d}v = 0,$$

since both total knowledge and wealth are conserved in the wealth exchange (4.2). That implies that any distribution function with a straight line support solves the Boltzmann equation (with $Q_W(f, f)$ only) in a distributional sense.

OUTLOOK

In this last chapter we present the open questions and the further works for each model we investigated.

5.1 CROSS-DIFFUSION HERDING

So far, relatively little attention has been devoted to the study of the parameter space interfaces of different mathematical methods. We have analysed as an example a cross-diffusion herding model to understand where, and how, the global nonlinear analysis approach via entropy variables is connected to bifurcation analysis techniques from dynamical systems. We have shown that both approaches encounter similar problems regarding the degeneracy of the diffusion matrix and we were able to cover different parameter regimes by combining the results of the two methods.

The result presented in chapter 2 is only a first starting point. Here we shall just mention a few ideas for future work.

The next step is to analyse the regime $\alpha \to 0$ and to check whether the limitation in (2.8) on α can be improved, or not. In this regard, one also has to consider in which sense the forward problem should be interpreted for moderate and small values of α and for $\delta < \delta_d$. Recent work [Lio15] suggests that one should not only use the notion of Petrovskii ellipticity for the stationary problem [SW09] but also consider it in the parabolic context; see the classical survey [AV64].

The next step is to expand the approach to other examples. In particular, many reaction-diffusion systems as well as other classes of PDEs have natural entropies, which can be used to study global existence and convergence properties. In the nonlinear case, one frequently can also employ approaches from dynamical systems to understand the dynamics of the PDE. Using a similar approach as we presented here could be illuminating for other examples. For example, it is natural to conjecture that there are examples in applications, which exhibit the following characteristics:

(Z1) There exists one fixed parameter region in which the entropy method yields global decay. Upon variation of a single parameter, the validity boundary of the entropy method coincides precisely with an isolated local supercritical bifurcation point.

(Z2) There exists one fixed parameter region in which the entropy method yields global decay. Upon variation of a single parameter, the validity boundary of the entropy method does not coincide with a local bifurcation point. Instead, the obstruction is a global bifurcation branch in parameter space with a fold point precisely at the validity boundary.

In this work, we apparently found a more complicated case as shown in Figure 1. However, it seems plausible that the cases (Z1)-(Z2) should occur even in classical problems without cross-diffusion, i.e. reaction-diffusion equations with a diagonal positive-definite diffusion matrix.

Determining whether this is true for several classical examples from applications is an interesting open problem.

Regarding the entropy method [CJM+01, DF06], it would be interesting to investigate in more detail parametric scenarios for its validity regime. For example, the question arises whether it is possible to find criteria for the validity range that are computable for entire classes of PDEs. The entropy approach relies on upper bounds. Although the bounds we present here turn out to be sharp in the sense of global decay dynamics in a suitable singular limit, this may not always be easy to achieve as demonstrated by the $\alpha \to 0$ case discussed above. It would be relevant to estimate a priori, which regime in parameter space one fails to cover if certain non-optimal upper bounds are used. As above, carrying this out for several examples could already be very illuminating.

Regarding the analytical and numerical bifurcation analysis, there are multiple strategies to deal with the problem of mass conservation, or more generally with higher-dimensional solution manifolds. For example, one may try to compute the entire solution family of steady states parametrized by the mass numerically [Hen02, DS13], which yields a numerical continuation problem for higher-dimensional manifolds and not only curves. Furthermore, we have focused on the numerical problem in the one-dimensional setup and computing the two- and three-space dimension cases could be interesting [Kue14, UWR14]. Regarding analytical generalizations, a possible direction is to view δ^* as a singular limit and phrase the problem as a perturbation problem [Ni98, Fif73, AK15].

5.2 KINETIC MODEL FOR HERDING AND RATIONALITY

In chart analysis, the bandwidth is employed to identify a band squeeze. When the asset value leaves the interval $[R^-, R^+]$, this situation may indicate a change of direction of the prices. Clearly, this interpretation cannot be directly applied to the situation presented in Chapter 3. On the other hand, the Bollinger bands are an additional tool to identify large changes in the mean asset value, for instance when the background value $W(t)$ is no longer deterministic but driven by some stochastic process. We leave this generalization for future work.

5.3 WEALTH DISTRIBUTION MODEL

In the last part of Chapter 4, we proved that any distribution function with a straight line support solves the Boltzmann equation in a distributional sense.

The straight lines depend on the initial datum, in a way we still have to understand, but the numerical simulations from Figure 27, where f^{in} is chosen as constant on the indicated domain and zero elsewhere, show an interesting behaviour: all the lines are concurring at the same point $(-1, 0)$ in Figure 27b. Unfortunately, for the time being, we still have to understand how the equation of the straight line can be computed from the data of the problem.
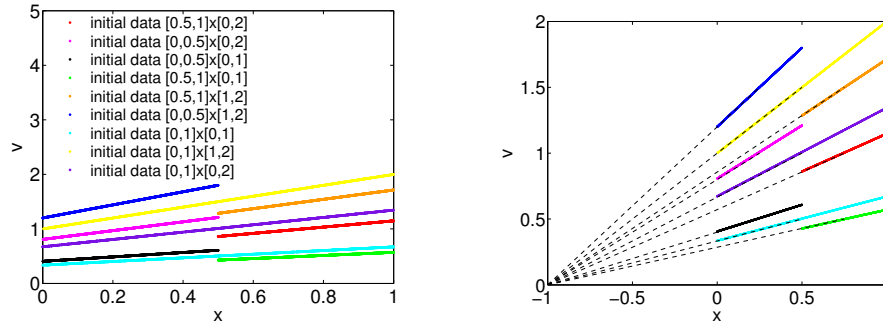
Figure 27: Distribution functions obtained with different initial data with large time.

Moreover it would be interesting to study the quasi invariant limit obtaining a Fokker-Planck equation and compare the numerical results that we obtained for the Boltzmann equation with the numerics for the Fokker-Planck.

AAN96   A. Arnold, N.B. Abdallah, and C. Negulescu. Liapunov functionals and large-time-asymptotics of mean-field nonlinear Fokker-Planck equations. *Transp. Theory Stat. Phys.*, 25(7):733–751, 1996.

AK15   F. Achleitner and C. Kuehn. On bounded positive stationary solutions for a nonlocal Fisher-KPP equation. *Nonl. Anal. A: Theor. Meth. & Appl.*, 112:15–29, 2015.

Ama89   Herbert Amann. Dynamic theory of quasilinear parabolic systems. iii. global existence. *Mathematische Zeitschrift*, 202(2):219–250, 1989.

AMTU01   A. Arnold, P. Markowich, G. Toscani, and A. Unterreiter. On convex Sobolev inequalities and the rate of convergence to equilibrium for Fokker-Planck type equations. *Comm. Partial Differential Equations*, 26(1-2):43–100, 2001.

AN03   A. L. Amadori and R. Natalini. Entropy solutions to a strongly degenerate anisotropic convection-diffusion equation with application to utility theory. *J. Math. Anal. Appl.*, 284(2):511–531, 2003.

AR93   Eric Abrahamson and Lori Rosenkopf. Institutional and competitive bandwagons: Using mathematical modeling as a tool to explore innovation diffusion. *The Academy of Management Review*, 18(3):487–517, 1993.

AR97   Eric Abrahamson and Lori Rosenkopf. Social network effects on the extent of innovation diffusion: A computer simulation. *Organization Science*, 8(3):289–309, 1997.

ARNn+05   E. Altshuler, O. Ramos, Y. Núñez, J. Fernández, A. J. Batista-Leyva, and C. Noda. Symmetry breaking in escaping ants. *The American Naturalist*, 166(6):643–649, 2005.

AV64   M.S. Agranovich and M.I. Vishik. Elliptic problems with a parameter and parabolic problems of general type. *Russ. Math. Surv.*, 19(3):53–157, 1964.

AZ98   Christopher Avery and Peter Zemsky. Multidimensional Uncertainty and Herd Behavior in Financial Markets. *American Economic Review*, 88(4):724–48, 1998.

Bad10   Michelle Baddeley. Herding, social influence and economic decision-making: socio-psychological and neuroscientific analyses. *Philos Trans R Soc Lond B*, 365:281–290, 2010.

Ban92   Abhijit V. Banerjee. A simple model of herd behavior. *The Quarterly Journal of Economics*, 107(3):797–817, 1992.

BdO04 Armando Ticona Bustillos and Paulo Murilo C. de Oliveira. Evolutionary model with genetics, aging, and knowledge. *Phys. Rev. E*, 69:021903, 2004.

BGL14 D. Bakry, I. Gentil, and M. Ledoux. *Analysis and Geometry of Markov Diffusion Operators*. Springer, 2014.

BHW92 Sushil Bikhchandani, David Hirshleifer, and Ivo Welch. A Theory of Fads, Fashion, Custom, and Cultural Change in Informational Cascades. *Journal of Political Economy*, 100(5):992–1026, 1992.

Bir95 G. A. Bird. *Molecular gas dynamics and the direct simulation of gas flows*, volume 42 of *Oxford Engineering Science Series*. The Clarendon Press, Oxford University Press, New York, 1995.

BM00 J.-P. Bouchaud and M. Mézard. Wealth condensation in a simple model of economy. *Physica A*, 282:536, 2000.

BMP11a M. Burger, P. Markowich, and J.-F. Pietschmann. Continuous limit of a crowd motion and herding model: analysis and numerical simulations. *Kinet. Relat. Mod.*, 4:1025–1047, 2011.

BMP11b Martin Burger, Peter Alexander Markowich, and Jan-Frederik Pietschmann. Continuous limit of a crowd motion and herding model: analysis and numerical simulations. *Kinet. Relat. Models*, 4(4):1025–1047, 2011.

Bol09 Ludwig Boltzmann. 1:317, 1909.

Bru01 Markus K. Brunnermeier. *Asset pricing under asymmetric information: bubbles, crashes, technical analysis, and herding*. Oxford University Press, 2001.

BS09 Laurent Boudin and Francesco Salvarani. A kinetic approach to the study of opinion formation. *M2AN Math. Model. Numer. Anal.*, 43(3):507–522, 2009.

BS10 Laurent Boudin and Francesco Salvarani. Modelling opinion formation by means of kinetic equations. In *Mathematical modeling of collective behavior in socio-economic and life sciences*, Model. Simul. Sci. Eng. Technol., pages 245–270. Birkhäuser Boston, Inc., Boston, MA, 2010.

BT15 Carlo Brugna and Giuseppe Toscani. Boltzmann-type models for price formation in the presence of behavioral aspects. *Netw. Heterog. Media*, 10(3):543–557, 2015.

CCC07 B.K. Chakrabarti, A. Chakraborti, and A. Chatterjee. *Econophysics and Sociophysics: Trends and Perspectives*. Wiley, 2007.

CDCT09 Valeriano Comincioli, Lucia Della Croce, and Giuseppe Toscani. A Boltzmann-like equation for choice formation. *Kinet. Relat. Models*, 2(1):135–149, 2009.

CJM⁺01 J.A. Carrillo, A. Jüngel, P.A. Markowich, G. Toscani, and A. Unterreiter. Entropy dissipation methods for degenerate parabolic problems and generalized Sobolev inequalities. *Monatshefte für Mathematik*, 133(1):1–82, 2001.

CKWW12 A. Chertock, A. Kurganov, X. Wang, and Y. Wu. On a chemotaxis model with saturated chemotactic flux. *Kinet. Relat. Mod.*, 5:51–95, 2012.

CMPP10 Stephane Cordier, Dario Maldarella, Lorenzo Pareschi, and Cyrille Piatecki. Microscopic and kinetic models in financial markets. In *Mathematical modeling of collective behavior in socio-economic and life sciences*, Model. Simul. Sci. Eng. Technol., pages 51–80. Birkhäuser Boston, Inc., Boston, MA, 2010.

CPT05 Stephane Cordier, Lorenzo Pareschi, and Giuseppe Toscani. On a kinetic model for a simple market economy. *J. Stat. Phys.*, 120(1-2):253–277, 2005.

CR71 M.G. Crandall and P.H. Rabinowitz. Bifurcation from simple eigenvalues. *J. Functional Analysis*, 8(2):321–340, 1971.

CR73 M.G. Crandall and P.H. Rabinowitz. Bifurcation, perturbation of simple eigenvalues and linearized stability. *Arch. Rational Mech. Anal.*, 52:161–180, 1973.

DARM⁺13 P. Degond, C. Appert-Rolland, M. Moussaïd, J. Pettré, and G. Theraulaz. A hierarchy of heuristic-based models of crowd dynamics. *J. Stat. Phys.*, 152(6):1033–1068, 2013.

DCD⁺07 E.J. Doedel, A. Champneys, F. Dercole, T. Fairgrieve, Y. Kuznetsov, B. Oldeman, R. Paffenroth, B. Sandstede, X. Wang, and C. Zhang. Auto 2007p: Continuation and bifurcation software for ordinary differential equations (with homcont). *http://cmvl.cs.concordia.ca/auto*, 2007.

DF06 L. Desvillettes and K. Fellner. Exponential decay toward equilibrium via entropy methods for reaction-diffusion equations. *J. Math. Anal. Appl.*, 319(1):157–176, 2006.

DF07 L. Desvillettes and K. Fellner. Entropy methods for reaction-diffusion systems. *Discrete Cont. Dyn. Sys. (suppl.)*, pages 304–312, 2007.

dFC06 Luciano da Fontoura Costa. Learning about knowledge: A complex network approach. *Phys Rew E*, 64:026103, 2006.

DJ12 M. Dreher and A. Jüngel. Compact families of piecewise constant functions in $L^p(0, T; B)$. *Nonlin. Anal.*, 75:3072–3077, 2012.

DJH⁺09 John R.G. Dyer, Anders Johansson, Dirk Helbing, Iain D. Couzin, and Jens Krause. Leadership, consensus decision making and collective behaviour in humans. *Philosophical transactions of the Royal Society. B, Biological sciences*, 364:781–789, 2009.

DL14   Marcello Delitala and Tommaso Lorenzi. A mathematical model for value estimation with public information and herding. *Kinet. Relat. Models*, 7(1):29–44, 2014.

DMPW09   Bertram Düring, Peter Markowich, Jan-Frederik Pietschmann, and Marie-Therese Wolfram. Boltzmann and Fokker-Planck equations modelling opinion formation in the presence of strong leaders. *Proc. R. Soc. Lond. Ser. A Math. Phys. Eng. Sci.*, 465(2112):3687–3708, 2009.

DNAW00   G. Deffuant, D. Neau, F. Amblard, and G. Weisbuch. Mixing beliefs among interacting agents. *Adv. Complex Systems*, 3:87–98, 2000.

DS13   H. Dankowicz and F. Schilder. *Recipes for Continuation*. SIAM, 2013.

DW96   Andrea Devenow and Ivo Welch. Rational herding in financial economics. *European Economic Review*, 40(3-5):603–615, 1996.

DW15   Bertram Düring and Marie-Therese Wolfram. Opinion dynamics: inhomogeneous Boltzmann-type equations modelling opinion leadership and political segregation. *Proc. A.*, 471(2182):20150345, 21, 2015.

DY00   A. Drăgulescu and V.M. Yakovenko. Statistical mechanics of money. *Eur. Phys. J. B*, 17:723–729, 2000.

EVZ94   M. Escobedo, J. L. Vázquez, and Enrike Zuazua. Entropy solutions for diffusion-convection equations with partial diffusivity. *Trans. Amer. Math. Soc.*, 343(2):829–842, 1994.

Fif73   P.C. Fife. Semilinear elliptic boundary value problems with small parameters. *Arch. Rational Mech. Anal.*, 52(3):205–232, 1973.

Gab12   P. Gabriel. Long-time asymptotics for nonlinear growth-fragmentation equations. *Commun. Math. Sci.*, 10:787–820, 2012.

GAEM+11   Juan Carlos González-Avella, Victor M. Eguíluz, Matteo Marsili, Fernado Vega-Redondo, and Maxi San Miguel. Threshold learning dynamics in social networks. *PLoS ONE*, 6:1–9, 05 2011.

GGS82   S. Galam, Y. Gefen, and Y. Shapir. Sociophysics: a new approach of sociological collective behavior. i. mean-behavior description of a strike. *J. of Math. Sociology*, 9:1–13, 1982.

Gov87   W.F. Govaerts. *Numerical Methods for Bifurcations of Dynamical Equilibria*. SIAM, Philadelphia, PA, 1987.

Gra85   Mark Granovetter. Economic action and social structure: The problem of embeddedness. *American Journal of Sociology*, pages 481–510, 1985.

GS14   G. Galiano and V. Selgas. On a cross-diffusion segregation problem arising from a model of interacting particles. *Nonlin. Anal.: Real World Appl.*, 18:34–49, 2014.

Ham71   W.D. Hamilton. Geometry for the selfish herd. *Journal of Theoretical Biology*, 31:295–311, 1971.

Hel93a   D. Helbing. Boltzmann-like and Boltzmann-Fokker-Planck equations as a foundation of behavioral models. *Phys. A*, 196(4):546–573, 1993.

Hel93b   D. Helbing. Stochastic and Boltzmann-like models for behavioral changes, and their relation to game theory. *Phys. A*, 193(2):241–258, 1993.

Hen02   M.E. Henderson. Multiple parameter continuation: Computing implicitly defined k-manifolds. *Int. J. Bif. Chaos*, 12(3):451–476, 2002.

Hir01   David Hirshleifer. Investor psychology and asset pricing. *J. Finance*, 56:1533–1597, 2001.

HJ11   S. Hittmeir and A. Jüngel. Cross diffusion preventing blow up in the two-dimensional Keller-Segel model. *SIAM J. Math. Anal.*, 43:997–1022, 2011.

HK02   R. Hegselmann and U. Krause. Opinion dynamics and bounded confidence: models, analysis and simulation. *J. Artif. Soc. Soc. Sim.*, 5(3), 2002.

Hor11   D. Horstmann. Generalizing the keller-segel model: Lyapunov functionals, steady state analysis, and blow-up results for multi-species chemotaxis models in the presence of attraction and repulsion between competitive interacting species. *J. Nonlin. Sci.*, 21:231–270, 2011.

HP02   T. Hillen and K. Painter. Volume filling and quorum sensing in models for chemosensitive movement. *Canad. Appl. Math. Quart.*, 10:501–543, 2002.

HPW13   Thomas Hillen, Kevin J. Painter, and Michael Winkler. Anisotropic diffusion in oriented environments can lead to singularity formation. *European J. Appl. Math.*, 24(3):371–413, 2013.

Jan98   A. Janušauskas. Classification of second-order partial differential equation systems elliptic in the petrovskii sense. *Lithuanian Mathematical Journal*, 38:59–63, 1998.

Jün15   A. Jüngel. The boundedness-by-emtropy method for cross-diffusion systems. *Nonlinearity*, 28:1963–2001, 2015.

JZ09   J. Jiang and Y. Zhang. On convergence to equilibria for a chemotaxis model with volume-filling effect. *Asympt. Anal.*, 65:79–102, 2009.

Kel77   H. Keller. Numerical solution of bifurcation and nonlinear eigenvalue problems. In P. Rabinowitz, editor, *Applications of Bifurcation Theory*, pages 359–384. Academic Press, 1977.

Key36   John Maynard Keynes. *The General Theory of Employment, Interest and Money*. Cambridge University Press, 1936.

Kie04   H. Kielhoefer. *Bifurcation Theory: An Introduction with Applications to PDEs*. Springer, 2004.

KOGV07   B. Krauskopf, H.M. Osinga, and J. Galán-Vique, editors. *Numerical Continuation Methods for Dynamical Systems: Path following and boundary value problems*. Springer, 2007.

KS70   E. Keller and S. Segel. Initiation of slime mold aggregation viewed as an instability. *J. Theor. Biol.*, 26:399–415, 1970.

Kue14   C. Kuehn. Efficient gluing of numerical continuation and a multiple solution method for elliptic PDEs. *arXiv:1406.6900*, pages 1–34, 2014.

LB95   Gustave Le Bon. *Psychologie des foules*. 1895.

Lio15   P.-L. Lions. Some new classes of nonlinear Kolmogorov equations. Talk at the 16th Pauli Colloquium, Wolfgang-Pauli Institute, November 18 2015.

LM99   Thomas Lux and Michele Marchesi. Scaling and criticality in a stochastic multi-agent model of a financial market. *Nature*, 397:498–500, 1999.

LM13   M. Liero and A. Mielke. Gradient structures and geodesic convexity for reaction-diffusion systems. *Phil. Trans. Roy. Soc. A*, 371:20120346, 2013.

LMM13   Annamaria Lusardi, Pierre-Carl Michaud, and Olivia S. Mitchell. Optimal financial knowledge and wealth inequality. Working Paper 18669, National Bureau of Economic Research, 2013.

LS08   H. Lambda and T. Seaman. Market statistics of a psychology-based heterogeneous agent model. *Intern. J. Theor. Appl. Finance*, 11:717–737, 2008.

Lux98   T. Lux. The socio-economic dynamics of speculative markets: interacting agents, chaos, and the fat tails of return distributions. *J. Econ. Behav. Organ.*, 33:143–165, 1998.

MP12   Dario Maldarella and Lorenzo Pareschi. Kinetic models for socio-economic dynamics of speculative markets. *Physica A*, 391:715–730, 2012.

MS00   R. N. Mantegna and H. E. Stanley. *An Introduction to Econophysics: Correlations and Complexity in Finance*. Cambridge University Press, 2000.

Ni98   W.-M. Ni. Diffusion, cross-diffusion and their spike-layer steady states. *Notices Amer. Math. Soc.*, 45(1):9–18, 1998.

NPT10   G. Naldi, L. Pareschi, and G. Toscani, editors. *Mathematical Modeling of Collective Behavior in Socio-Economic and Life Sciences*. Model. Simul. Sci. Eng. Technol. Birkhauser Basel, 2010.

PT13   Lorenzo Pareschi and Giuseppe Toscani. *Interacting Multiagent Systems: Kinetic equations and Monte Carlo methods*. Oxford University Press, 2013.

PT14   L. Pareschi and G. Toscani. Wealth distribution and collective knowledge: a Boltzmann approach. *Philos. Trans. R. Soc. Lond. Ser. A Math. Phys. Eng. Sci.*, 372(2028):20130396, 15, 2014.

Rog03   Everett M. Rogers. *Diffusion of innovations*. Free Press, New York, NY [u.a.], 5th edition, 2003.

Roo06   Laurens Rook. An economic psychological approach to herd behavior. *J. Econ.*, 40:75–95, 2006.

RRF09   N. Chater R. Raafat and C. Frith. Herding in humans. *Trends Cognitive Sci.*, 13:420–428, 2009.

Sch71   Thomas Schelling. Dynamic models of segregation. *Journal of Mathematical Sociology*, 1, 1971.

Shi00   Robert J. Shiller. *Irrational exuberance*. Princeton Univ. Press, 2000.

Sim55   Herbert A. Simon. A behavioral model of rational choice. *The Quarterly Journal of Economics*, 69(1):99–118, 1955.

Smi59   Adam Smith. *The Theory of Moral Sentiments*. McMaster University Archive for the History of Economic Thought, 1759.

SW09   J. Shi and X. Wang. On the global bifurcation for quasilinear elliptic systems on bounded domains. *J. Differential Equat.*, 246:2788–2812, 2009.

Tem97   R. Temam. *Infinite-Dimensional Dynamical Systems in Mechanics and Physics*. Springer, 1997.

Tos06   Giuseppe Toscani. Kinetic models of opinion formation. *Commun. Math. Sci.*, 4(3):481–496, 2006.

Tro06   Wilfred Trotter. *Instincts of the Herd in Peace and War*. 1906.

Uhl72   K. Uhlenbeck. Eigenfunctions of Laplace operators. *Bull. Amer. Math. Soc.*, 78:1073–1076, 1972.

UWR14   H. Uecker, D. Wetzel, and J.D.M. Rademacher. pde2path - A Matlab package for continuation and bifurcation in 2D elliptic systems. *Num. Math.: Th. Meth. Appl.*, 7:58–106, 2014.

Veb09   Thorstein Veblen. The limitations of marginal utility. *History of Economic Thought Articles*, 17, 1909.

Wei71   W. Weidlich. The statistical description of polarization phenomena in society. *Br. J. Math. Stat. Psychol.*, 24:251–266, 1971.

Wol02   G. Wolansky. Multi-components chemotactic system in the absence of conflicts. *Europ. J. Appl. Math.*, 13:641–661, 2002.

Wrz04   D. Wrzosek. Global attractor for a chemotaxis model with prevention of overcrowding. *Nonlin. Anal.*, 59:1293–1310, 2004.

WX13   X. Wang and Q. Xu. Spiky and transition layer steady states of chemotaxis systems via global bifurcation and Helly's compactness theorem. *J. Math. Biol.*, 66(6):1241–1266, 2013.

Zei90   Eberhard Zeidler. *Nonlinear functional analysis and its applications. II/A*. Springer-Verlag, New York, 1990.

ZM15   J. Zinsl and D. Matthes. Transport distances and geodesic convexity for systems of degenerate diffusion equations. *arXiv:1409.6520*, pages 1–32, 2015.